Radiation transfer modeling and land surface parameter inversion from multi source remote sensing data

Qinhuo Liu
(qhliu@irsa.ac.cn)

State Key Laboratory of Remote Sensing Sciences
Institute of Remote Sensing Applications,
Chinese Academy of Sciences

2010-11-30
NESDIS/NOAA, Camp Springs, Maryland

Contents

0. Brief introduction of SKLRSS and IRSA

- **IRSA: Institute of Remote Sensing Applications, Chinese Academy of Sciences**
- **SKLRSS: State Key Laboratory of Remote Sensing Science**
- **Division of Remote Sensing Radiation Transfer Modeling and Inversion**

(1) IRSA Milestone

1979 IRSA established: **There are 4 academicians, 58 senior researchers, 200+ staffs, 167+ contractors, 200+ PhD students and post doctors, 100+ MS students**

- **1986 Airborne Remote Sensing Centre established**
- **1994 Laboratory of Remote Sensing Information Science**
- **1997 National Engineering Research Center for Geoinformatics**
- **2003 National Demonstration Center for Spaceborne Remote Sensing / National Space Administration**
- **2004 State Key Lab of Remote Sensing Science**

IRSA Organization Structure

research units:

- Remote Sensing Radiation Transfer Modeling and inversion
- Environmental Remote Sensing application technology
- Hyperspectral Remote Sensing
- Microwave Remote Sensing
- Remote Sensing Calibration and Validation
- Remote Sensing Image processing
- Agriculture and Ecological Remote Sensing
- Disaster and Emergency Remote Sensing
- Land Resource Remote Sensing
- Non-Renewable Remote Sensing
- Spatial Information System
- Digital Earth and Navigation Positioning
- Environment Protection Remote Sensing

(2) Brief Introduction of SLRSS

- **1994, Key Laboratory of Remote Sensing Information Science, Institute of Remote Sensing Applications, Chinese Academy of Sciences**
- **1999, Centre for Remote Sensing, Beijing Normal University**
- **2003, State Key Laboratory of Remote Sensing Science was approved to be jointly established.**
- **2005, formally opened to public after state acceptance in 2005.**

- **53 fixed researchers, including 46 researchers (28 professors and 9 associate professors) and 7 staff members.**
- **Among adjunct members, there are 7 visiting professors, 8 associate professors,18 lecturers and 27 post-doctors.**

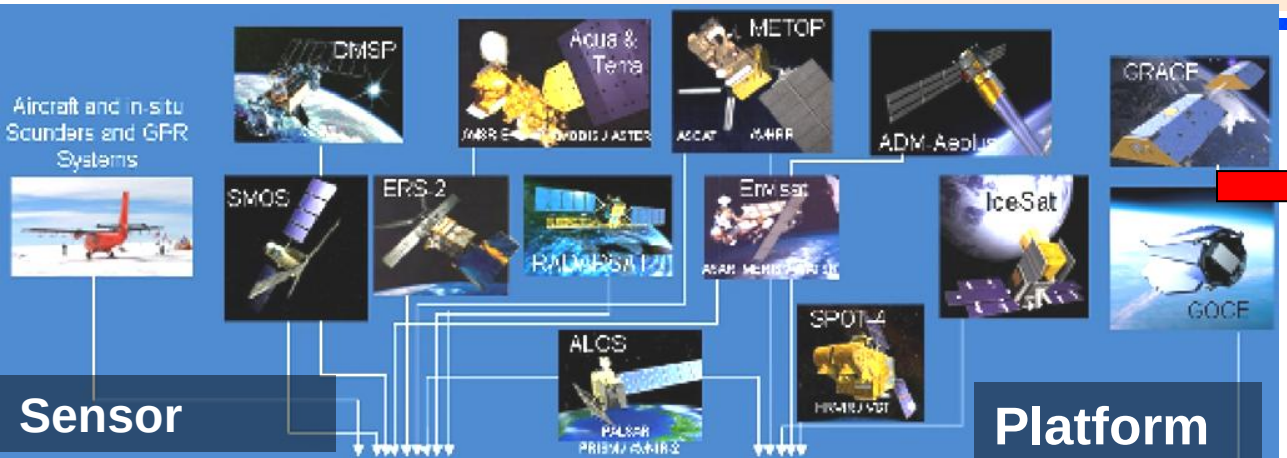

Basic Theory: EM radiation transfer

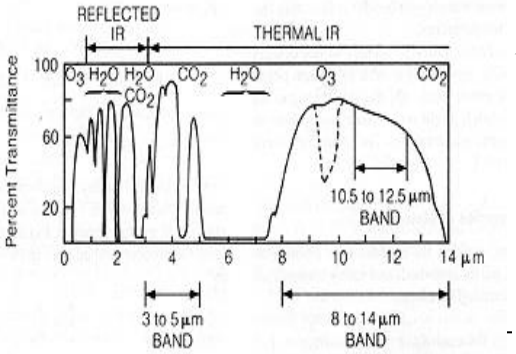

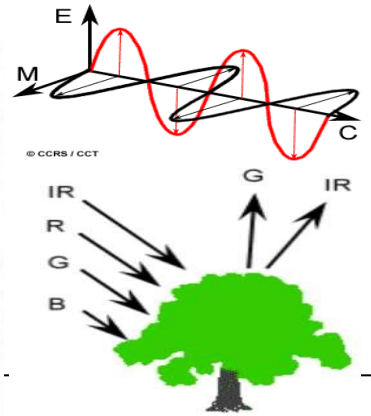

Information extraction
Parameter inversion

Earth Science

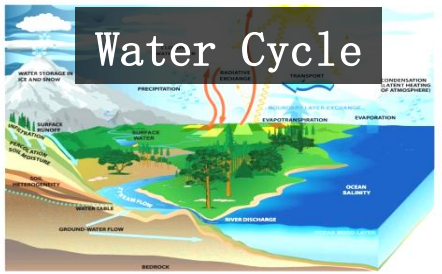

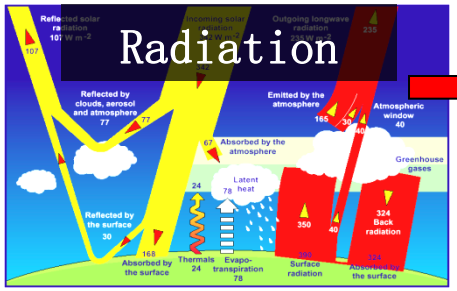

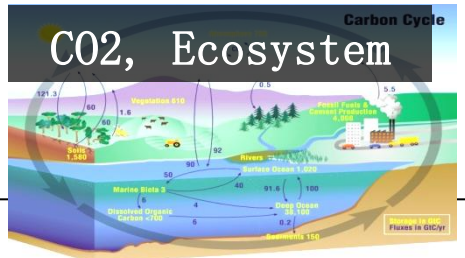

Applications

Research Directions（1/3）

- **Radiative transfer mechanism and inversion theory**
  - improve radiative transfer models in RS
  - integrate multi-scale remote sensing models
  - synergistic inversion of multi-sensor data
  - assimilate multi-scale data and land surface process models.

Research Directions（2/3）

- **Technogies for RS data acquisition and processing**
  - remote sensing detection, data processing and information extraction techniques
  - such as multiangle, polarization, full polarization multi-band microwave, hyper-spectral, LIDAR, high spatial resolution imaging, and wireless sensor networks.

Research Directions（3/3）

- **Geospatial information integration and applications**
  - communication networks, integration and information services, simulation and visualization
  - monitoring & simulation platforms for land surface radiation, energy balance studies and key element cycle (Carbon, Water,…).
  - conduct exemplary applications of agriculture, resources, disaster, environment and health

Research Areas

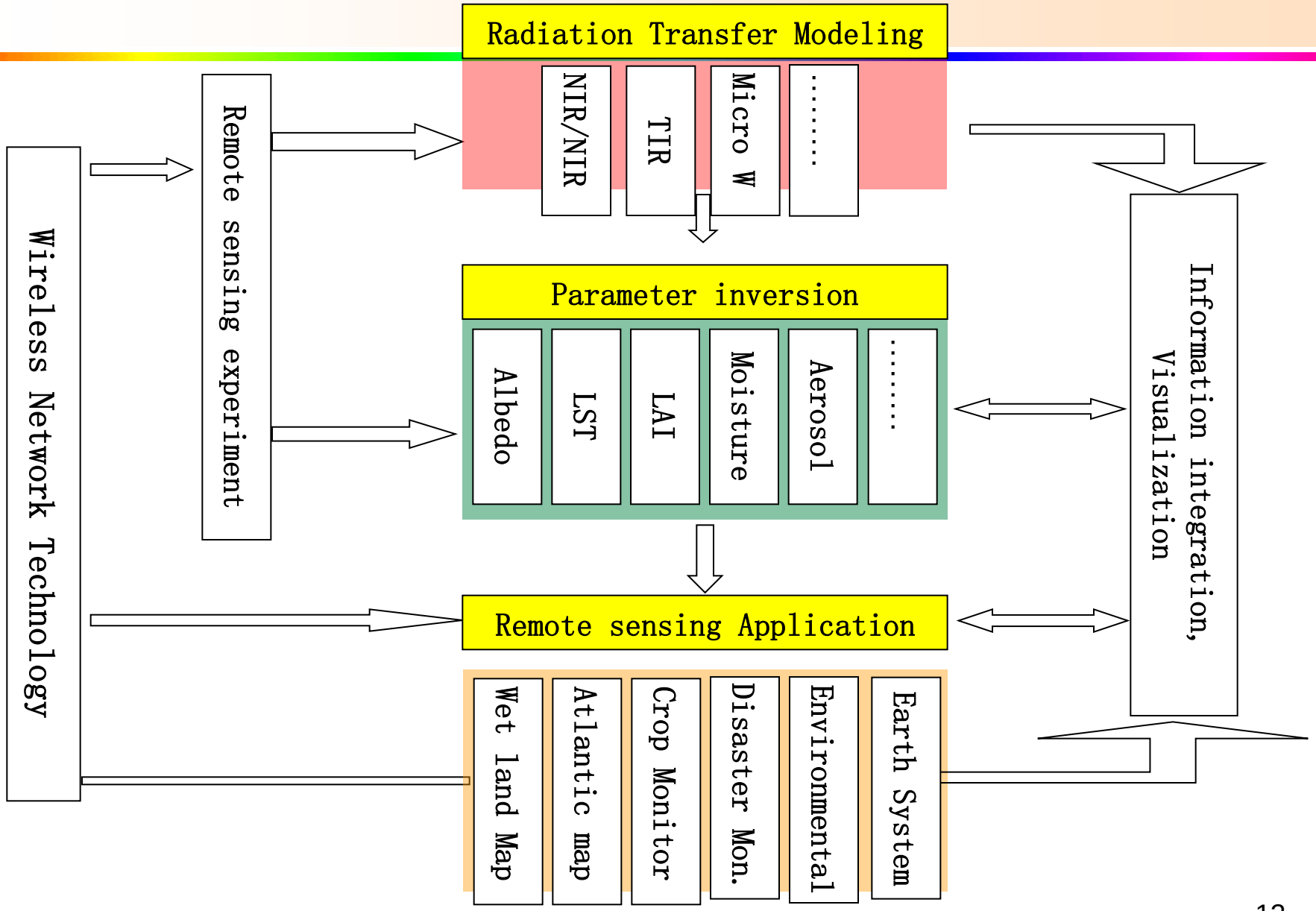

Radiation Transfer Modeling and inversion

1. Research Background
2. Recent advances on radiation transfer modeling
3. Land surface parameters inversion based on multi-source remote sensing data
4. Multi-scale field experiment system design and field experiment campaign
5. Software system development and product generation
6. Discussion

Research Background

Atmosphere

Ice, Snow

Biosphere

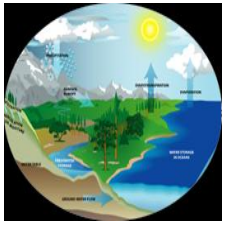

hydrosphere

lithosphere

Earth system

Hydrosystem, Water cycle

Radiation balance

Ecosystem C cycle

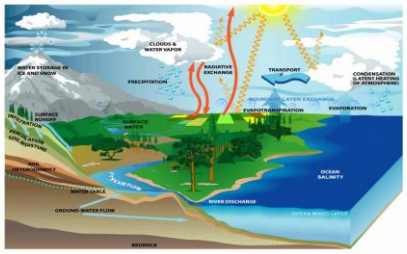

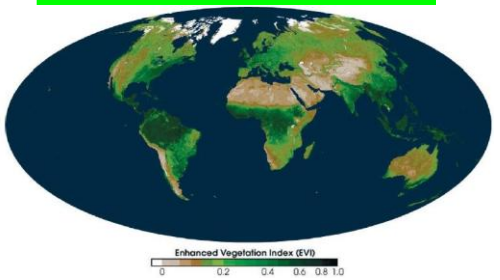

Control effects for global system

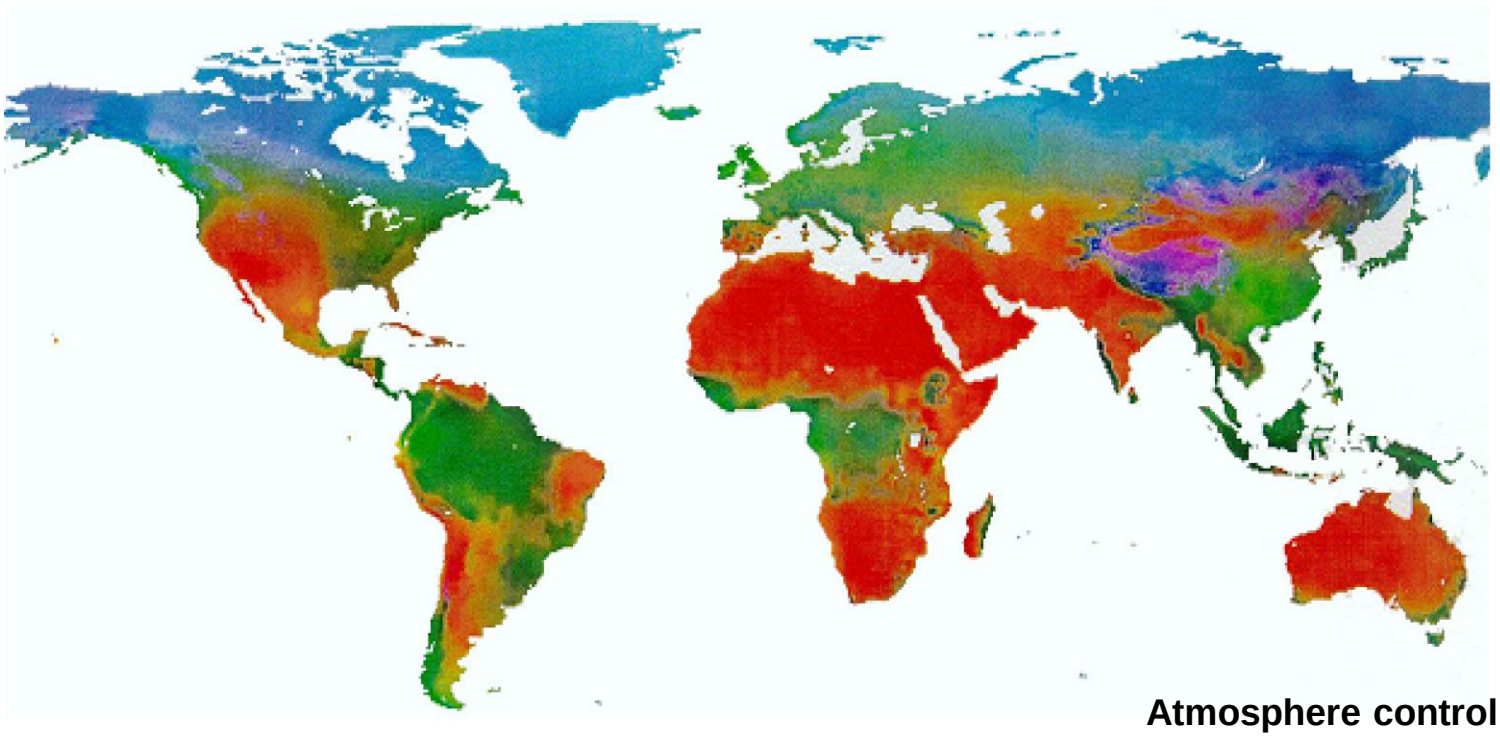

Atmosphere control
(solar radiation)

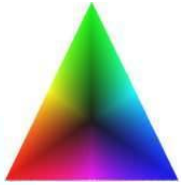

Land surface control
(soil moisture)

Land surface control
(temperature/vegetation)

Churkina & Running, 1998

Radiation and energy balance

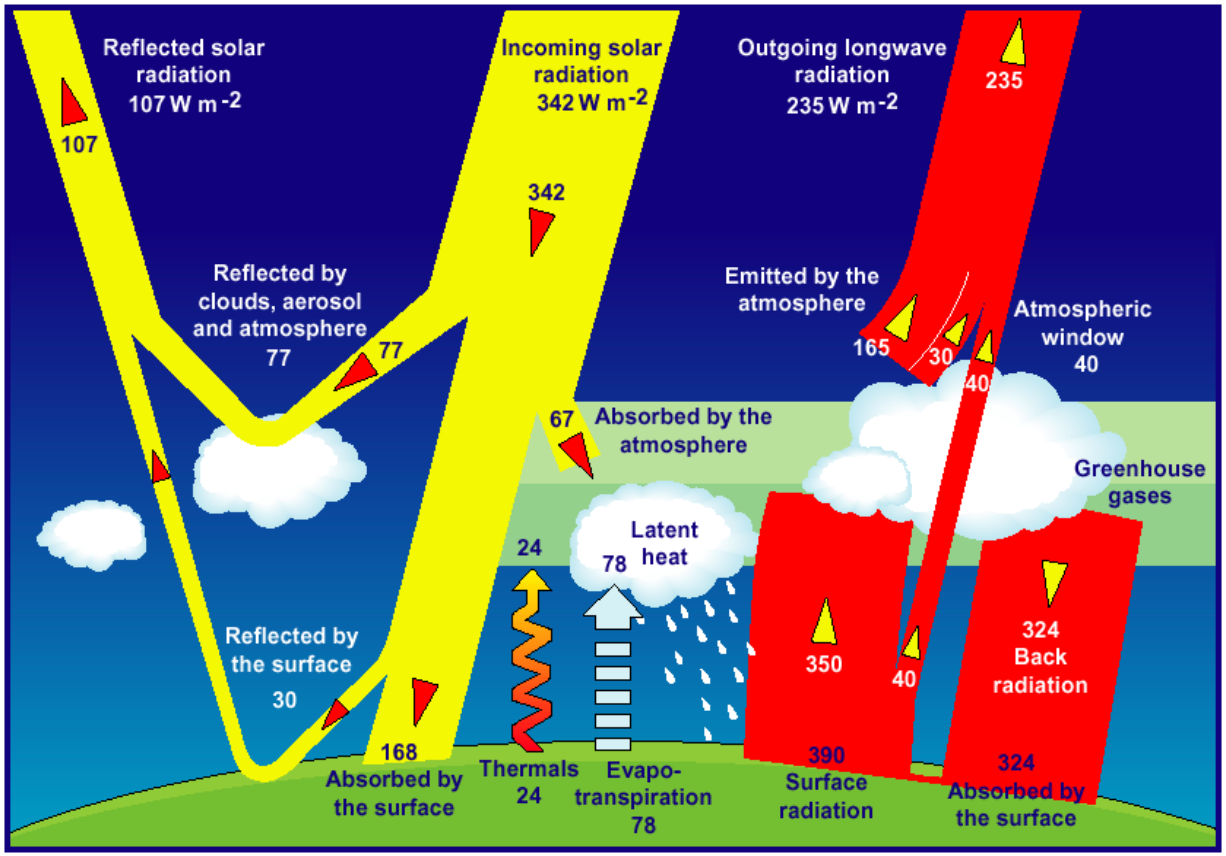

Radiation and land surface energy balance

Key parameters:

Atmospheric optical depth

Solar Radiation

Albedo

Land surface temperature
Emissivity

Latent Heat Flux

Sensible Heat Flux

Classification

Leaf Area Index

Soil Moisture

Land surface process model scale issues

Land surface process model need different spatial scale observation: 1KM, 5KM, 10KM, 100KM

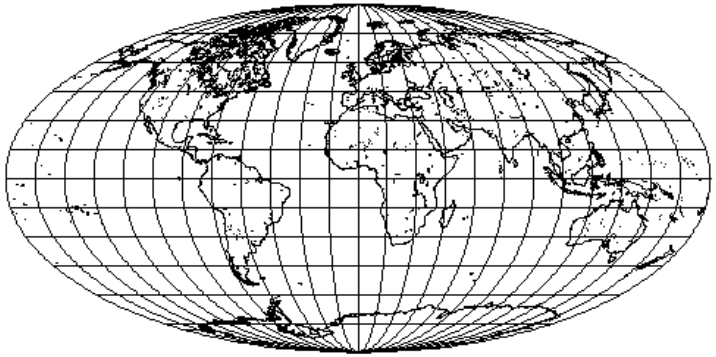

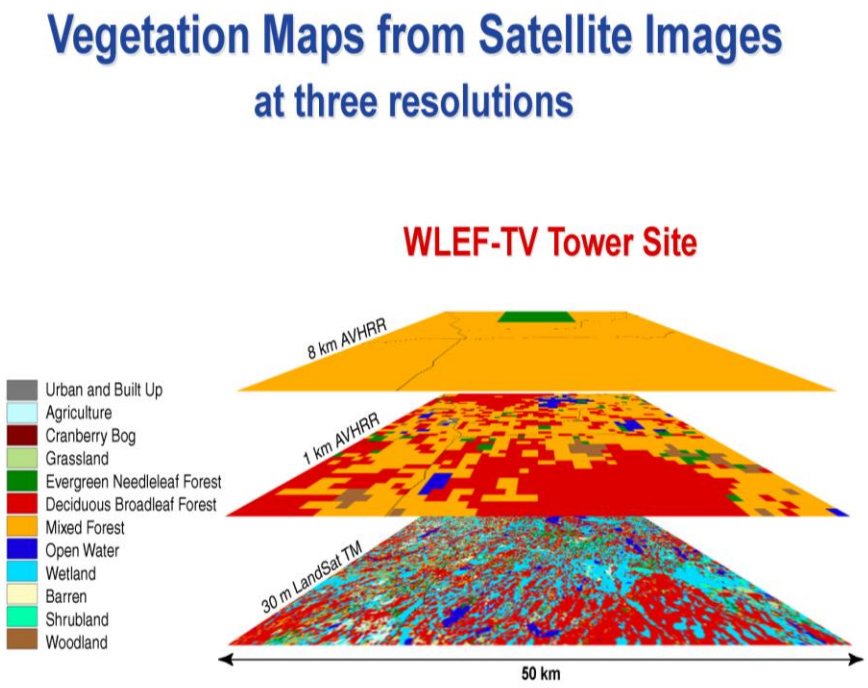

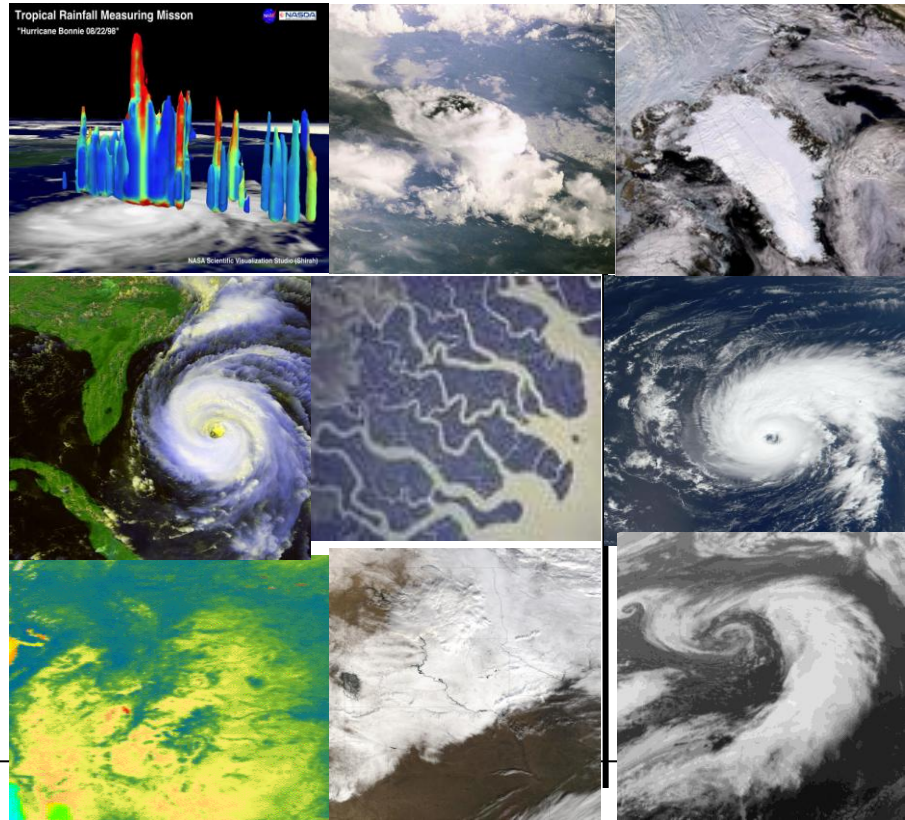

Traditional observation system

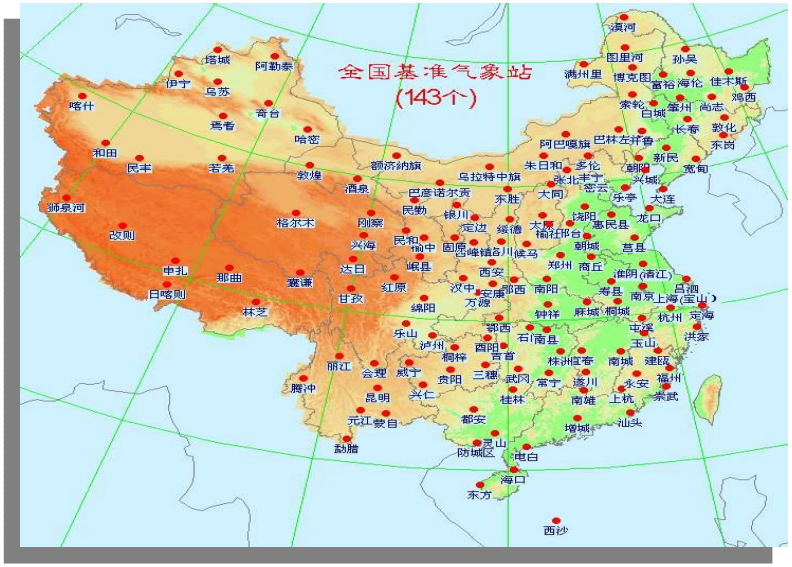

1. Ground observation station: sparsely distributed
2. Ground station observation doesn't agree with model scales
3. Remote sensing can provide spatially distribution information

Soil moisture

at 25 km x 25 km

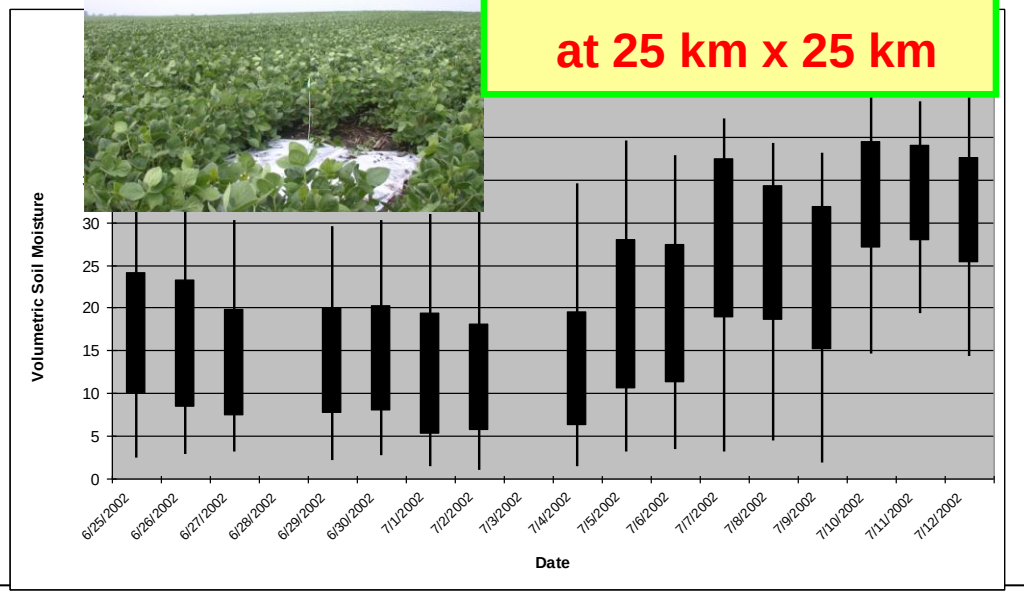

New observation system wanted

Remote sensing+ground station observation

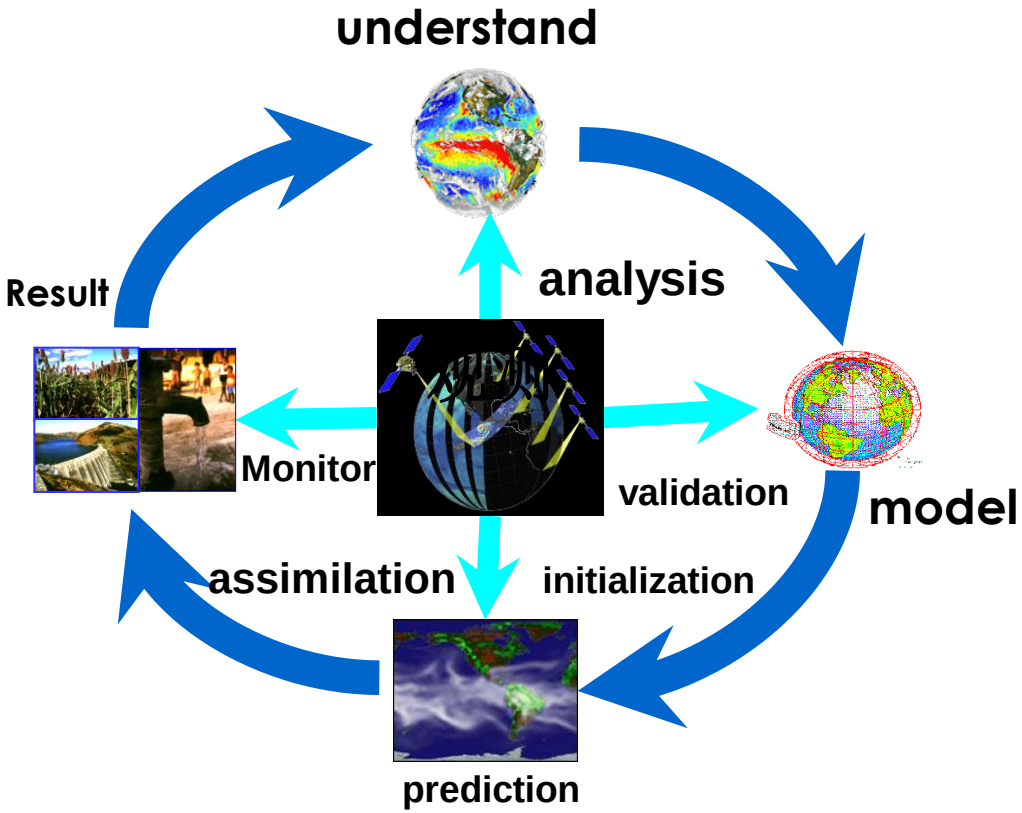

EM radiation transfer modeling and inversion

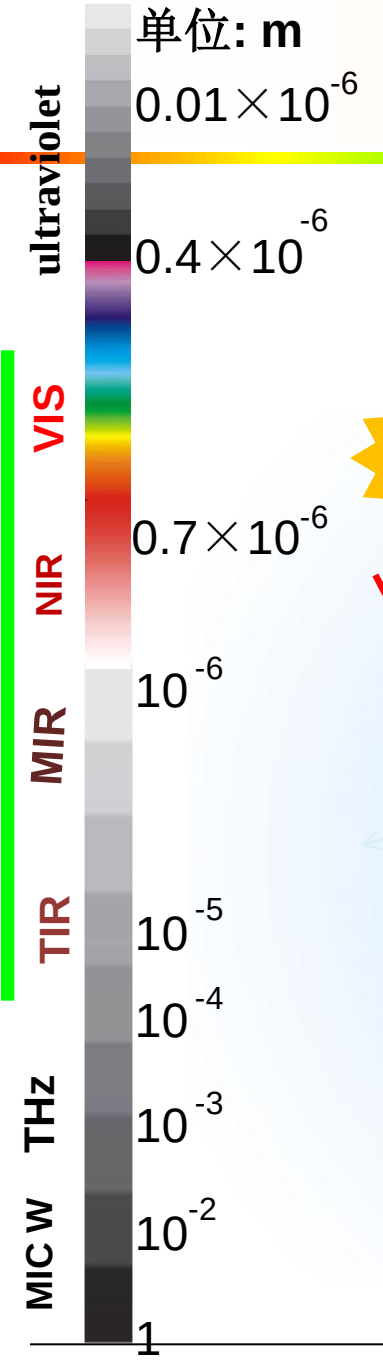

$$L = f\left(\lambda, s_{x,y,z}, t, \theta, P, \Omega\right)$$

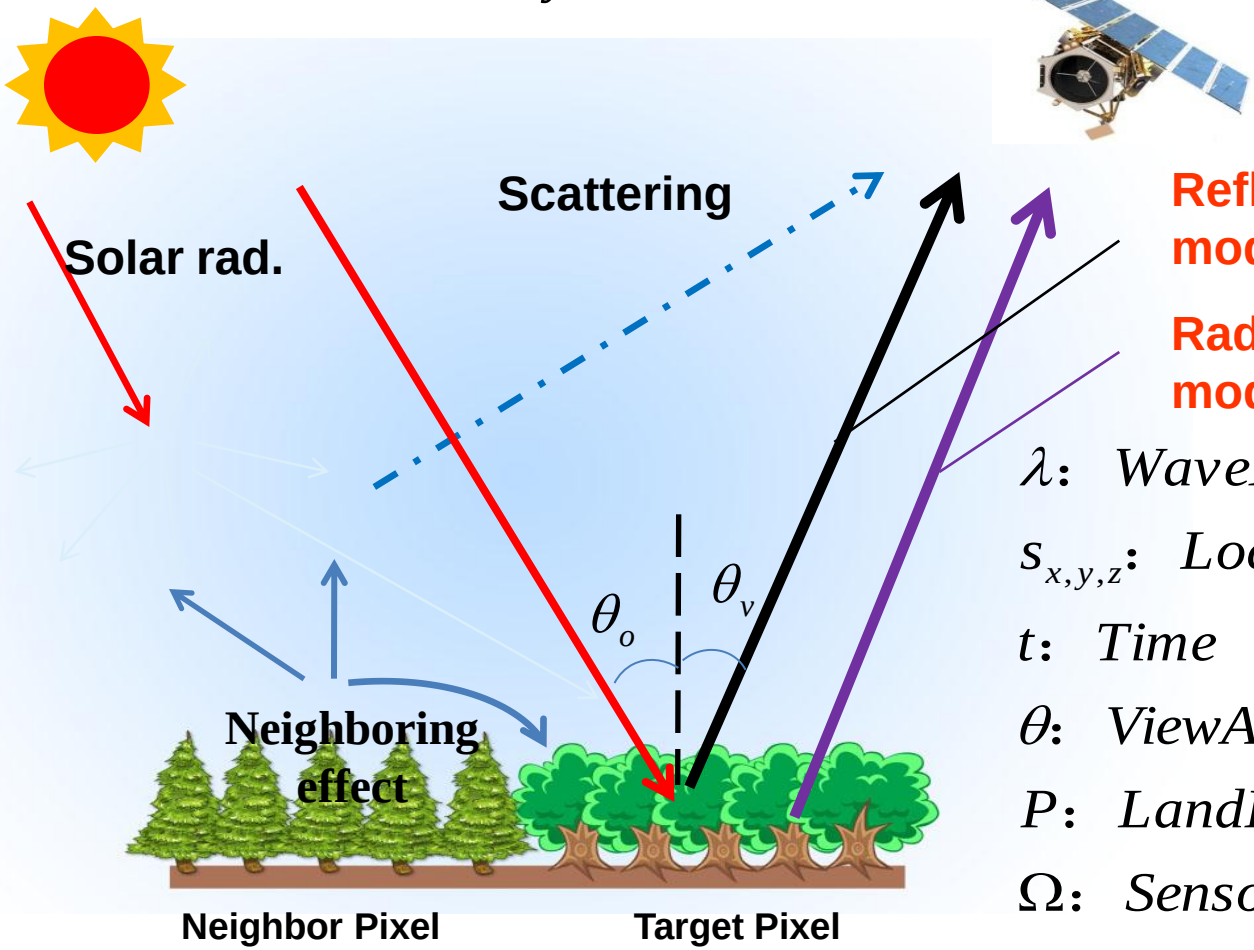

Reflectance modeling

Radiation modeling

λ: *WaveLenght*

$s_{x,y,z}$: *Location*

t: *Time*

θ: *ViewAngle*

P: *LandParameter*

Ω: *SensorParameter*

2. Recent advances on radiation transfer modeling

- The angular effect and scaling effect of remote sensing data due to the earth surface heterogeneity and 3-D structure;
- The Bi-directional reflectance Distribution Function modelling and Thermal emission directionality modelling are the basic issues for quantitative remote sensing。

(1)Basic Principle

(2) Recent Advances

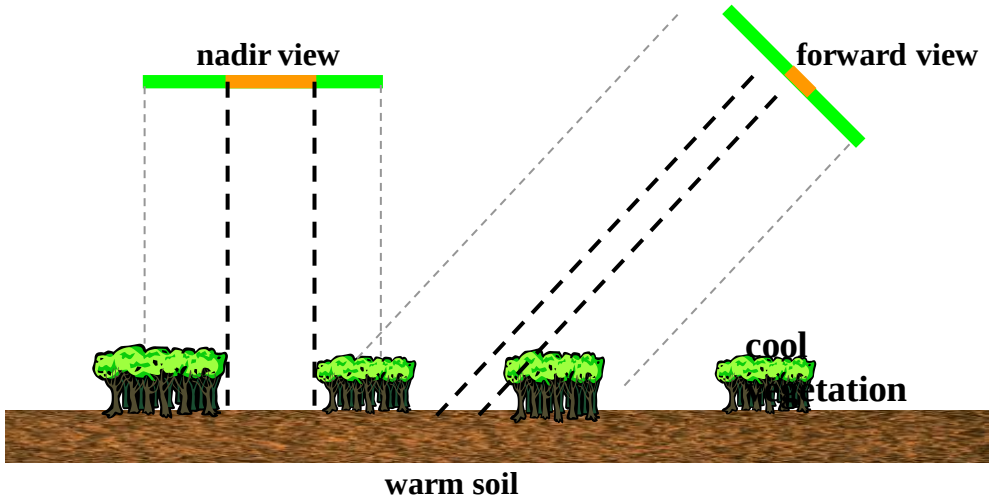

Basic Principle

Radiance L

Radiation Flux at unit area, unit wavelength, unit solid angle:

$$L=\partial^3 \Phi / \partial A \partial \lambda \partial \Omega$$

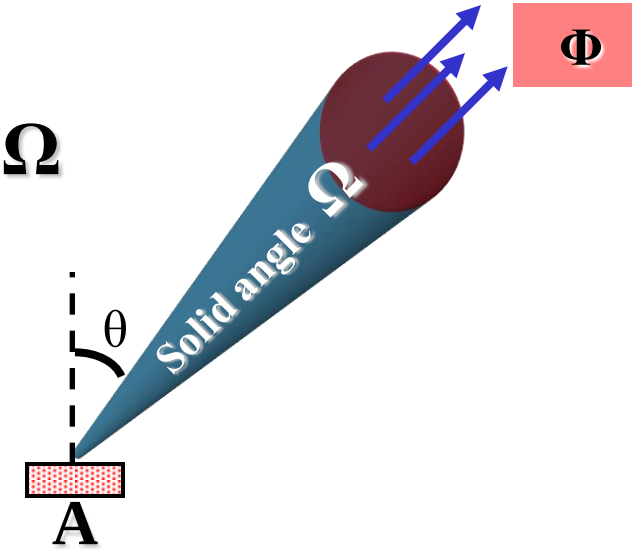

（W/m² • μm • Sr）

Bi-directional Reflectance Distribution Function (BRDF)

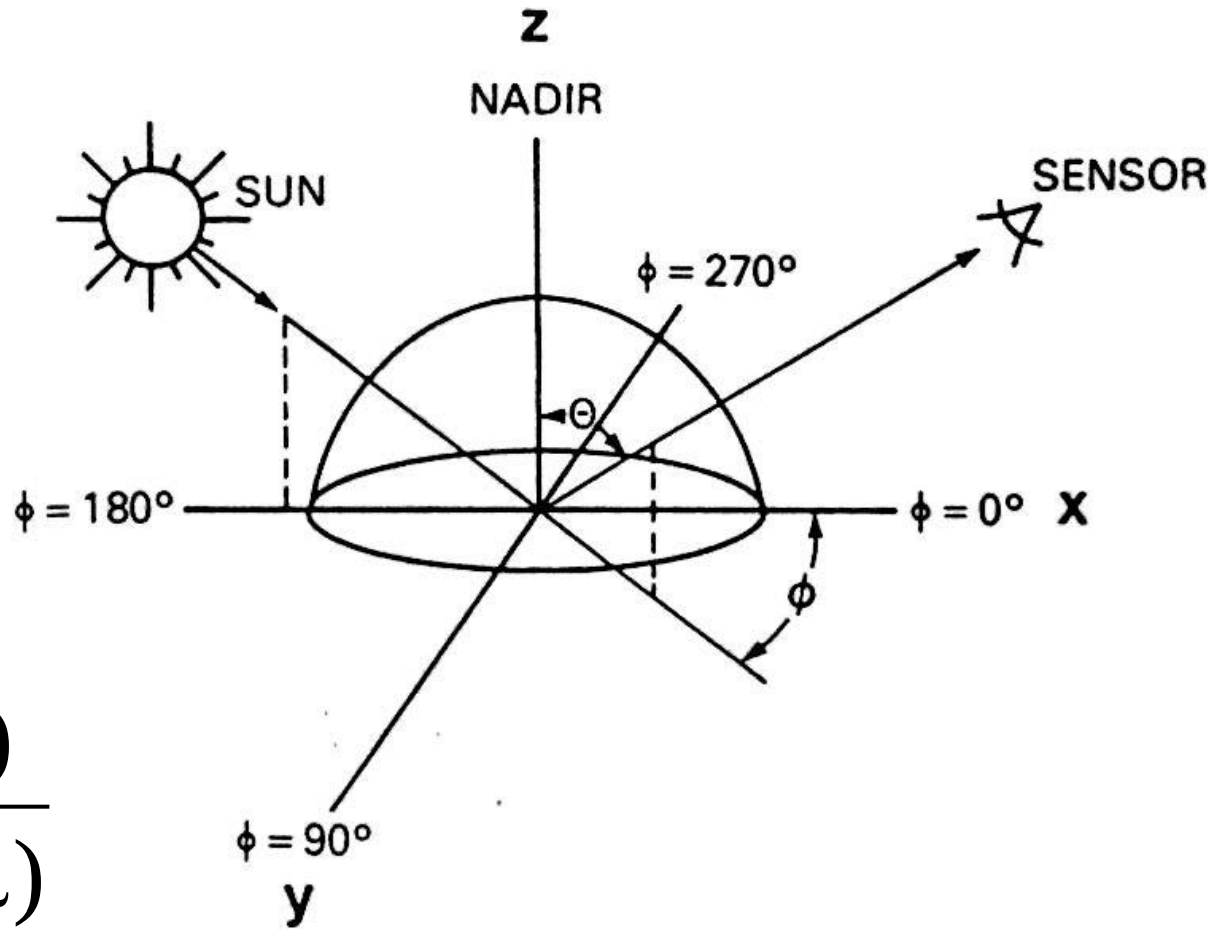

$$f = \frac{dL(\theta, \varphi, \lambda)}{dE(\theta_0, \varphi_0, \lambda)}$$

Multi-scales of remote sensing radiation transfer

Vegetation canopy： 3D structure

Leaf： Component Spetrum

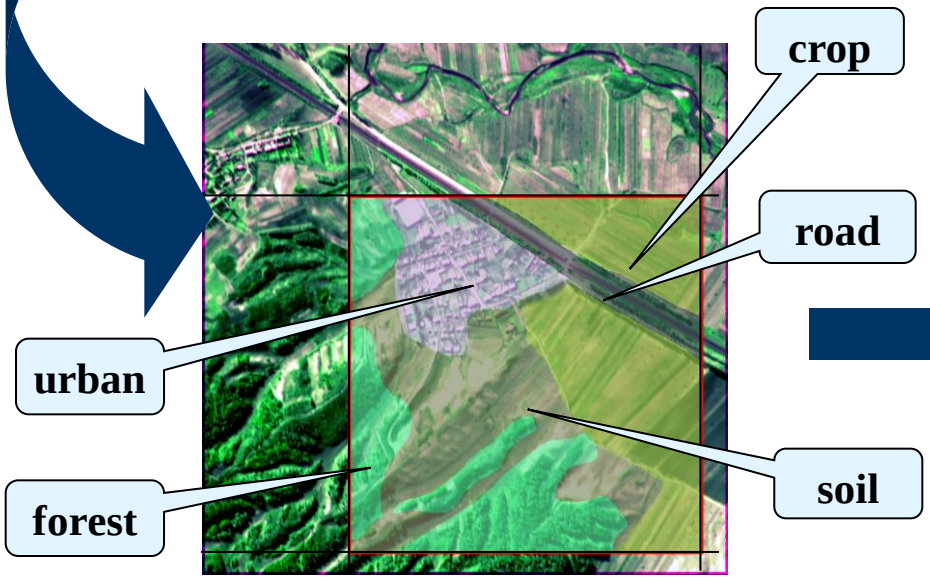

Mixed pixel, terrain effect

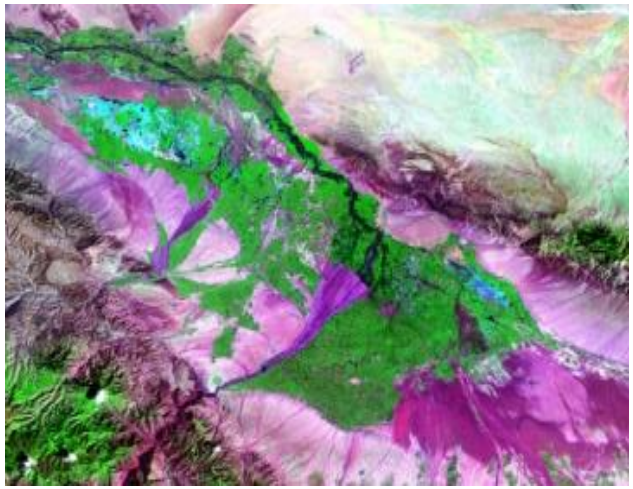

Image： earth surface－atmosphere－sensor

Multi-scale remote sensing radiation transfer modeling

Recent advances:

① d-Prospect model for leaf spectrum

② Radiosity-Graphic combined model on large scale (LRGM)

③TIR emission directionality modeling

④Topographic effect modeling

⑤Remote Sensing Image simulation system

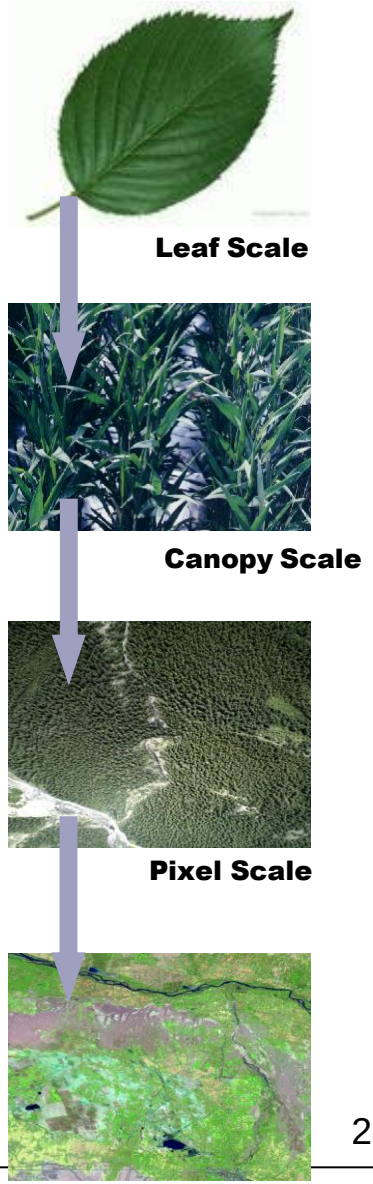

d-Prospect model for leaf spectrum

- **Leaf Spectrum Model：**
  - Flat layer models： PROSPECT (Jacquemoud and Baret, 1990)
  - Needle leaf models： LIBERTY(Dawson, et. al. 1998)
  - Ray tracing model
  - Stochastic model
  - Hybrid medium model

PROSPECT model is one of the most popular leaf spectrum models。

① d-Prospect model for leaf spectrum

A Model to Simulate Optical Properties Spectra of Double Leaf Surfaces

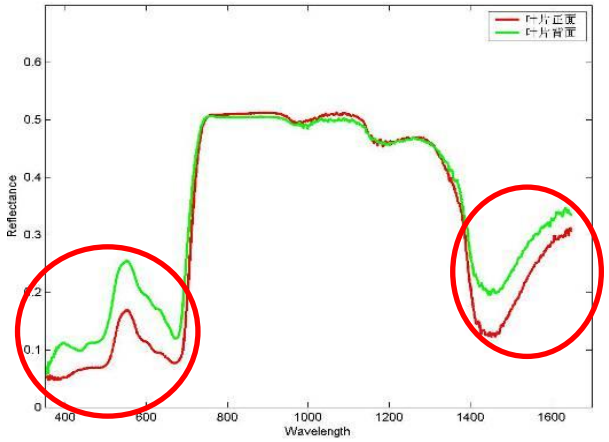

Experiment Measurement results:
The both side reflectance of crop leaves are not equal as the prospect model predicted.

Leaf Spectra model development: from PROSPECT to d-PROSPECT

Thus the assumption that leaf upper and lower surfaces have the same reflectance is not always true, especially for some dicotyledonous leaves.

- Leaf Structure and Model Structure

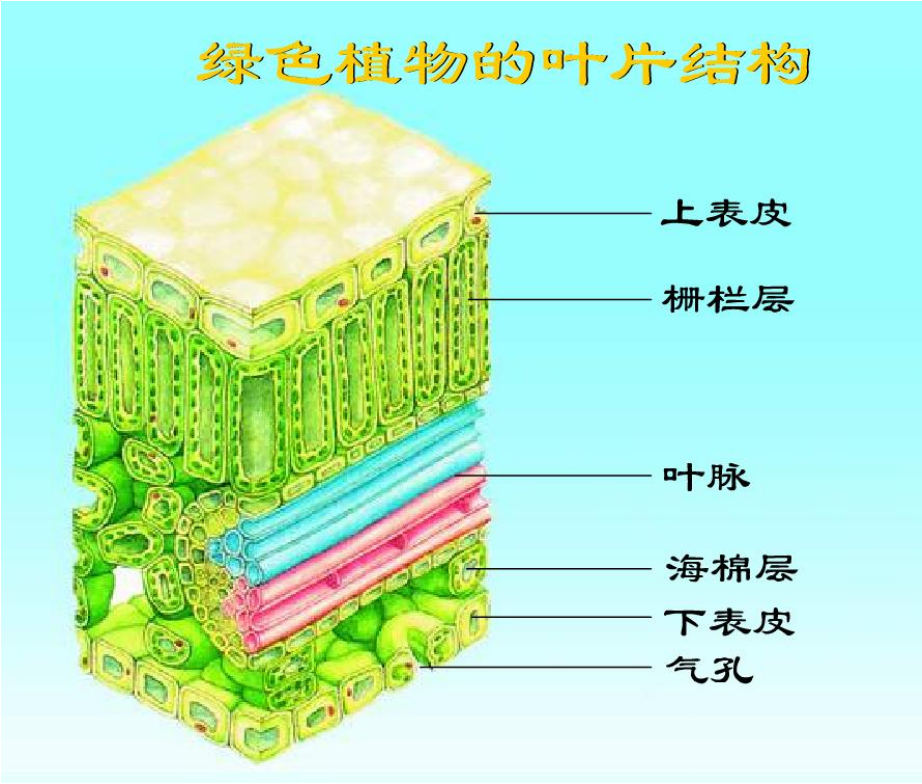

A typical dicotyledonous leaf has an obvious layer structure. It includes four layers of upper epidermis, palisade mesophyll, spongy mesophyll, and lower epidermis. The water, chlorophyll and pigment features distribute in the palisade mesophyll and spongy mesophyll.

the distribution of chlorophyll and leaf water can not be well-proportioned within the leaf

structure of dicotyledonous leaf 双子叶植物叶片结构

Asymmetric Biochemical material distribution → **Optic property asymmetry** → **Up and bottom side reflectance are equal?**

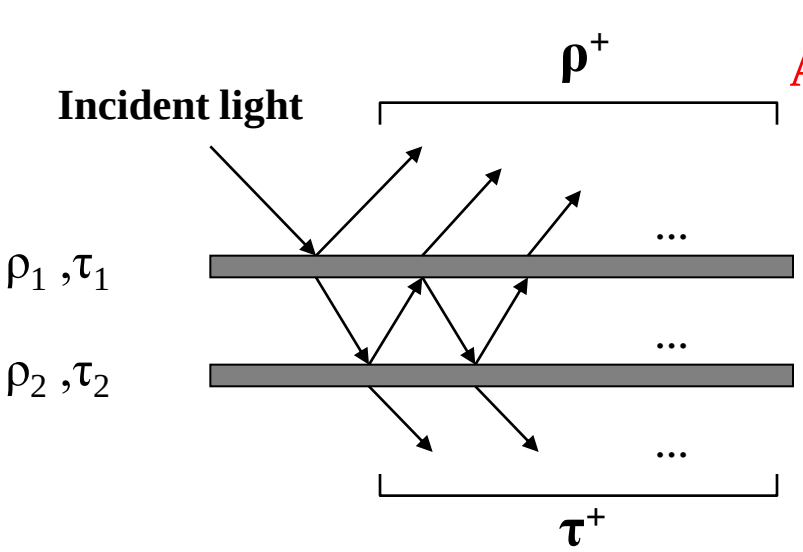

Analyze with plat model

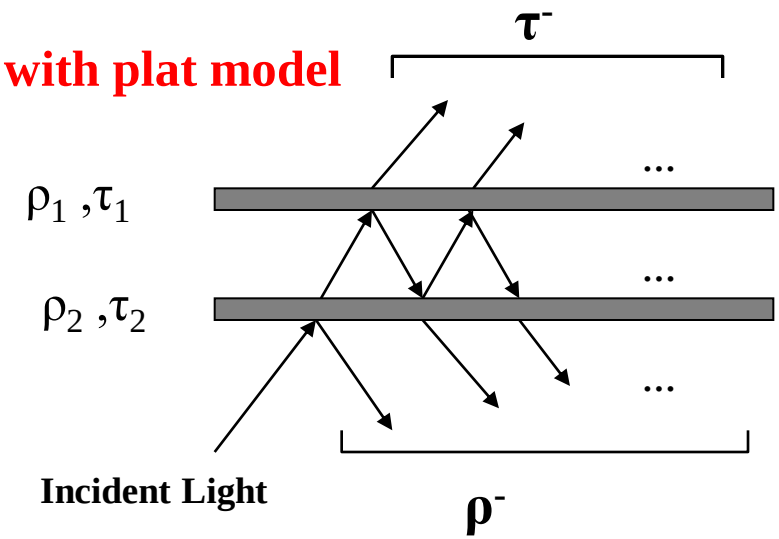

$$\rho^{+} = \rho_1 + \frac{\tau_1^2 \rho_2}{1-\rho_1\rho_2} \quad \neq \quad \rho^{-} = \rho_2 + \frac{\tau_2^2 \rho_1}{1-\rho_1\rho_2}$$

$$\tau^{+} = \frac{\tau_1\tau_2}{1-\rho_1\rho_2} \quad = \quad \tau^{-} = \frac{\tau_1\tau_2}{1-\rho_1\rho_2}$$

It is found out that the biochemical material asymmetric distribution cause to Up and bottom side reflectance are equal

- PROSPECT
- dPROSPECT

新

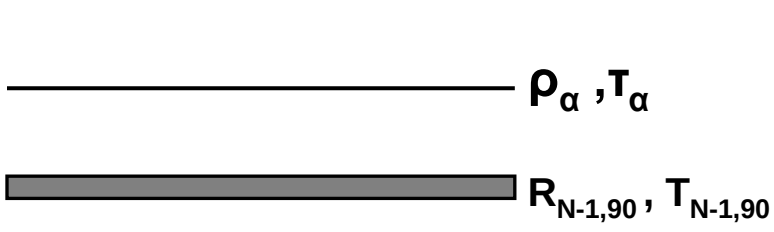

Chlorophyll asymmetric distribution ratio

Water asymmetric distribution ratio

$$k_1(\lambda) = (K_{Cab}(\lambda) * (1 + W_{Cab}) * Cab + K_{Cw}(\lambda) * (1 + W_{Cw}) * Cw + \sum K_i(\lambda)) / 2 * N + k_e(\lambda)$$

$$k_2(\lambda) = (K_{Cab}(\lambda) * (1 - W_{Cab}) * Cab + K_{Cw}(\lambda) * (1 - W_{Cw}) * Cw + \sum K_i(\lambda)) / 2 * N + k_e(\lambda)$$

Leaf up surface reflectance ρ^+, and bottom surface reflectance ρ^-

Jing Li, Qinhuo Liu, and Qiang Liu, D-PROSPECT: A Model to Simulate Optical Properties Spectra of Double Leaf Surfaces

SAIL model to SAILE model

散射系数 σ 和 σ',

$$\sigma(\theta_i) = L'(f_1^2\rho^+ + f_2^2\rho^- + 2\tau f_1 f_2)$$

$$\sigma'(\theta_i) = L'\left[\tau(f_1^2 + f_2^2) + f_1 f_2(\rho^+ + \rho^-)\right]$$

散射系数 s 和 s',

$$s(\theta_i) = \frac{1}{2}[f_1(\rho^+ + \tau) + f_2(\rho^- + \tau)]k(\theta_i) - \frac{1}{2}[f_1(\rho^+ - \tau) - f_2(\rho^- - \tau)]L'\cos\theta_i$$

$$s'(\theta_i) = \frac{1}{2}[f_1(\rho^+ + \tau) + f_2(\rho^- + \tau)]k(\theta_i) + \frac{1}{2}[f_1(\rho^+ - \tau) - f_2(\rho^- - \tau)]L'\cos\theta_i$$

散射系数 v 和 u,

$$v(\theta_i) = \frac{1}{2}[f_1(\rho^+ + \tau) + f_2(\rho^- + \tau)]K(\theta_i) + \frac{1}{2}[f_1(\rho^+ - \tau) - f_2(\rho^- - \tau)]L'\cos\theta_i$$

$$u(\theta_i) = \frac{1}{2}[f_1(\rho^+ + \tau) + f_2(\rho^- + \tau)]K(\theta_i) - \frac{1}{2}[f_1(\rho^+ - \tau) - f_2(\rho^- - \tau)]L'\cos\theta_i$$

散射系数 w

$$w(\theta_i) = \frac{L'}{2\pi}\{\left[\pi\rho^+ - \beta_2(\rho^+ + \tau)\right](2\cos^2\theta_i + \sin^2\theta_i \tan\theta_i \tan\theta_o \cos\varphi)$$
$$+(\rho^+ + \tau)\sin\beta_2\left[\frac{2\cos^2\theta_i}{\cos\beta_i \cos\beta_o} + \cos\beta_1\cos\beta_3\sin^2\theta_i \tan\theta_i \tan\theta_o\right]$$
$$+Z\}$$

new

Replace ρ^+, ρ^- in Sail Model, new scattering coefficients are deduced

=>SAILE

Brief summery

Double *N*-layer structure assumption is suggested here, different from the assumption of a pile of *N* homogeneous layers in PROSPECT model. Two new parameters, *Wab* and *Ww* are introduced to represent the vertical distribution fraction of leaf chlorophyll and water contents. The sensitivity analysis proves that D-PROSPECT model has the capability to simulate the spectra reflectance of both leaf sides fitted with the experiment results well.

- **Vegetation Canopy BRDF models：**
  - **Physical models**
    - **Radiation tranfer models：SAIL model(Verhoef, 1984, …)**
    - **Geometrical Optical models：Li-Strahler GO model (Li, et al., 1986)**
    - **Hybrid Models：GORT (Li, et al., 1995)、5 Scale model (J.M. Chen）**
    - **Computer simulation models：MC model, RGM**
  - **Statistical (empirical) models：Walthall (Walthall, et al., 1985)**

The radiosity-graphics model (RGM) is an important branch of computer simulation modelling for the vegetation BRDF;

As the radiosity method is based on a global solving technique, the RGM can only deal with limited numbers of polygons, and has only been used for small-scale flat terrain scenes.

However, the land surface is generally rugged, so it is necessary to extend the RGM to simulate the remote sensing pixel leaving radiance of the vegetation canopy at a large scale with complex topography.

We have developed a new methodology (Huaguo HUANG, Min CHEN, Qinhuo LIU, et. al., IJRS V. 30, No. 20, 2009, 5421–5439):

(1) virtual forest scene generation combined with a digital elevation model;

(2) scene division method, shadowing effect correction and multiple scattering calculation;

(3) merging the simulated sub-scene bidirectional reflectance factors (BRFs) to get the whole-scene BRF.

(4)We have compared this new method with other models by choosing a large-scale conifer forest scene with a GAUSS terrain from RAMI3 (http://rami-benchmark.jrc.it).

(5)Multi-angle imaging spectroradiometer (MISR) data are used to validate the extended RGM in a Picea crassifolia forest area at a satellite pixel scale in the field campaign in Gansu Province, China.

Model validation using multi-angle imaging spectroradiometer (MISR) data

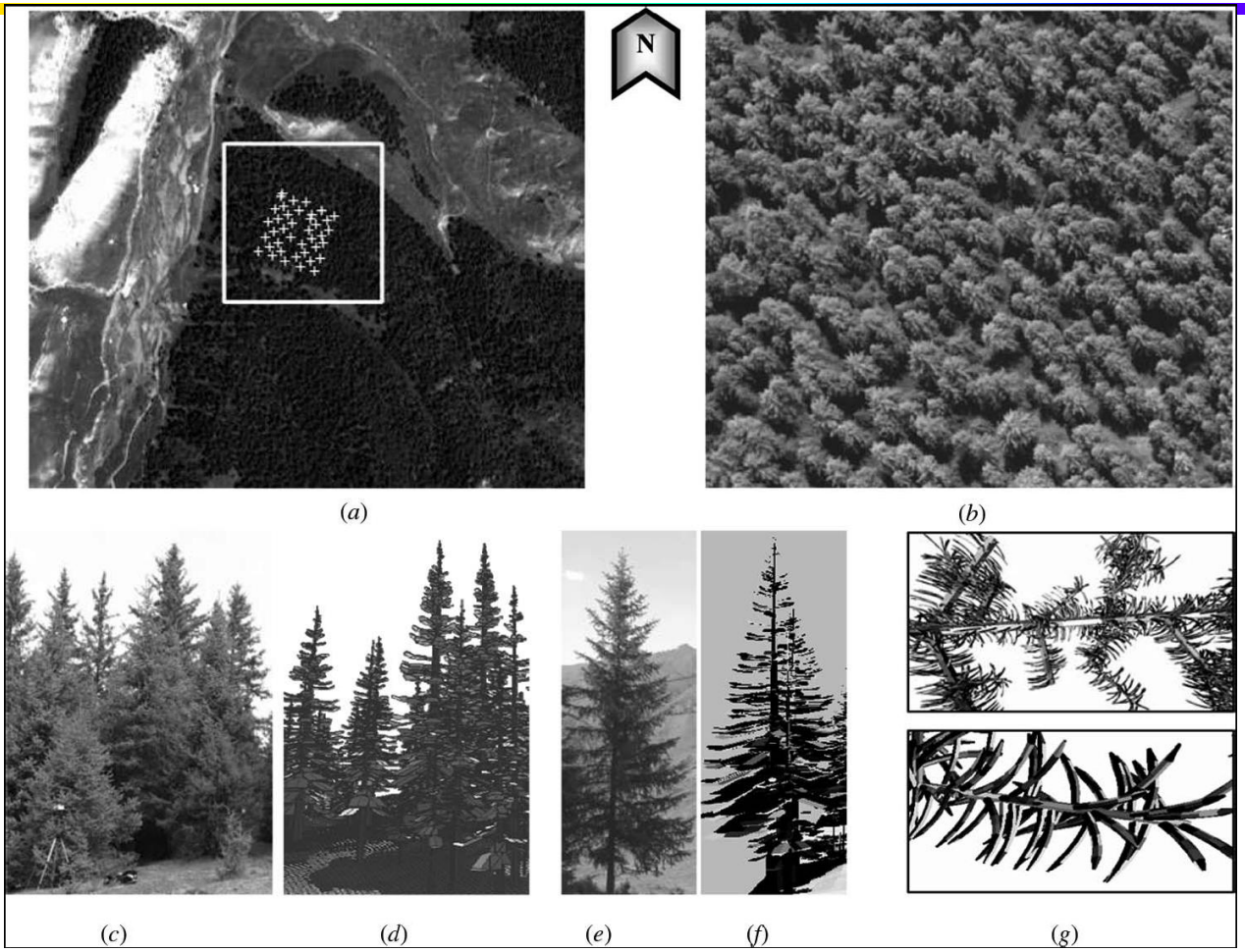

Spruce forest: (a) sample plot (white cross points) in an MISR pixel (white square box), (b) aerial photos of the spruce trees, (c) real trees, (d) virtual trees, (e) real-tree, (f) simplified virtual tree and (g) virtual branches and needles.

Model validation using multi-angle imaging spectroradiometer (MISR) data

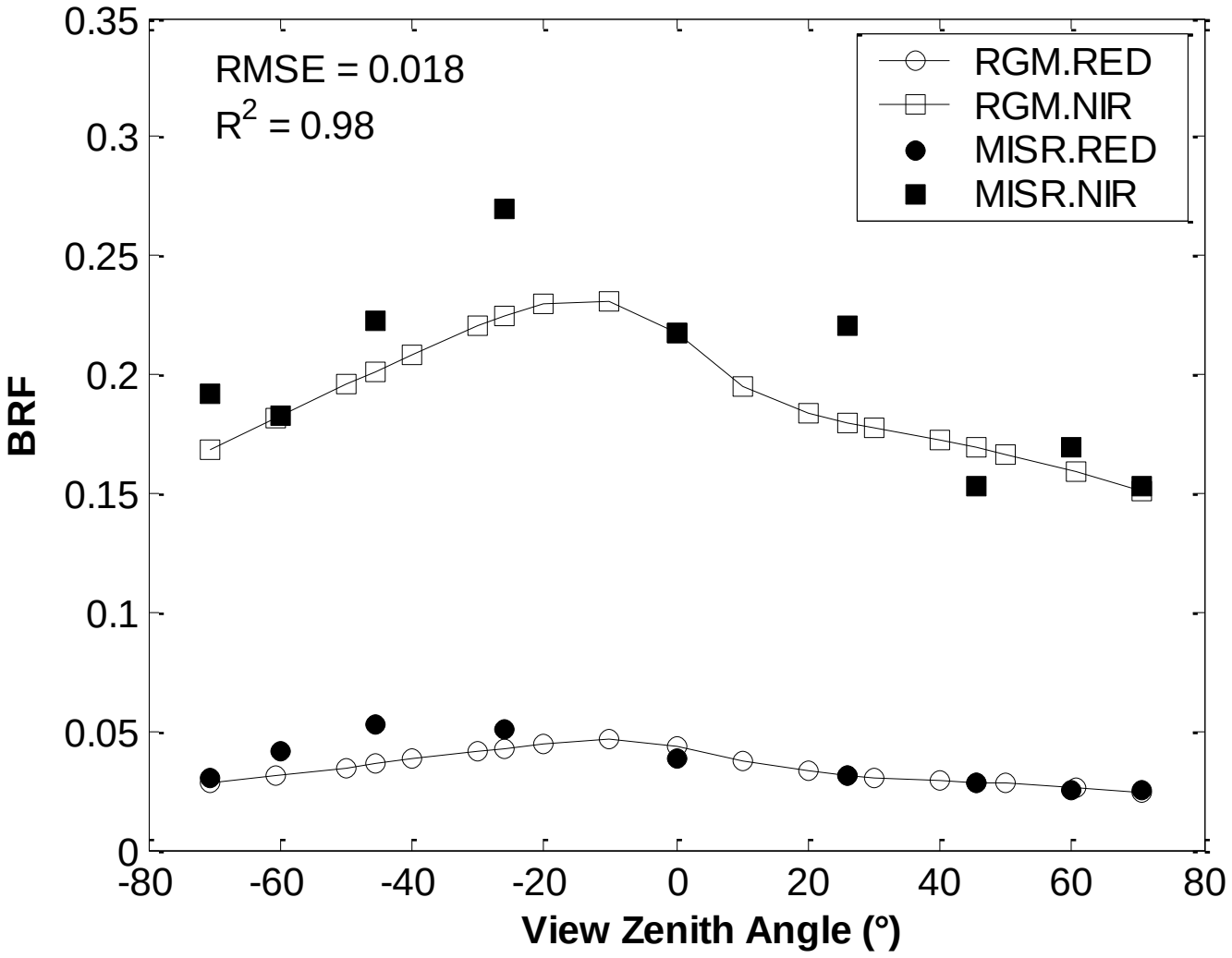

BRF comparisons between our extended RGM and other 3D radiative transfer models in RAM3

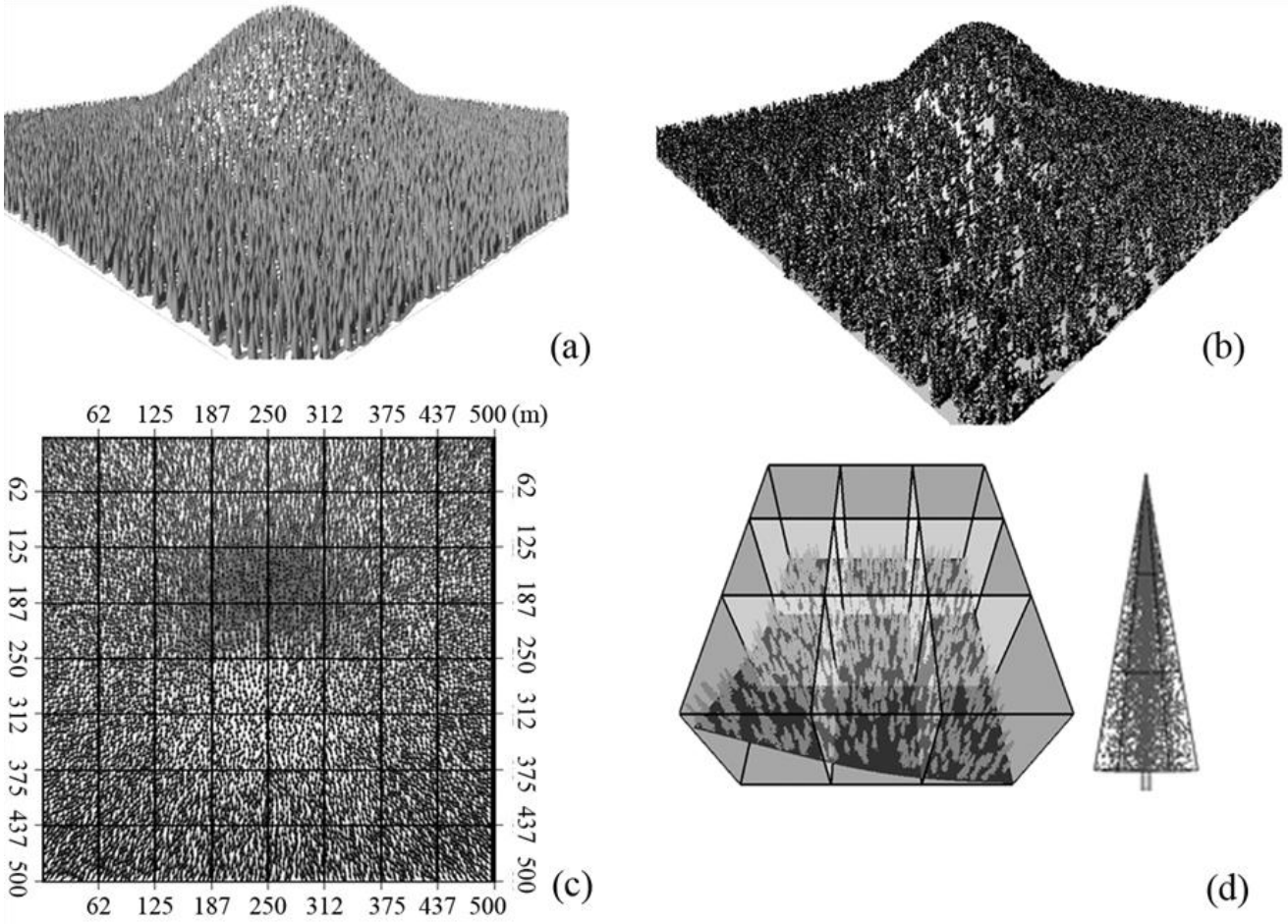

Conifer forest scenes: (a) from RAMI-3; (b) our simulated large forest scene; (c) The sub-division strategy for the whole forest scene; there are 36 sub-scenes, each (187.5m×187.5m) contains nine boxes with around 1400 trees in it; (d) a sample sub-scene and a single cone tree with leaf scatterers in it.

BRF comparisons between our extended RGM and other 3D radiative transfer models in RAM3

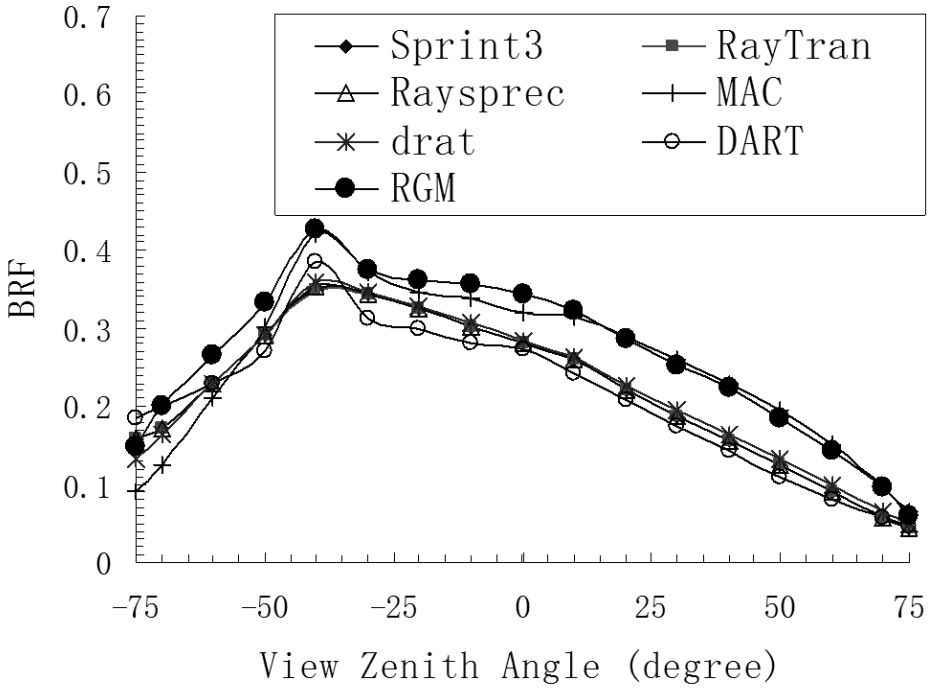

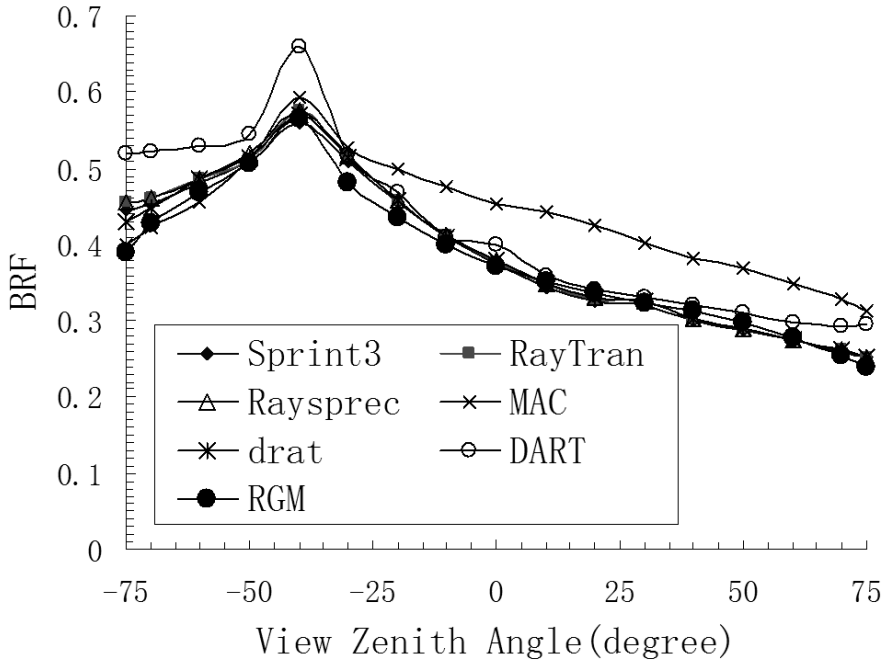

(a) the red band; (b) the NIR band.

Brief summery

A a sub-scene division algorithm based on RGM (Qin *et al.* 2000) as well as a method to generate large-scale virtual forest scenes is developed to simulate forest radiosity for large-scale forests under complex topographic conditions. The extended RGM sub-divides the whole forest landscapes into several smaller scenes, which can overcome the limitation of the maximum polygon number found in the original version of RGM.

③ TIR emission directionality modeling

Remote sensing Land surface temperature

- Instantaneous observation with continuous variation
- Directional effect (depends on view angle)
- Uncertainty (LST+Emissivity: ill-poised inversion problem)

Difficulties of TIR experiment

- Temporal scale effect (observation time)
- Heterogeneous surface (view field)
- Spatial scale different with satellite

TIR emission directionality observations

The vegetation TIR emission directionality is significant that have been observation by lots of field experiment（Fuchs et al. 1967）。

Bare soil （Lagouarde, 1995） Grass land (Chehbouni et al. 2001）
Sunflower （Paw U,1989）； Cotton (Kimes et al. 1980; Kustas, 1990)
Corn (Lagouarde et al. 1995)； Winter wheat （Qinhuo Liu, 2001）
Soy Bean （ Fuchs et al. 1967 、Nielsen,1984）

Needle leaf forest (Balick et al. 1986，Lagouarde, 2000)
Broad leaf forest（McGuire，1989）

Urban surface（Lagouarde et al. 2004)

The observed directional brightness temperature can vary up to 10K depend on the view angle 。

Directional measurement system is designed to observe the TIR emission directionality

- Coniometer system
- Computer control system
- ASD Spectrum Radiometer、Thermal Infrared Camera）
- Date processing

Directional Brightness temperature distribution

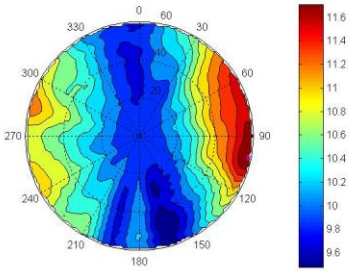

2001/04/21 08:00

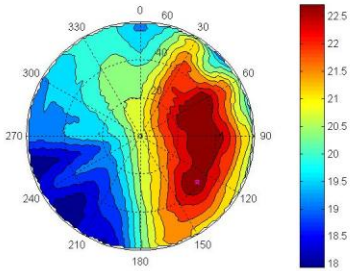

2001/04/21 10:00

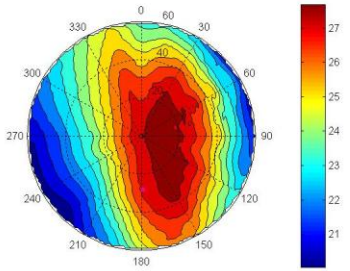

2001/04/21 12:00

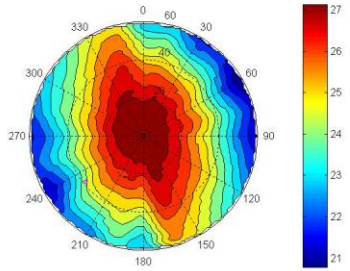

2001/04/21 14:00

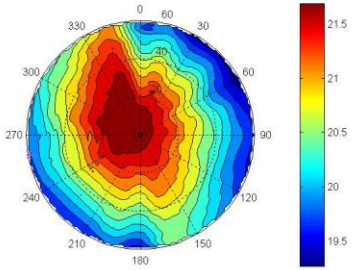

2001/04/21 16:00

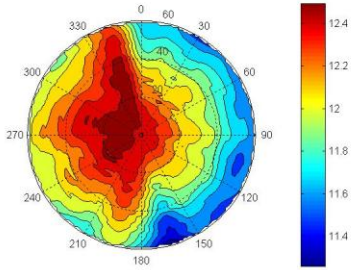

2001/04/21 18:00

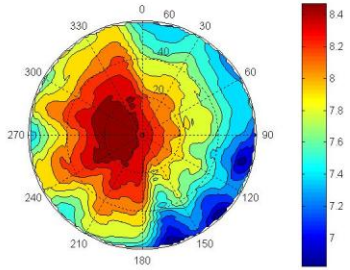

2001/04/21 20:00

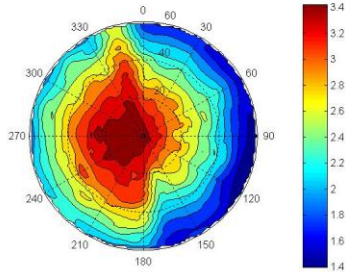

2001/04/22 00:00

"Hot Spot" Center varies as solar view angle

a. Soil-leaf-Ear canopy model (SLEC）for Thermal Emission Directionality

Experiment results:

- the sunlit and shaded ear have more than 3K temperature differences
- The directional emission brightness temperature of wheat canopy at tasseling stage can be more than 3-5K；

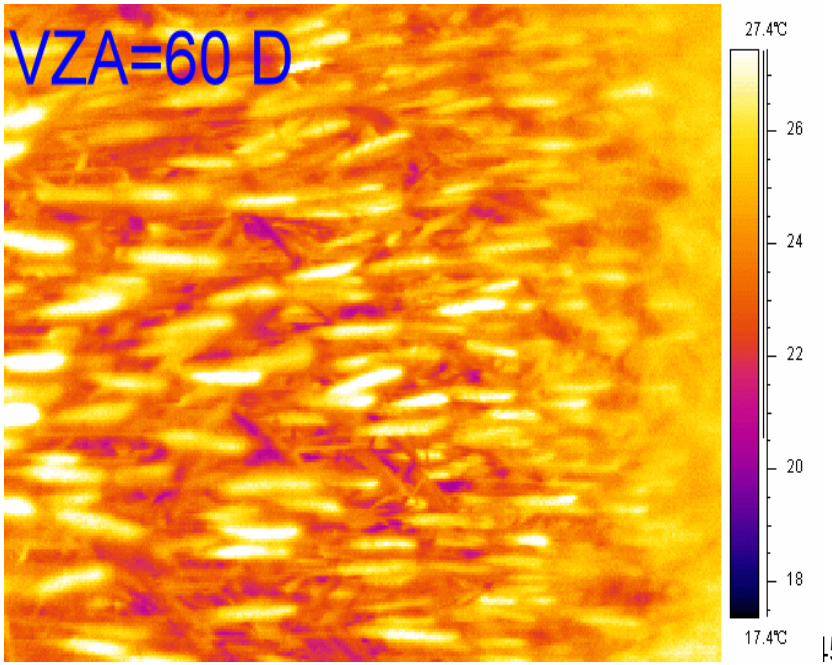

SLEC DBT model development:

How to calculate the view factor of ear ;

How to calculate the thermal radiation from ear, leaf and soil layers and the coupling effects;

How to express the directional emission characteristics of wheat canopy at tasseling stage.

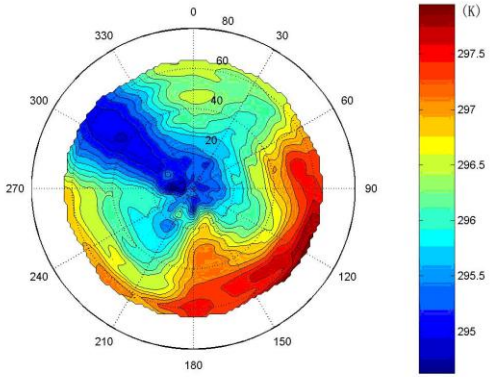

Measured DBT

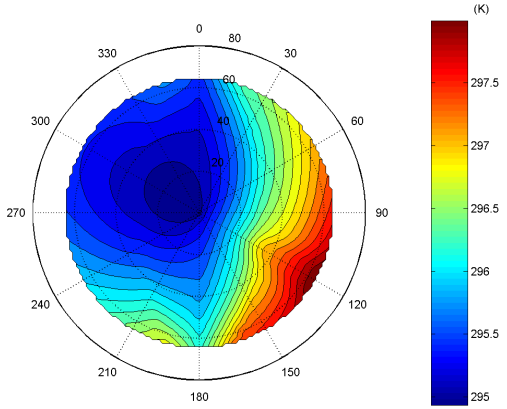

Model predicted DBT

Du, Y.M., Liu, Q.H, et. al. 2007. Modeling directional brightness temperature of the winter wheat canopy at the ear stage. IEEE TGRS, 45 (2): 3721~3739

b. Thermal Radiosity-Graphic combined model for Thermal Emission Directionality （TRGM）

RGM to TRGM

- **Expand RGM to TRGM by adding the thermal emission term in the model；**
- **Describe the relationship of DBT with the canopy structure, component temperature and emissivity；**
- **To calculate the multi-scattering effect to Thermal emission directionality；**
- **Coupling the TRGM and CUPID model to analyze the thermal emission directionality variation with the meteorological condition at different spatial and temporal scale, et.。**

Liu, Q.H., Huang, H et. a., 2007． An Extended 3-D Radiosity–Graphics Combined Model for Studying Thermal-Emission Directionality of Crop Canopy ． IEEE TGRS, 45(9)：2900~2918

RGM(Qin,2000) to TRGM(Liu, 2007)

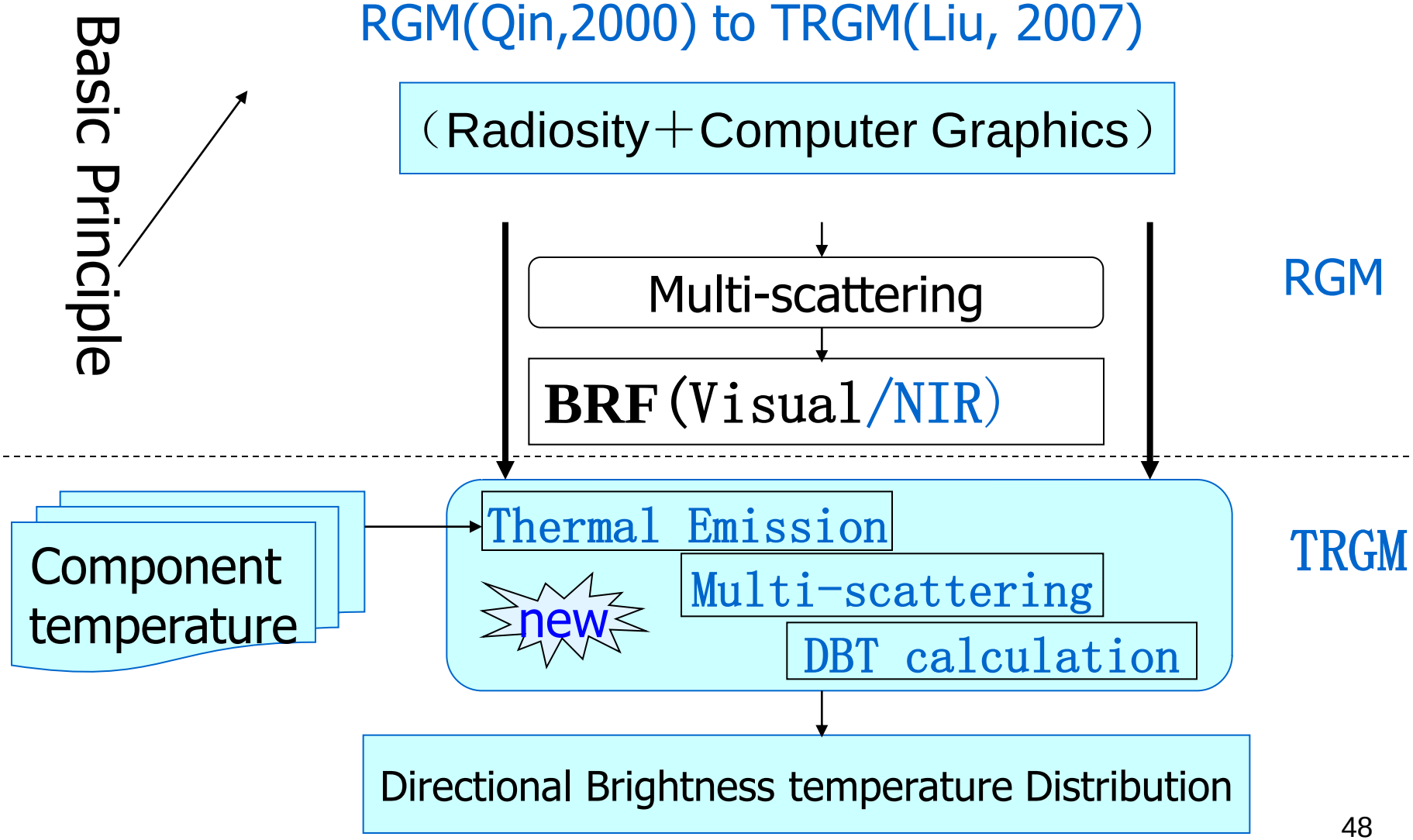

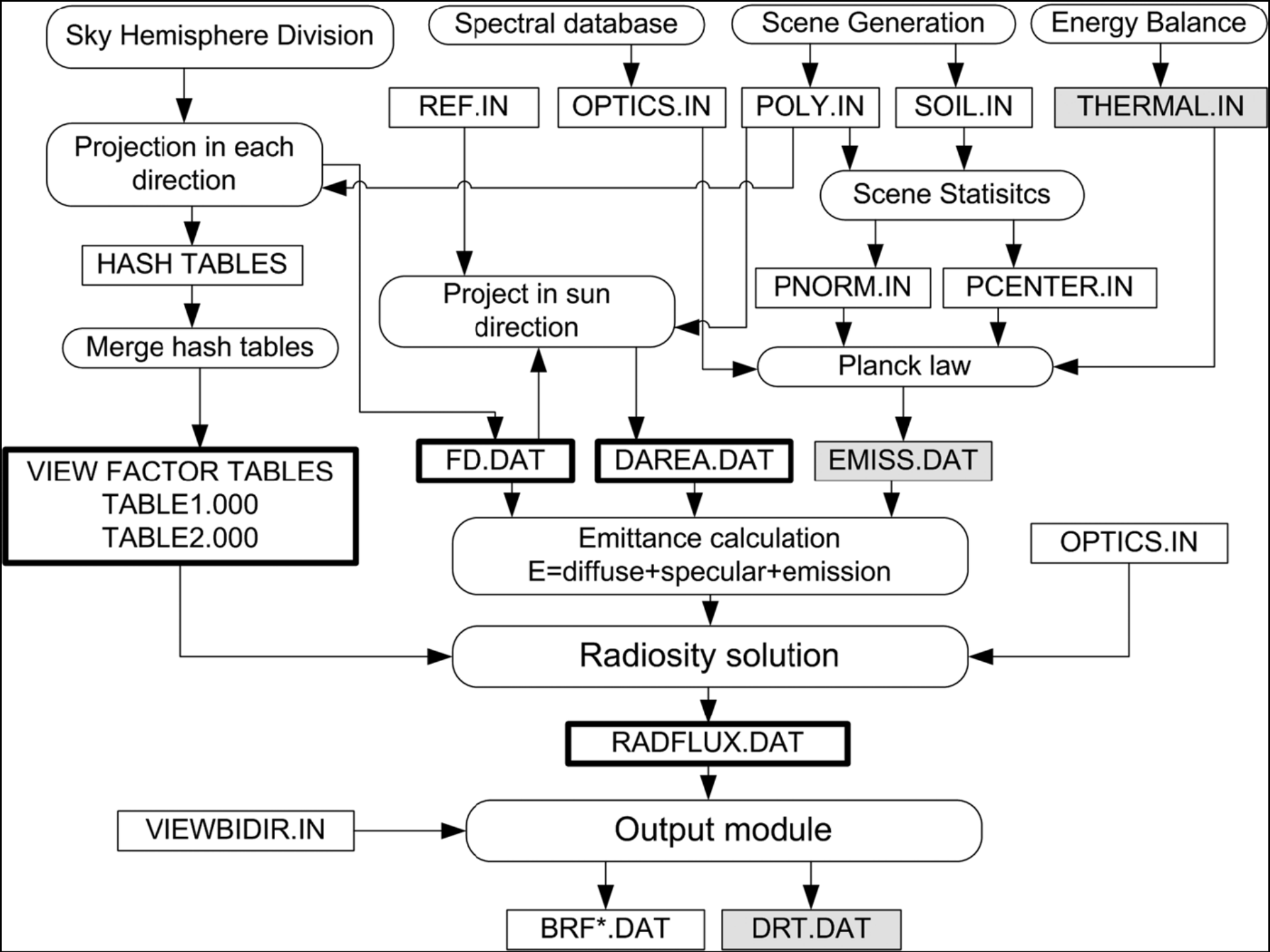
Sky Hemisphere Division
Spectral database
Scene Generation
Energy Balance
REF.IN
OPTICS.IN
POLY.IN
SOIL.IN
THERMAL.IN
Projection in each direction
Scene Statisitcs
HASH TABLES
PNORM.IN
PCENTER.IN
Project in sun direction
Merge hash tables
Planck law
VIEW FACTOR TABLES
TABLE1.000
TABLE2.000
FD.DAT
DAREA.DAT
EMISS.DAT
Emittance calculation
E=diffuse+specular+emission
OPTICS.IN
Radiosity solution
RADFLUX.DAT
VIEWBIDIR.IN
Output module
BRF*.DAT
DRT.DAT

TRGM model

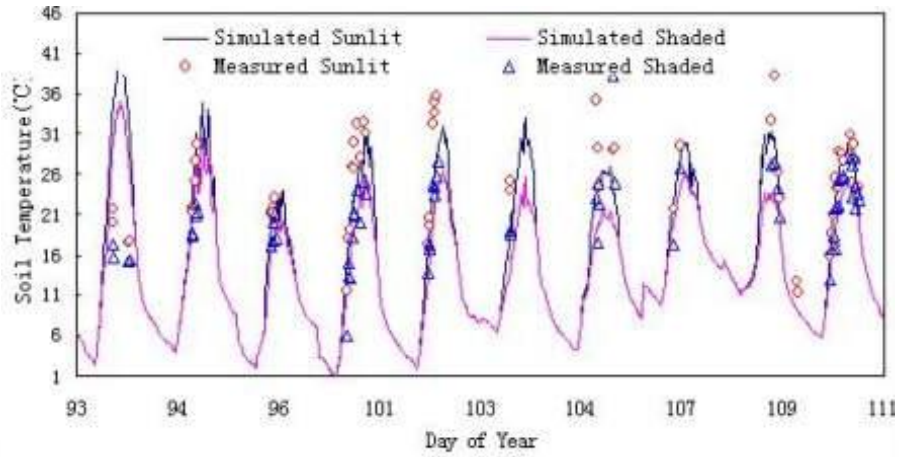

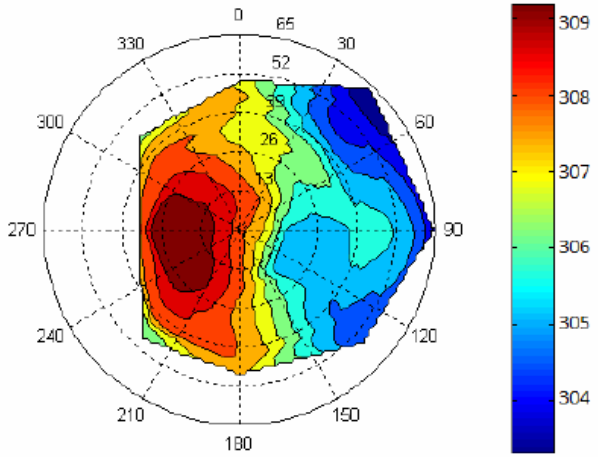

measurement

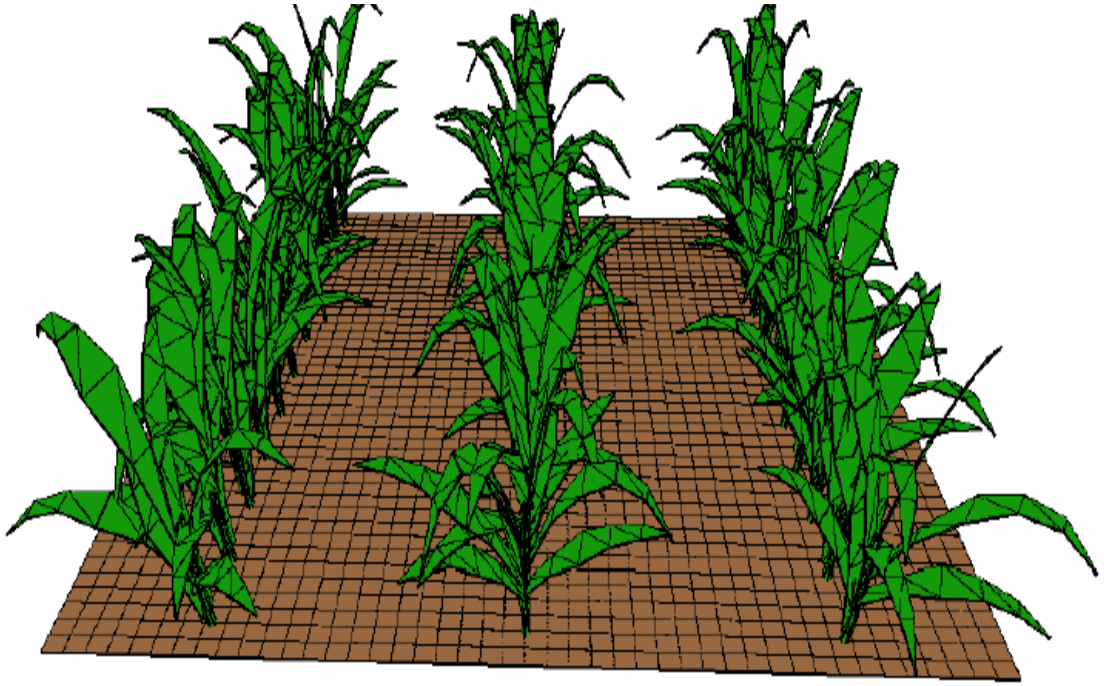

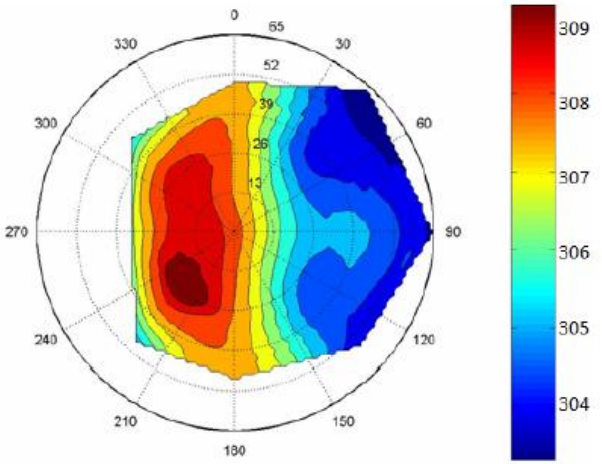

Model simulation

④Topographic effect modeling

Remote sensing radiation model for flat surface may have a significant error on radiatoin calculation, up to 900wm^{-2} when used at mountains area(Hansen et al. 2002)。

There are about 2/3 land of China is mountains area.

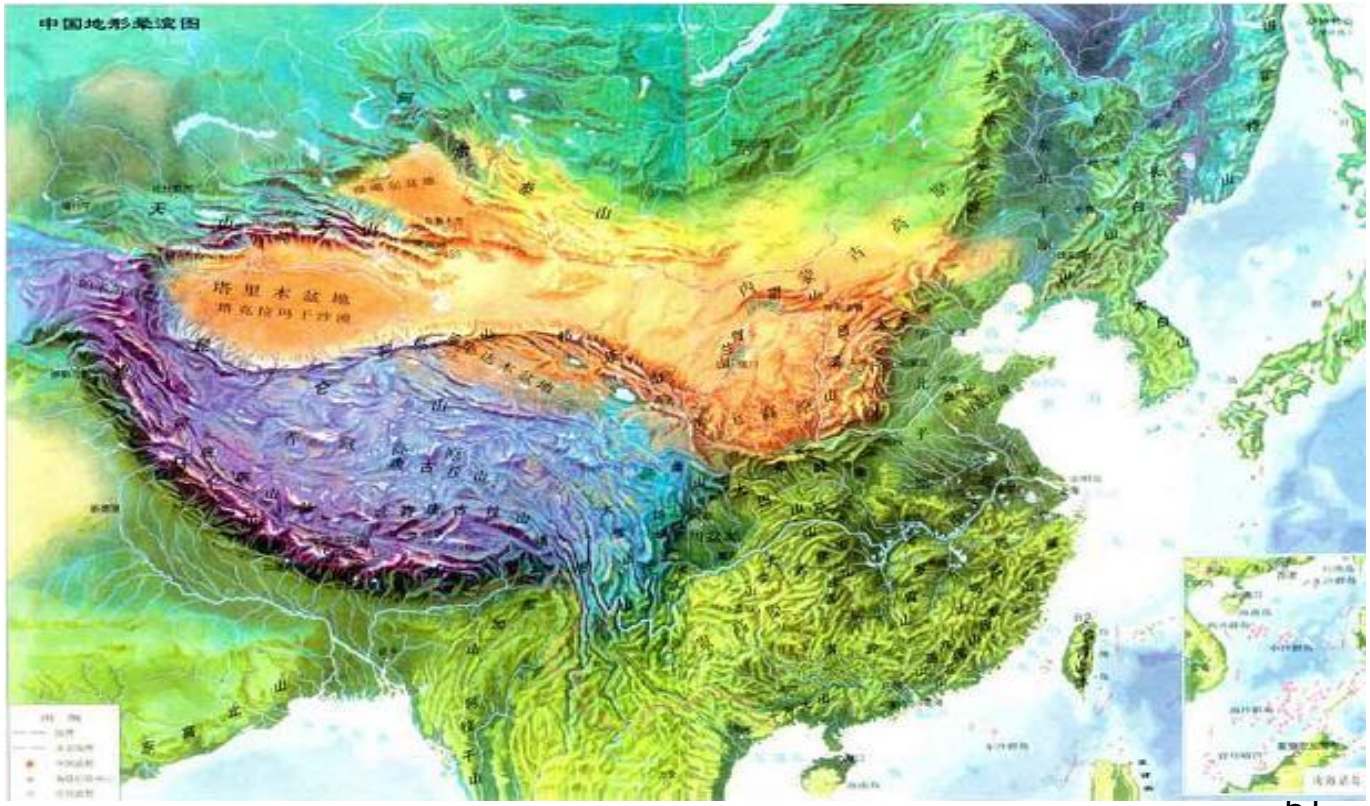

Topographic effects at mountains areas due to：elevation、pixel slope、in pixel slope；

The interaction of radiation transfer in mountains area：Atmospheric radiation, multi-scattering, shadow effects

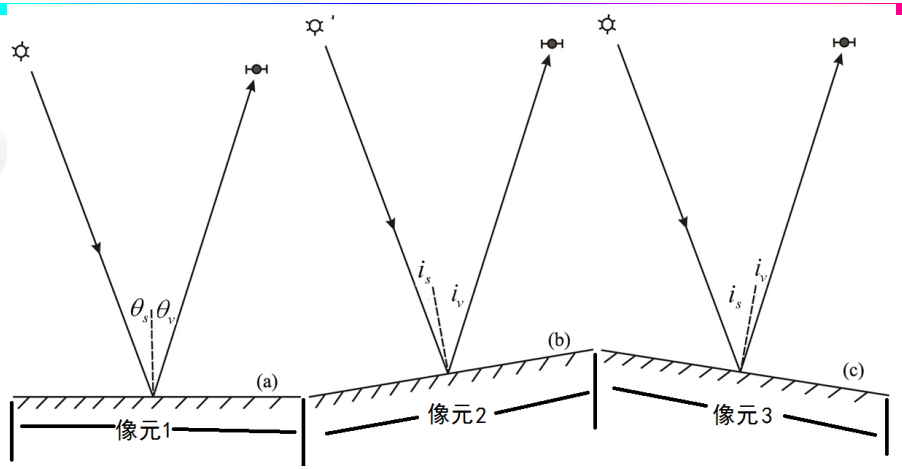

Slope at pixel scale

Existing models: solar radiation cosine correction, Lambertian radiation transfer models…

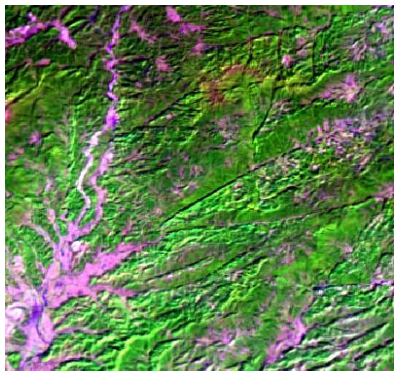

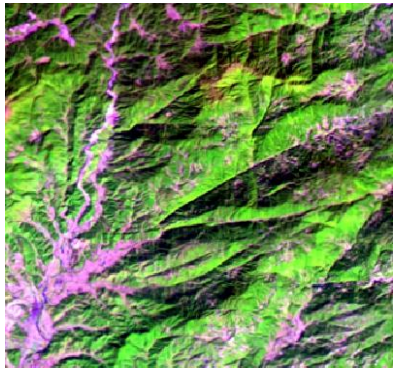

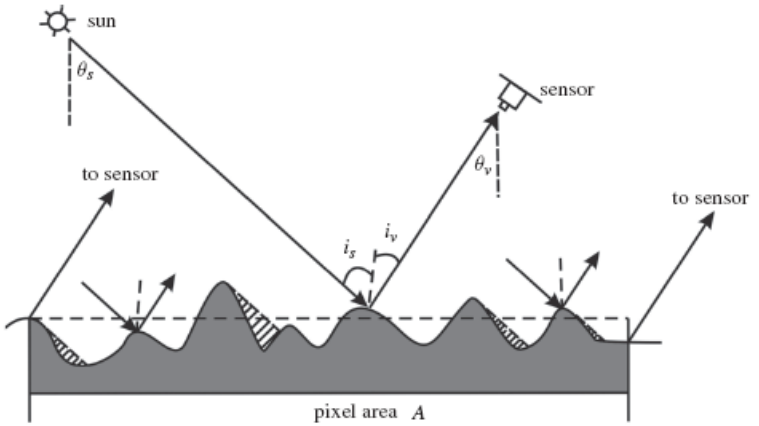

In pixel slop and shadow effects

☹ **Reflectance is over corrected!**

BRDF model for mountains area

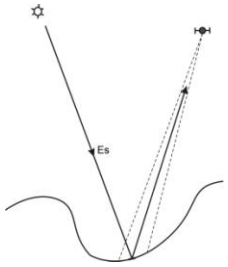

E_s^h

Solar radiaion

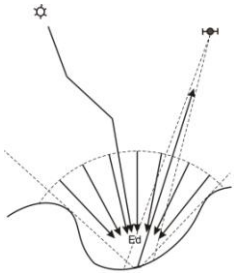

E_d^h

Diffuse radiation

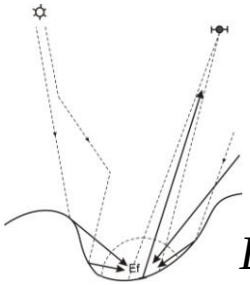

E_a

Neighbor effect

$$\rho_H(\theta_s,\varphi_s,\theta_v,\varphi_v)=\frac{\pi(L-L_p)e^{\tau/\cos(\theta_v)}}{\Theta\dfrac{(E_s^h+E_d^h K)\cos i_s}{\cos\theta_s}\dfrac{\Omega(i_s,\phi_s,i_v,\phi_v)}{\Omega(\theta_s,\varphi_s,\theta_v,\varphi_v)}+\dfrac{[E_d^h(1-K)V_d+E_a]}{\pi\Omega(\theta_s,\varphi_s,\theta_v,\varphi_v)}\int_{2\pi\pi/2}\int\Omega(i_s,\phi_s,i_v,\phi_v)d\Omega_{i_s}}$$

BRDF effect **H-D effect**

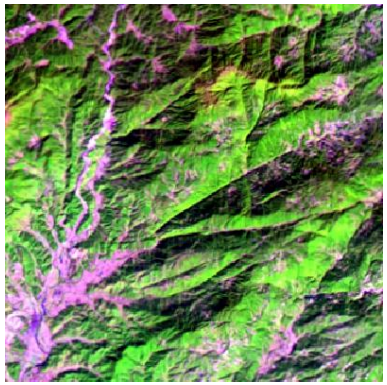

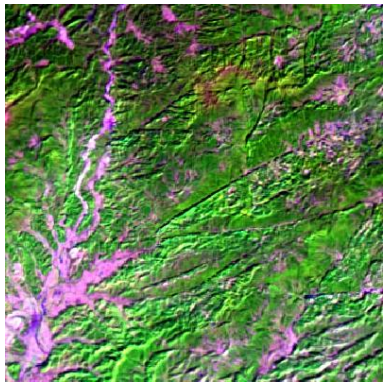

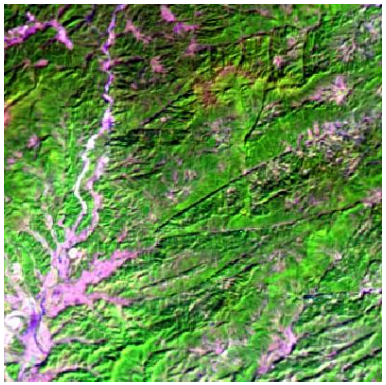

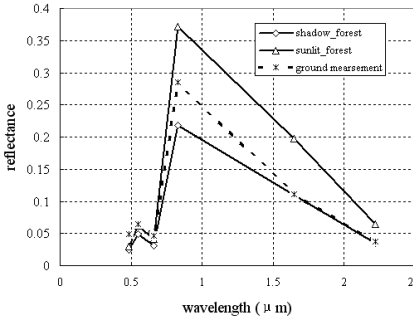

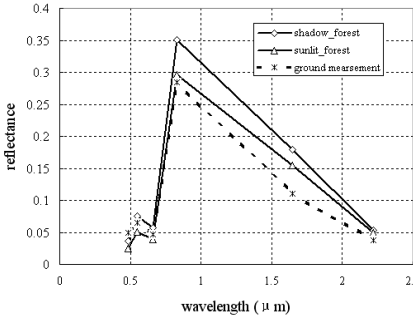

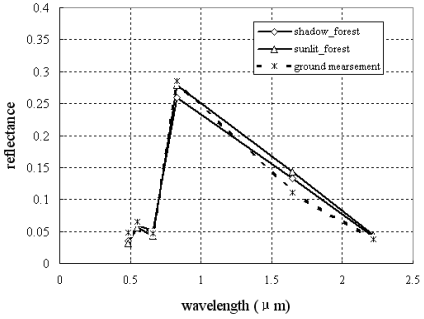

Atmos. correction **Radiation model** **New model**

（Huang,HB， Gong P et. al. IJRS 2008， Wen,JG, Liu QH，et. al, IJRS 2008）

⑤Remote Sensing Image simulation system

Remote sensing image simulation based on radiation transfer model coupling：land surface－atmosphere－sensor

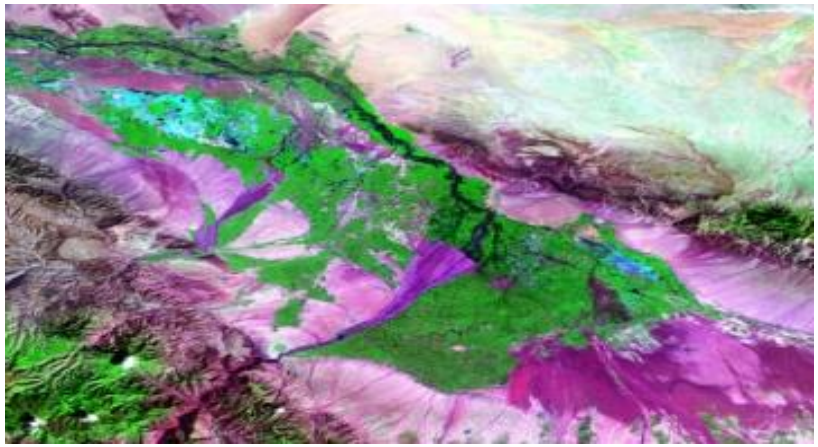

RS Image simulation technology development

phase	time	character	software
1	1960s	Physical simulation	ISF, Itek ,USA
2	1990s	Software: image to image simulation	PATCOD, LaRC
3	2000s	Simulation based on models	SENSOR; DIRSIG

Remote sensing image simulation systems are widely used in satellite remote sensing, including sensor design, system development and application demonstration:

- ✓**NEMO, OrbView-4, EO-1,**
- ✓ **WASP, MISI**
- ✓ **FIRES**

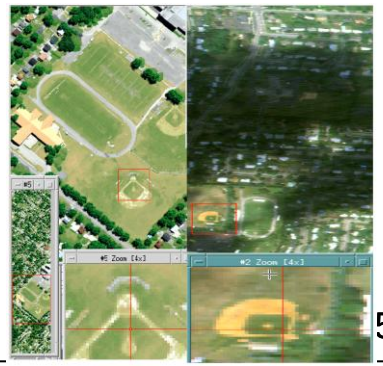

An optical remote sensing image simulation system has been developed:

Coupling the land surface radiation transfer models, atmospheric radiation transfer models, Remote sensor imaging models, and satellite orbiting models;

Ma, JW; Li, XW; et. al. IEEE TGRS 2006, Yang, GJ; Liu, QH;et. al. IJRS 2009

HJ1、CBERS03/04

- HJ-1A：CCD
- HJ-1B：CCD、IRMSS
- CBERS-03/04：Pan、Multi-spectrum，IR，WFI，MUX

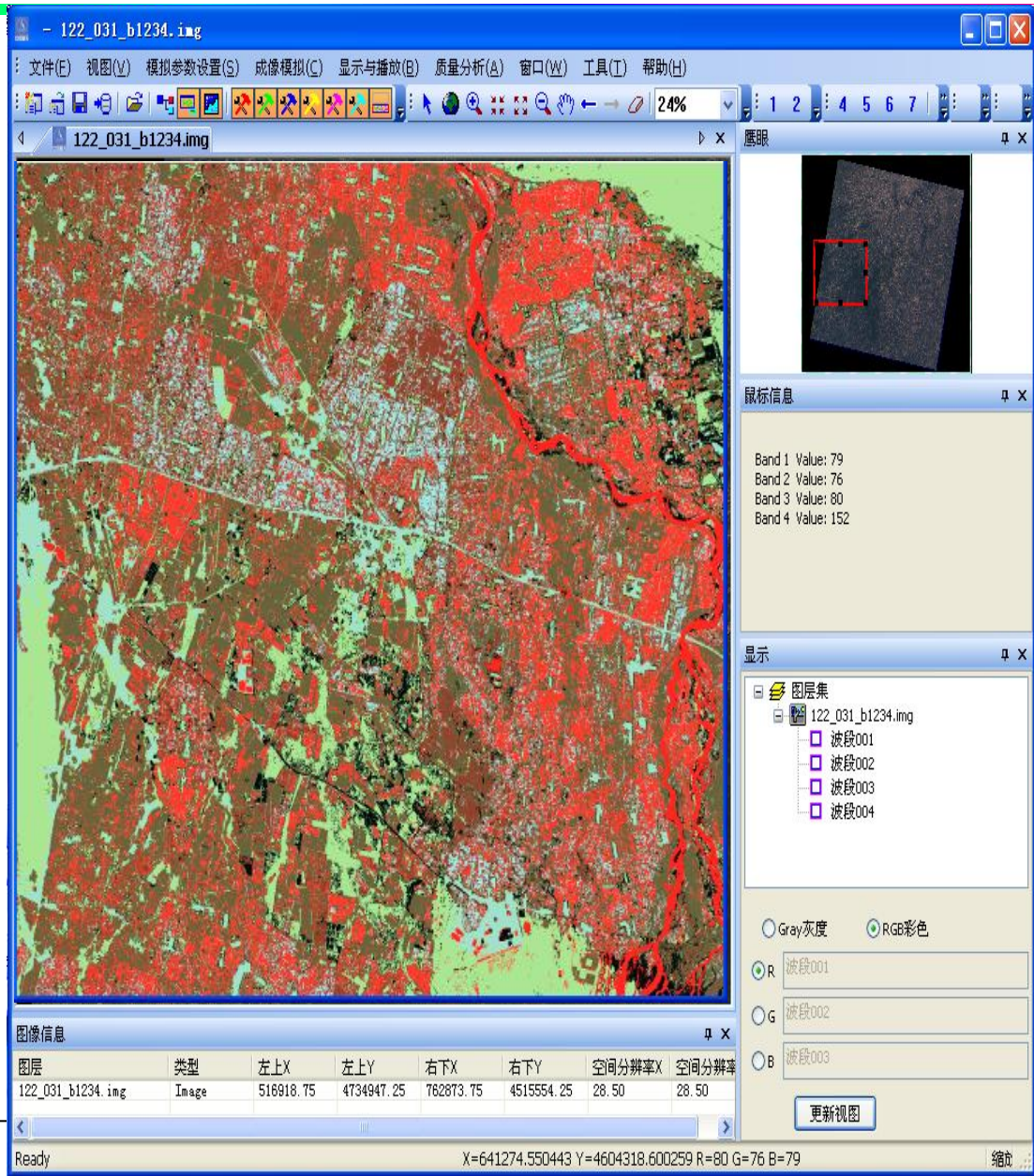

Simulated images at different view angles:

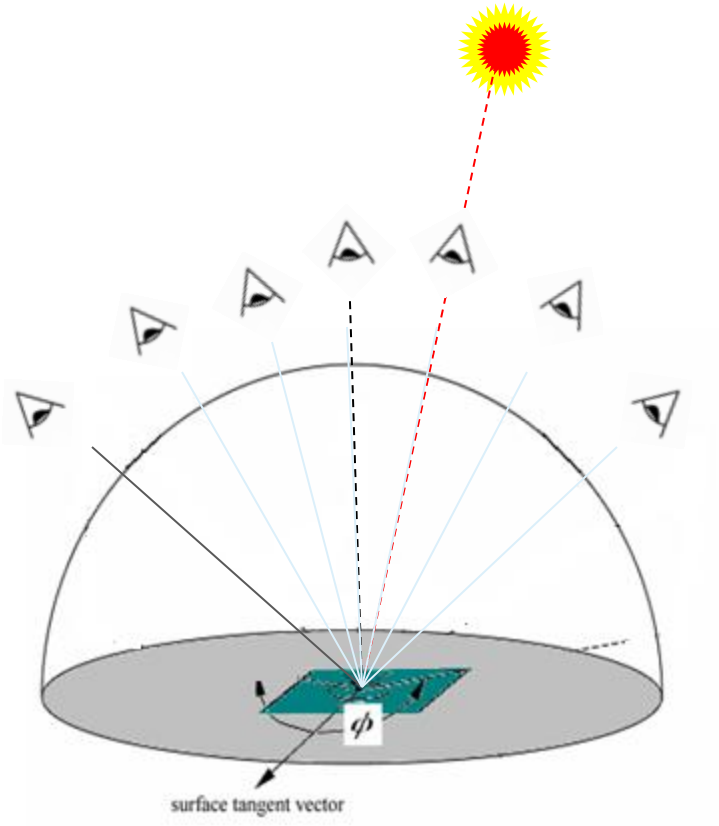

3. Land surface parameters inversion based on multi-source remote sensing data

(1) Introduction to HJ-1 Constellation

(2) Parameter Inversion algorithm development

(3) Model Assimilation for Environmental monitoring

(1) Introduction to HJ-1 Constellation

Not only in China, but also in the Asia and Pacific region or from the globe view:

Environment pollution and ecological destruction seriously affected sustainable development of economy and society: air, water, …

Natural disasters occur with great frequency, injuring or killing thousands and thousands of people and inflicting huge economic losses: earth quakes, volcano, floods, droughts, and forest fires

The application of remote sensing technology for disaster mitigation and environment protection is urgently needed both in China and in the world.

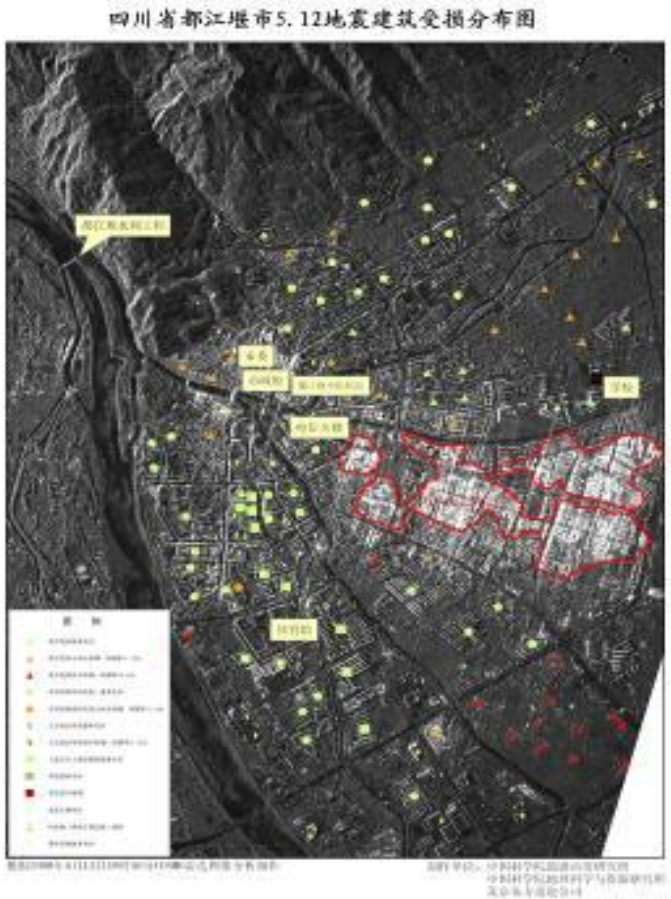

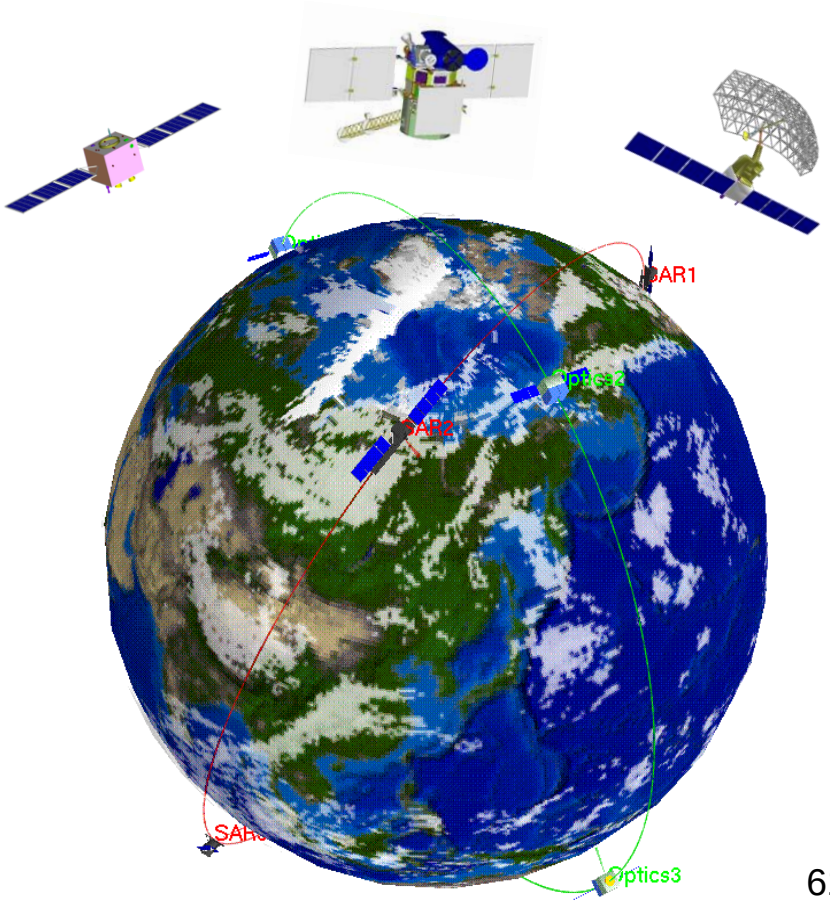

The requirements of monitoring of environment and disaster are very complicated. Although existing satellites have played an important role in the monitoring, but they cannot meet all the requirements.

- **spatial resolution**
- **spectral bands**
- **revisit interval.**

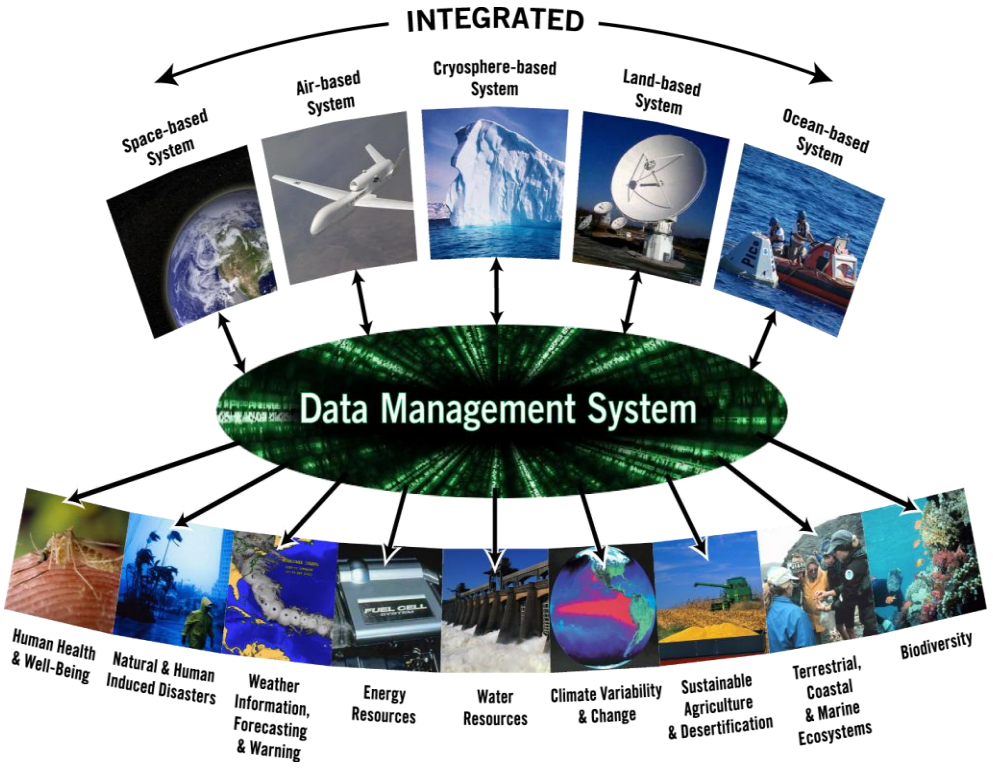

Only one satellite is not able to meet all the requirements.

	Revisit interval	Resolution (m)	Spectral bands (μm)	All weather
Flood	12h~2d	3~100	0.4~14, 3~21	need
Drought	1d~20d	3~100	0.4~14, 3~21	
Forest fire	6h~2d	3~300	3~5, 8~14	
Earthquake	6h~2d	3~100	0.4~1.1, 10~12.5	need
Sand storm	12h~2d	3~300	0.4~2.76， 8.0~14.0	
Storm tide	6h~2d	10~1000	0.4~1.1	need
Sparry flow	12h~2d	3~100		need
Bio-disaster	6h~10d	20~100	0.4~2.5, 8~14	
Environment pollution	1d~5d	3~500	0.4~0.9 high spectrum resolution, 3.5~14	
Environment event	4h~1d	3~100	0.4~0.9 high spectrum resolution, 3.5~14	
Red tide	4h~5d	20~50	0.52~0.6, 8.0~14.0	
Ecology	5d~60d	10~100	0.4~0.76, 1.55~1.75, 8.0~14.0	

a. Spatial resolution:

Although some large-scale phenomena observation can be monitored with low resolution remote sensor, most disaster and environment monitoring need middle-high resolution remote sensing data: from 3 to 100m will be needed.

b. Revisit interval:

The revisit interval needed for monitoring of disaster and environment are from hours to many days: flood, earthquake, forest and grass fire, plant diseases, and insect pests and pollution accident.

c. Large-scale:

Natural disasters and environment pollution often occur in a very large area: the wide swath is needed for most applications.

d. Multi-spectrum bands:

Multi-spectrum bands with high spectral resolution are needed to sense different surface characteristics of objects. Besides optical observation, microwave remote sensing is very important as well.

e. All weather observation:

Many natural disasters occur under clouds and at night. Visible optical observation only is not enough for monitoring of disaster and environment. Infrared remote sensing will be used day and night and microwave sensor will be very useful for observation through clouds and at night.

The Environmental Monitoring and Disaster mitigation small satellite constellation

The first stage (baseline) includes three satellites (two optical satellites and one SAR satellites): HJ1-1A, HJ-1B was launched on Sept. 6th, 2008, HJ1-C is to be launched on 2010.

And it is expected to expand to the second stage of eight satellites (four optical satellites and four SAR satellites): international cooperation.

Payload on HJ-1

a. Wide field multi-spectrum camera (WFC) on HJ1－A/B

Four bands from 0.43~0.90μm. The pixel resolution is 30m, the swath is about 720km.

b. Infrared scanner (IRS) on HJ1A

Four IR bands (from 0.75 ~12.5μm), three with 150m resolution, and the fourth 300m (10.5μm~12.5μm). The swath is 720km.

c. Hyper-spectrum imager (HSI) on HJ1B

118 bands (from 0.4 ~0.9μm), 100m resolution, the swath is 50km.

System Specification Outline

Item	Sub-item	Performance
Orbit	Type	Sun synchronous orbit
	Average altitude	~650km
	Local time at descending node	～10:45
Mass	Total mass	~450kg/460kg
	Payloads	147kg/157kg
Satellite body size	Satellite body size	1200×1100×980mm^3
	Maximal envelope	Φ1900mm×1200mm
WFC	Spectral band	4
	Ground pixel resolution	30m
	Swath width	720km
IRS	Number of spectral band	4
	Ground pixel resolution	150m/300m
	Swath width	720km
HSI	Number of Spectral band	118
	Resolution/Swath	100m/ 50KM
Data transmission	Frequency band	X
	Storage capacity	8Gbit
	Data rate	~70Mbps or 57Mbps
AOCS	Three-axis stabilization	
TT&C	System	S-band unified system
	orbit measurement system	GPS
OBDH		
Power supply	Solar array area	5.66m
	Output power	BOL 618W/ EOL 554W
Thermal control	Mode	Passive thermal control accompanied with active
	Inside the module	0～+45°C
Lifetime	3 years	

e. Synthetic aperture radar (SAR) on HJ-1C

Main Payload Specification of SAR

Operation mode:	single mode
Ground resolution:	30m
Imaging Width:	100km
Operation band:	S
Polarization:	HH or VV
Angle of incidence:	25°-47°
Size of antenna:	6m×2.8m
Bit rate:	280Mbps
Onboard operation time:	10min/orbit

Environment Application System

To establish national satellite monitoring and forecasting center and form the capacity to produce environmental remote sensing products and process all kinds of environmental data from disaster and environment monitoring satellite constellation and other satellite system.

To provide remote sensing information service, remote sensing data products and decision-making support.

Concluding Remarks

Disaster mitigation and environment protection is urgently needed in the world.

A small satellite constellation composed of optical satellites and synthetic aperture radar satellite(s) can meet the basic requirement of monitoring of disaster and environment.

Although the Baseline will be constructed by China, the international cooperation is the best way for construction and utilization of the whole constellation.

(2) Parameter Inversion algorithm development

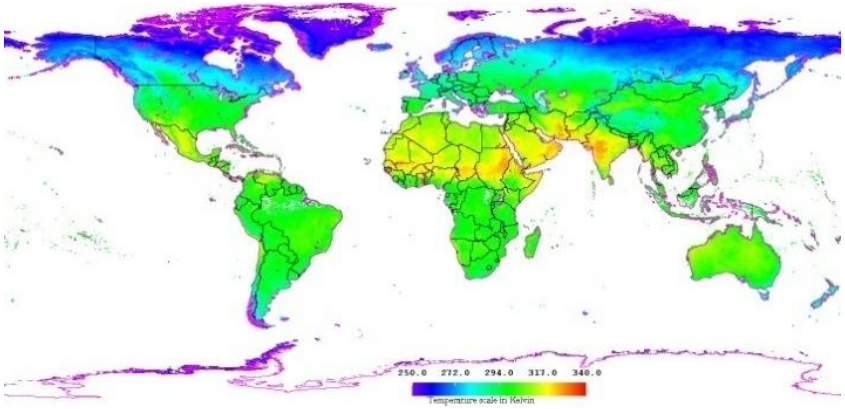

Preprocessing

Calibration corretion
Geometric correction
Cloudy mask
Atmospheric correction

Qualitative application: Classification and identification

Quantitative Monitoring: Inversion

Prediction : assimilation

Information extraction

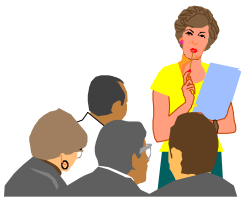

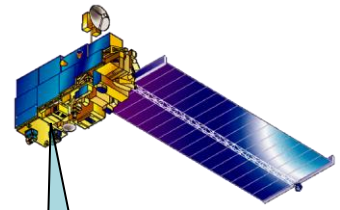

Product design

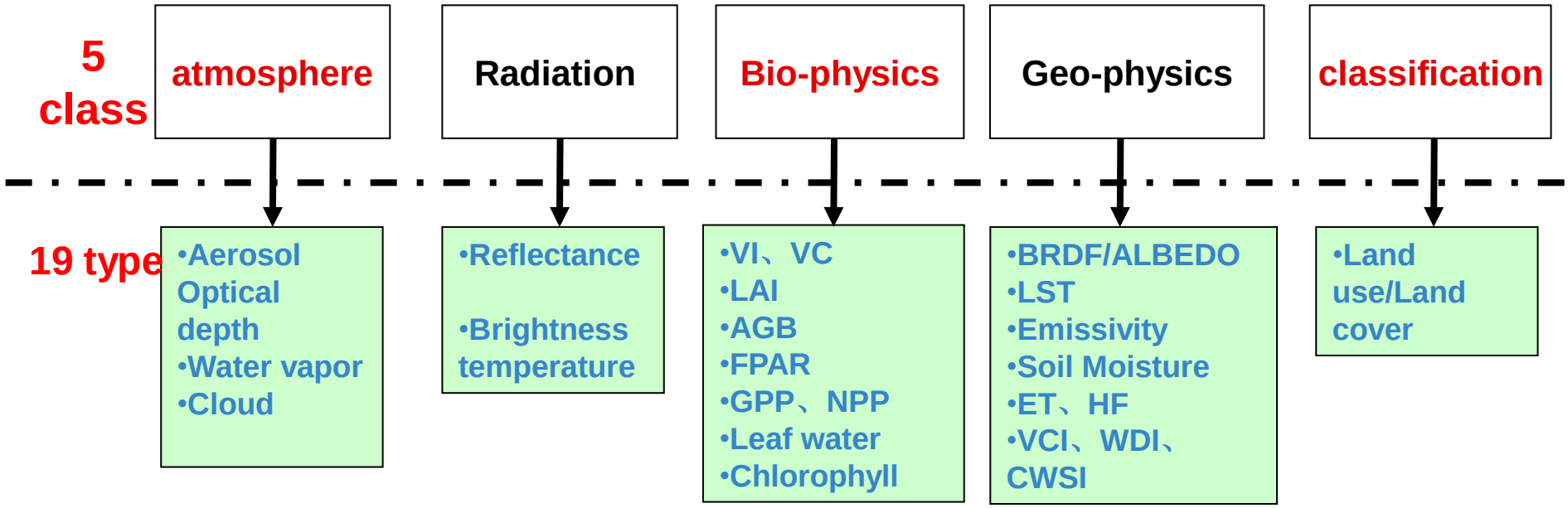

2007－2010， National Key Project of Scientific and Technical Supporting Programs(2008BAC34B03, 4.44 million Yuan) : Environmental Parameter Inversion and Assimilation using Environmental and Natural Disaster Monitoring Small Satellite Constellation and other multi-source data

① Pre-processing

calibration

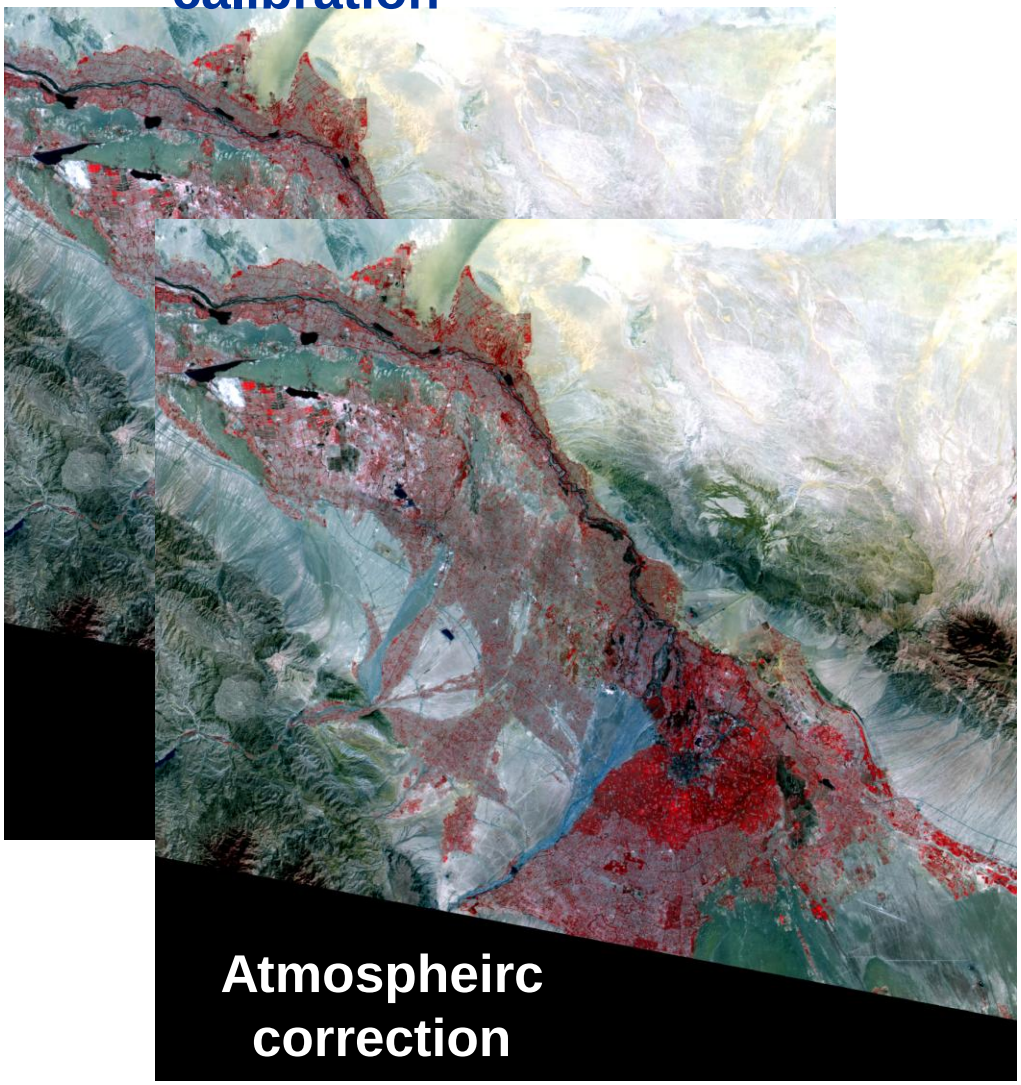

Azimuth angle

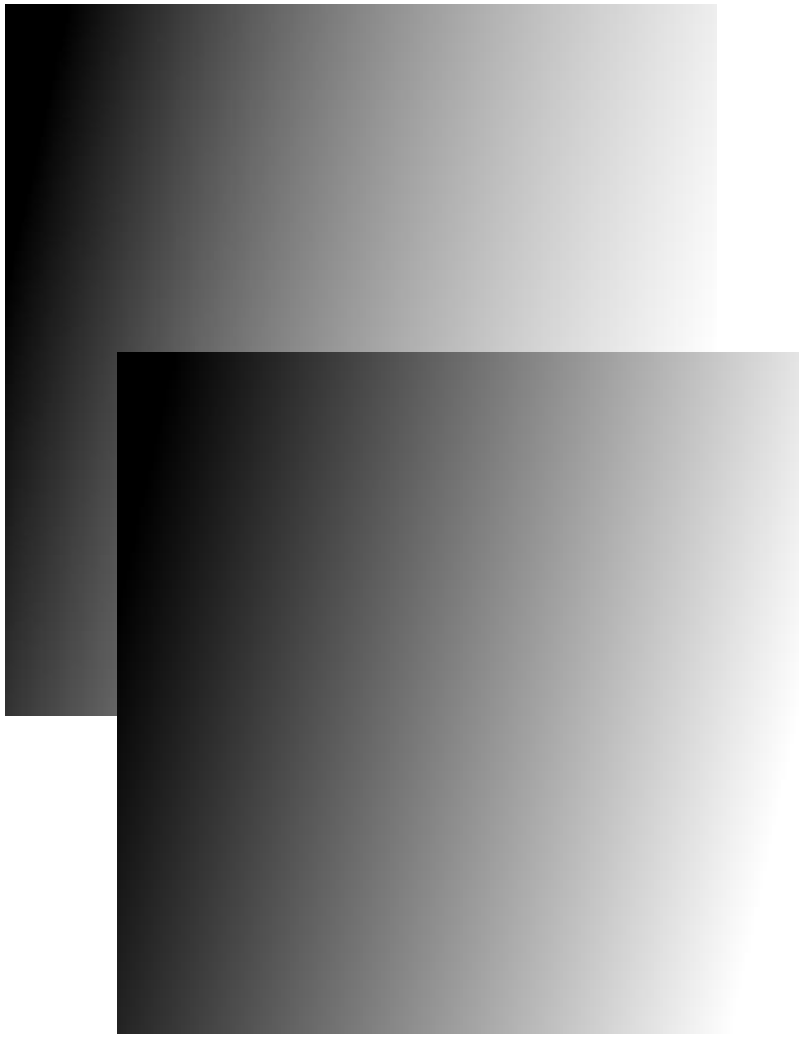

View zenith angle

② Classification for land use

1、Land cover classification

7 classes, 23 sub-classes。

2、ecological system classification

6 class ecosystems

一级类型	一级编码	二级类型	二级编码	含　义
森林	1	常绿针叶林	11	郁闭度>30%，高度>2 米的常绿针叶天然林和人工林
		常绿阔叶林	12	郁闭度>30%，高度>2 米的常绿阔叶天然林和人工林
		落叶针叶林	13	郁闭度>30%，高度>2 米的落叶针叶天然林和人工林
		落叶阔叶林	14	郁闭度>30%，高度>2 米的落叶阔叶天然林和人工林
		针阔混交林	15	郁闭度>30%，高度>2 米的针阔混交天然林和人工林
		灌丛	16	郁密度>40%，高度>2 米的灌丛和矮林

一级类型	编码	含　义
森林生态系统	1	森林（主要有热带雨林、常绿阔叶林、落叶阔叶林、针叶林等）生态系统分布在湿润或较湿润的地区，其主要特点是动植物种类繁多，群落的结构复杂，种群的密度和群落的结构能够长期处于较稳定的状态，尤其是热带雨林生态系统。森林中的植物以乔木为主，也有灌木和草本植物。
草原生态系统	2	草原生态系统分布在中纬度的大陆内部、干旱、年降雨量少地区，面积大约占全球陆地总面积的 1/5。动植物的种类比森林少，植物以多年生草本植物为主，其中以禾本科、豆科和莎草科植物占优势；

Change detection software development

Change detection based on the existing land use map and new remote sensing Image

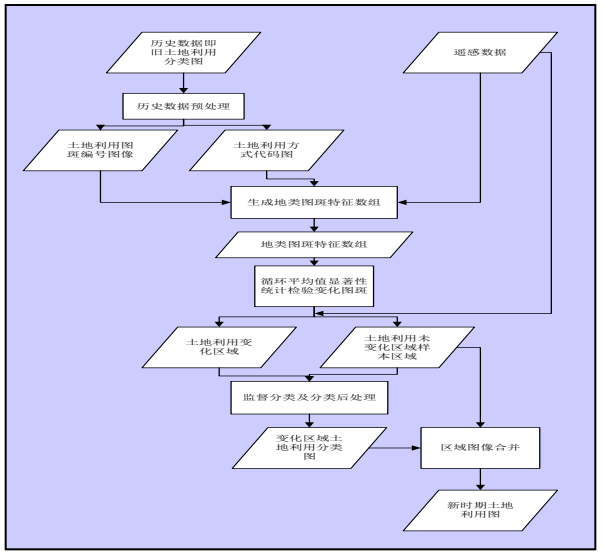

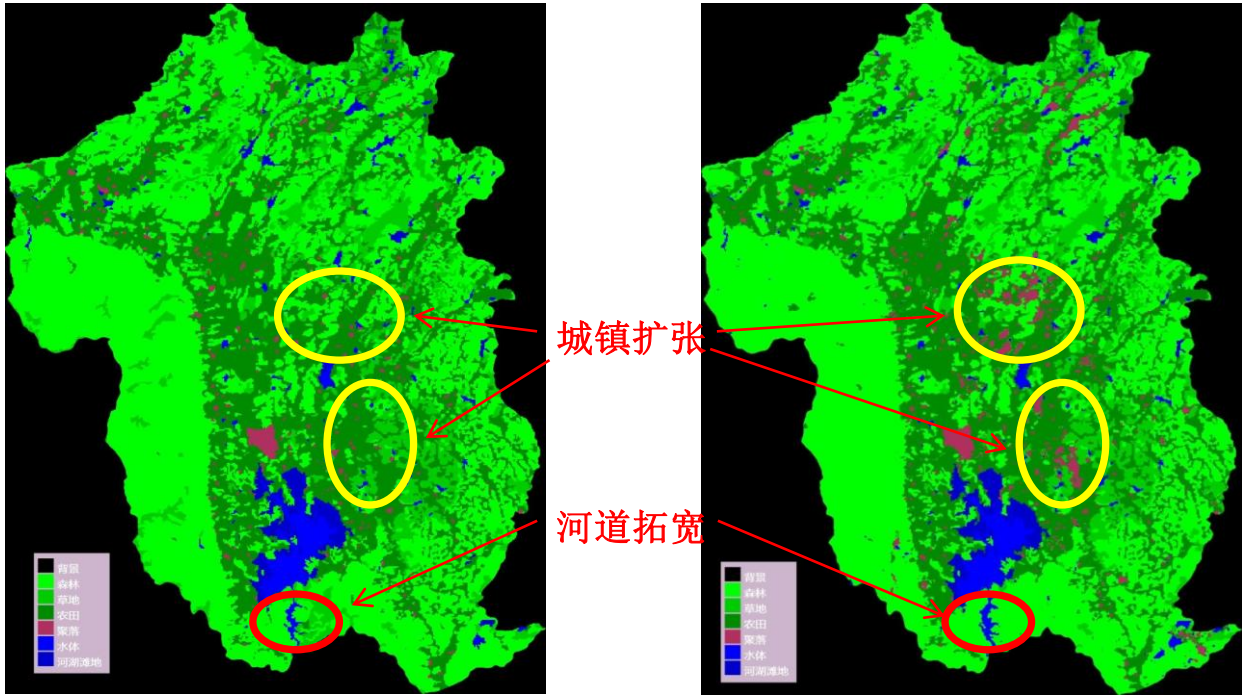

黑河地区土地覆盖分类图

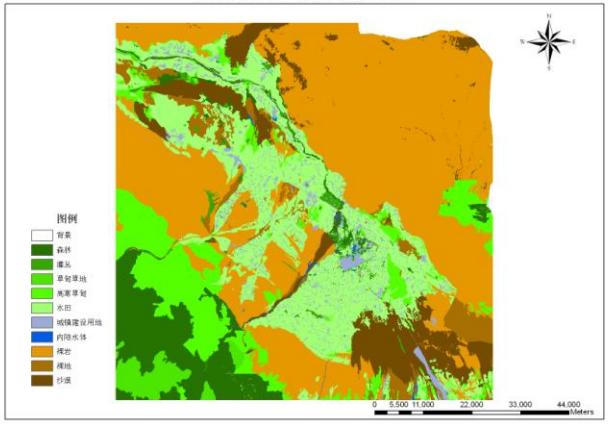

③ aerosol optical depth inversion algorithm

a. MODIS aerosol optical depth （500m）

b. HJ-1 AOD algorithm supported by MODIS

a. MODIS Aerosol Optical Depth product（500m）

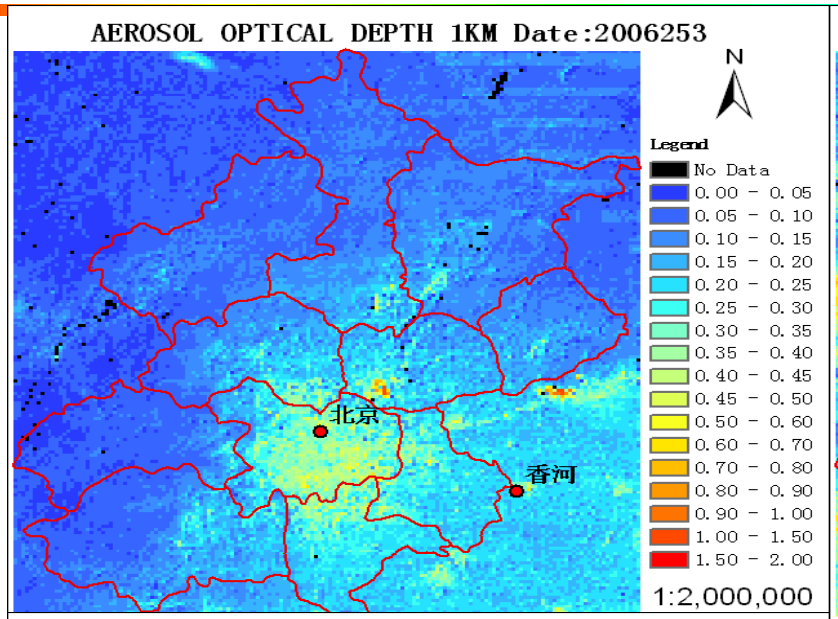

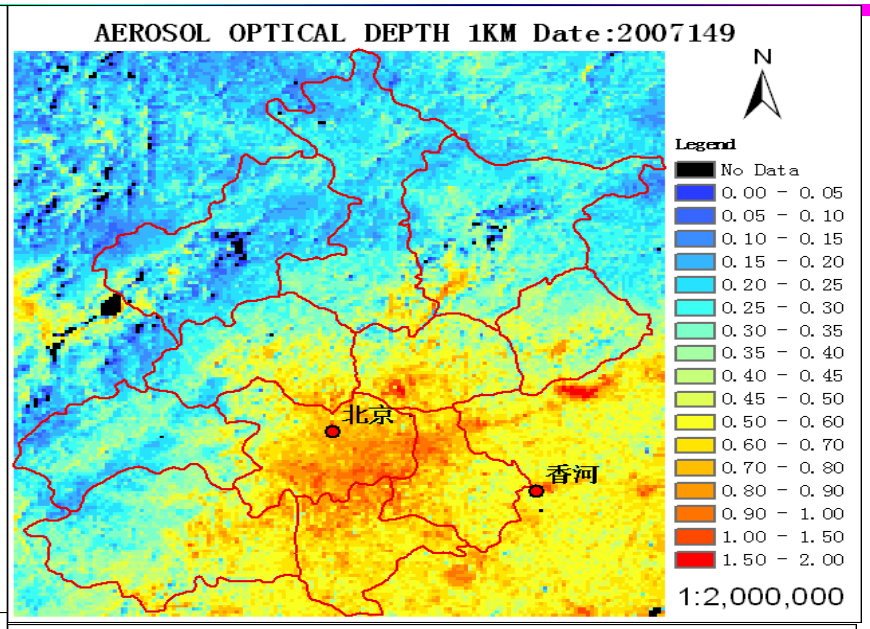

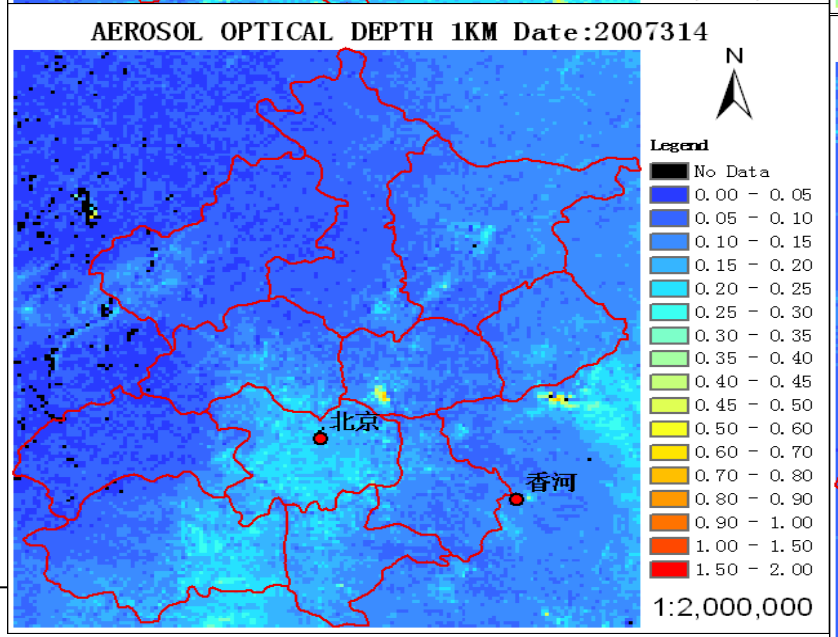

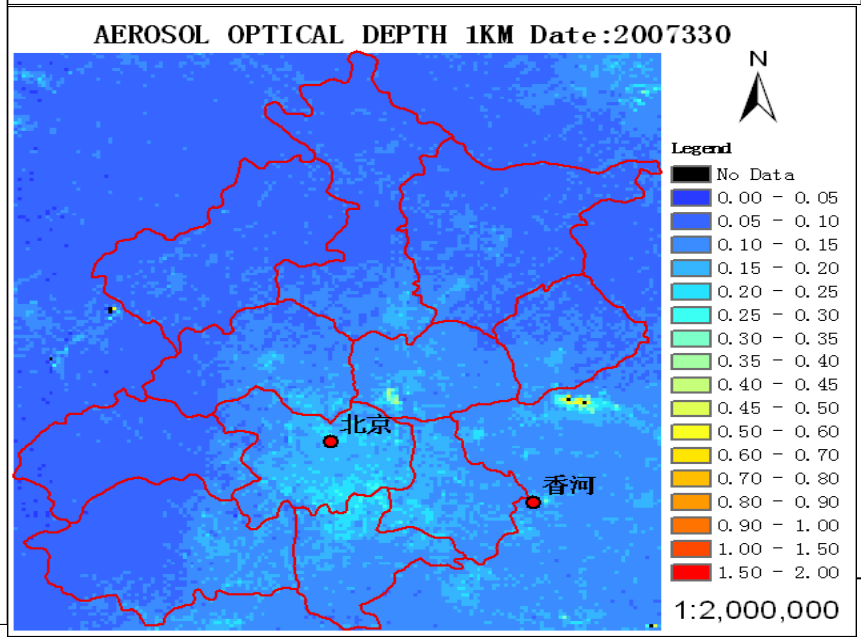

MODIS AOD ACCURACY

date	Beijing			xianghe		
	AERONET	MODIS	error	AERONET	MODIS	error
2006253	0.2015	0.3268	0.1253	0.2425	0.2292	0.0133
2007129	0.3255	0.4696	**0.1441**	0.3253	0.4039	0.0786
2007134	0.1979	0.2914	0.0935	0.1655	0.2508	0.0853
2007149	-	-	-	0.4744	0.6008	0.1264
2007289	0.1528	0.1928	0.0400	-	-	-
2007305	0.0991	0.1582	0.0591	0.1515	0.1010	0.0505
2007307	0.0825	0.1083	0.0258	0.1448	0.0998	0.0450
2007314	0.1648	0.1722	**0.0074**	0.0949	0.1040	0.0091
2007330	0.1587	0.1825	0.0238	0.1746	0.1419	0.0327

The accuracy is about 0.1.

HJ-1 CCD AOD supported by the MOD09

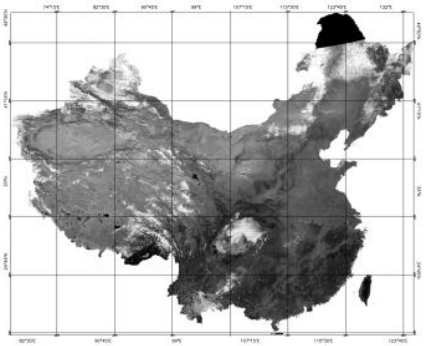

Reflectance (MOD09)

projection

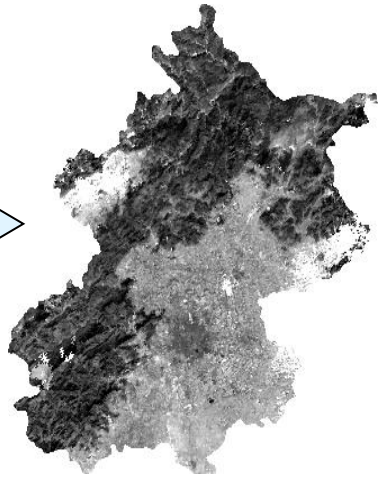

MODIS Reflectance
（500 m）

inversion

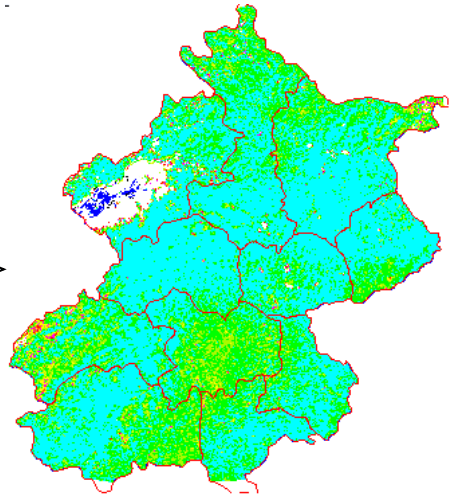

HJ-1 CCD AOD
（500m）

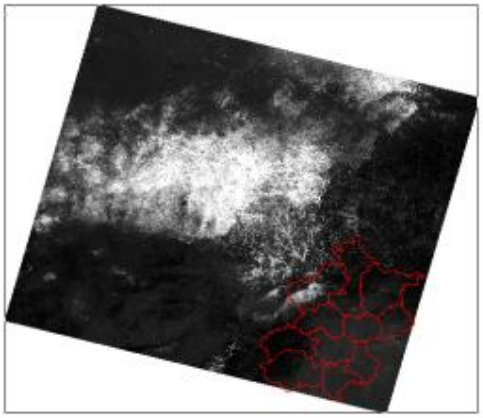

HJ-1 CCD

projection

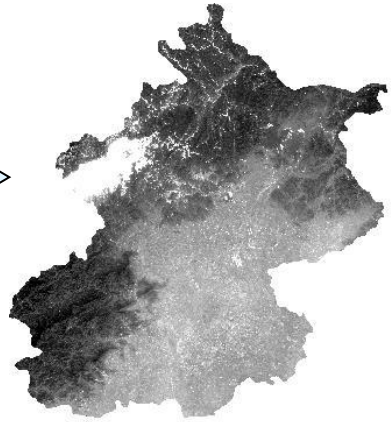

Reflectance of HJ-1 CCD (500m）

HJ-1 CCD AOD of Beijing

2008.12.25

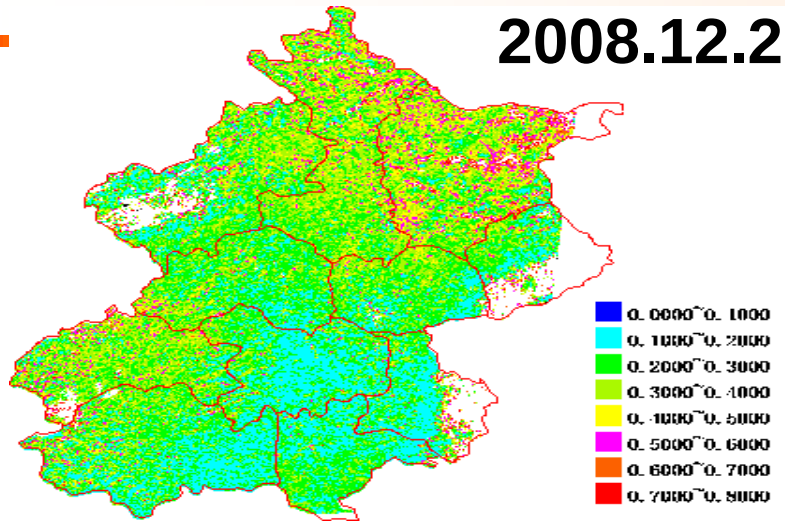

2008.12. 22

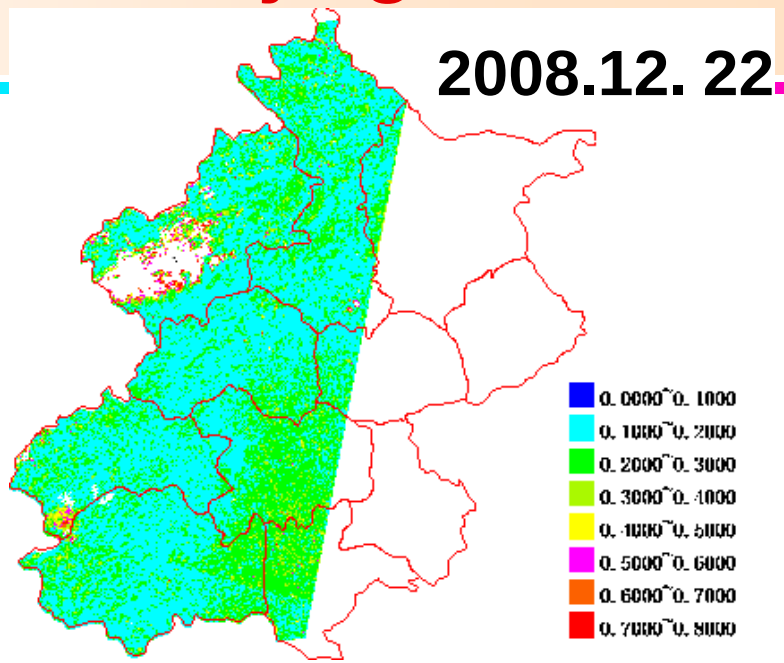

2008.12.20

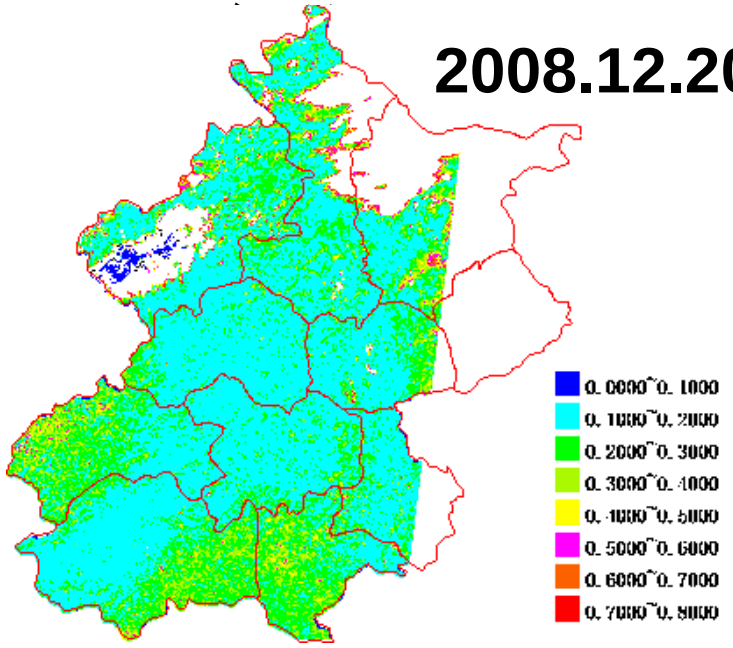

2008.12.18

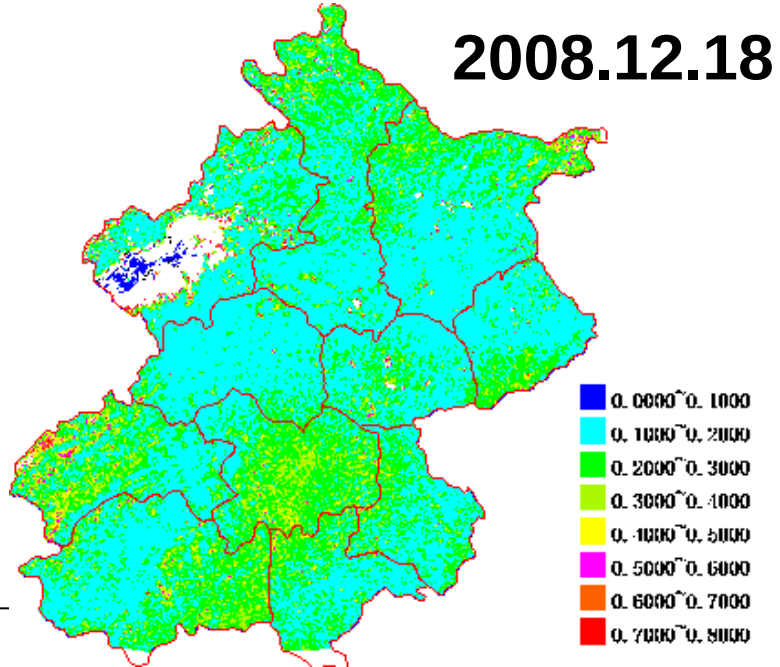

HJ-1 CCD AOD accuracy

AERONET	HJ-1 CCD	error
0.3054	0.3602	-0.0548
0.1885	0.08	0.1085
0.2298	0.1849	0.0449
0.1526	0.1637	-0.0111
0.1347	0.0748	0.0599

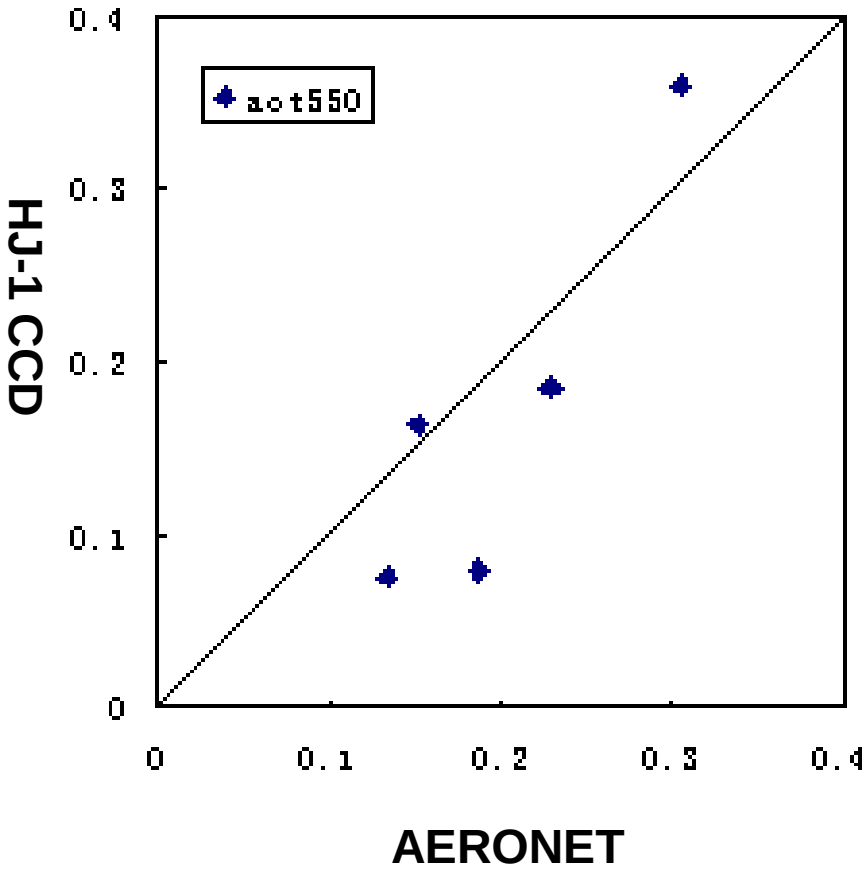

HJ-1 CCD AOD error is about 0.1。

④ Albedo inversion algorithm

(a) Empirical algorithm for HJ-1 Albedo estimation

(b) Albedo inversion combining MODIS/BRDF and HJ-1/CCD data to get higher resolution product

(a) Empirical algorithm for HJ-1 Albedo estimation

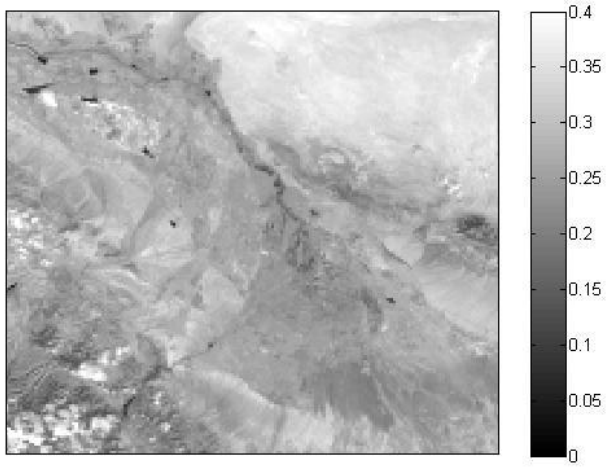

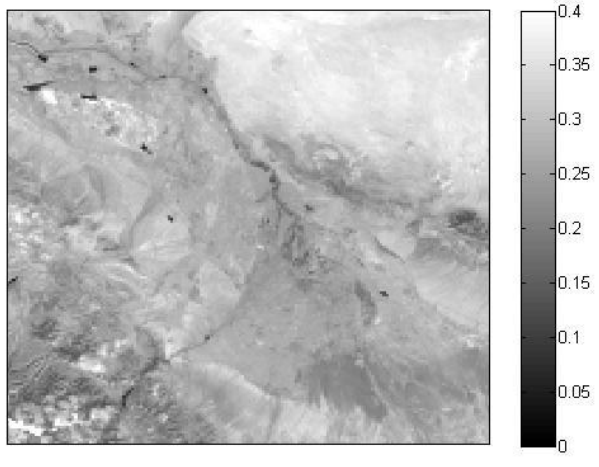

HJ-1 black sky albedo and white sky albedo by date on 051909,052209

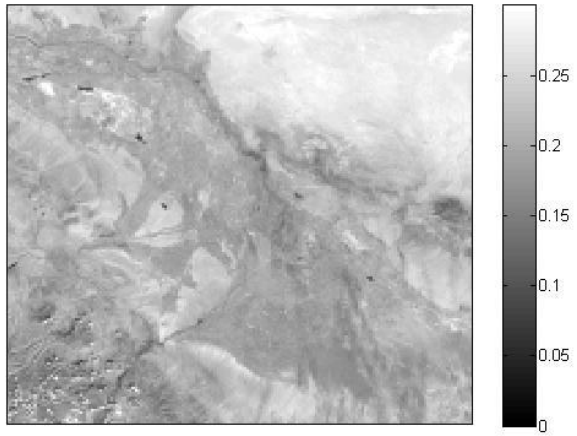

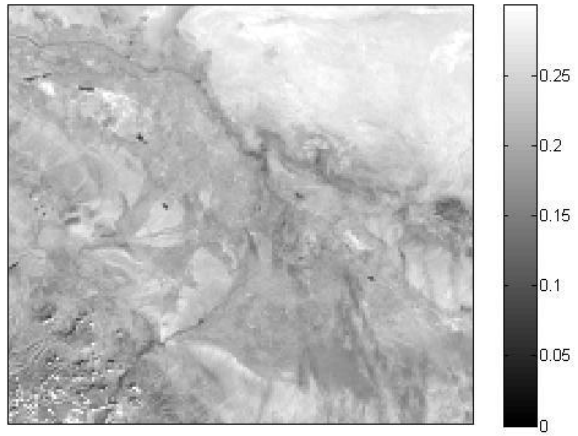

HJ-1 black sky albedo and white sky albedo by date on 062009，062409，062809

(b) Albedo inversion combining MODIS/BRDF and HJ-1/CCD data to get higher resolution product

HJ+MODIS: Spatial and Temporal resolution improved

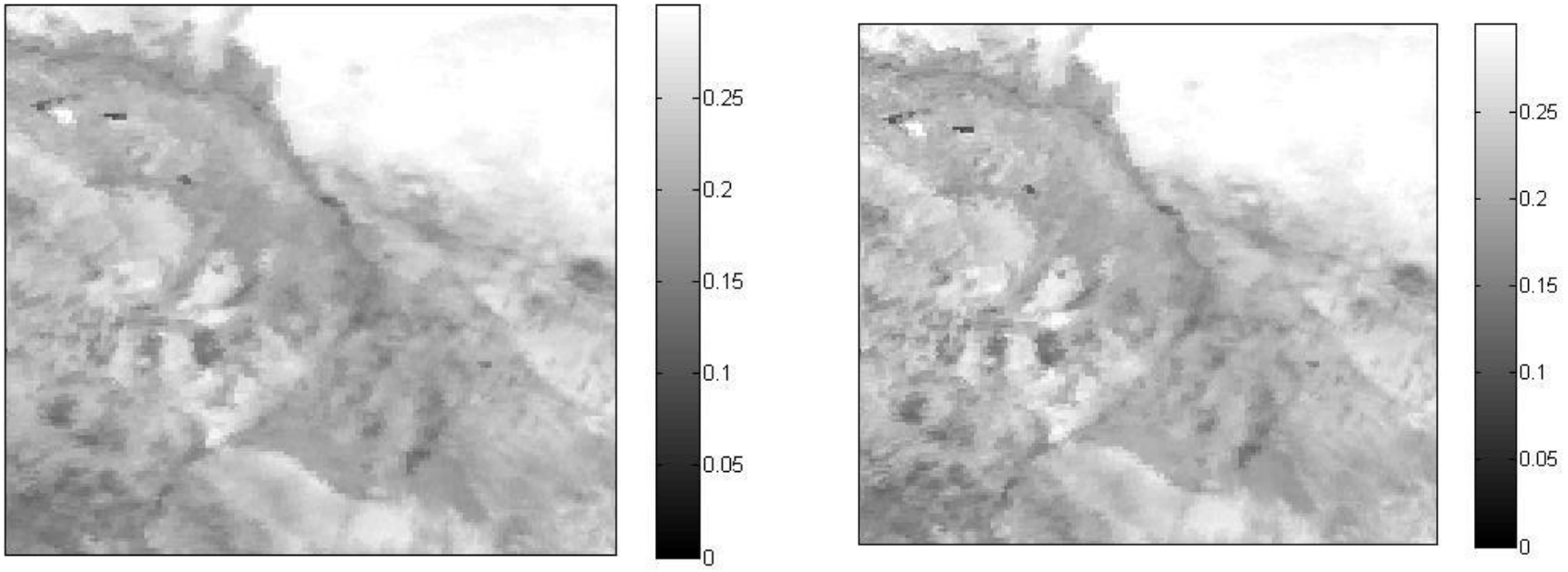

HJ+MODISGA09 inversed black sky and white sky albedo（062009）

Sihan Liu, Qiang Liu, Qinhuo Liu, et. al., IEEE JSTARS, VOL. 3, NO. 3, 2010

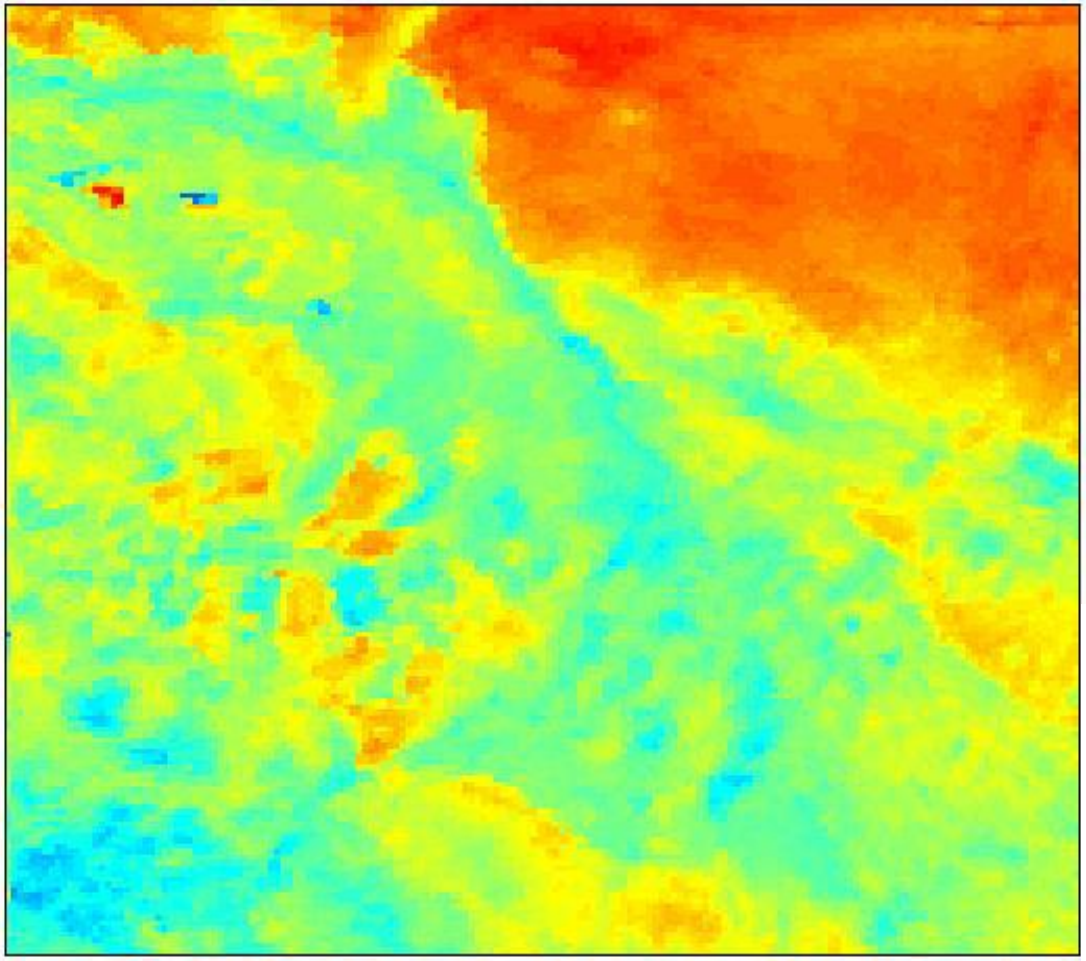

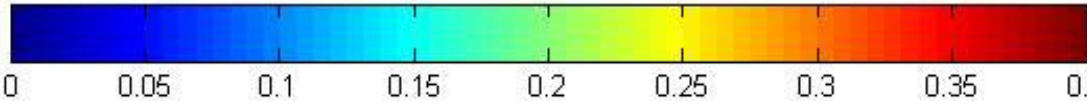

HJ+MODIS albedo

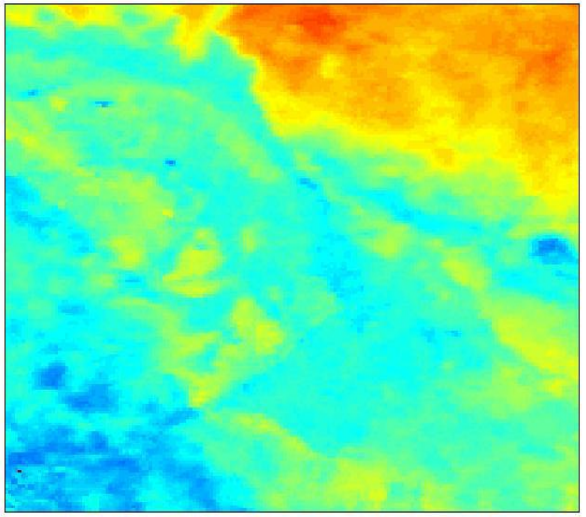

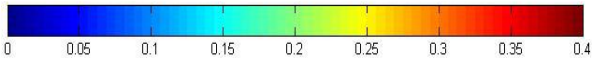

MODIS albedo

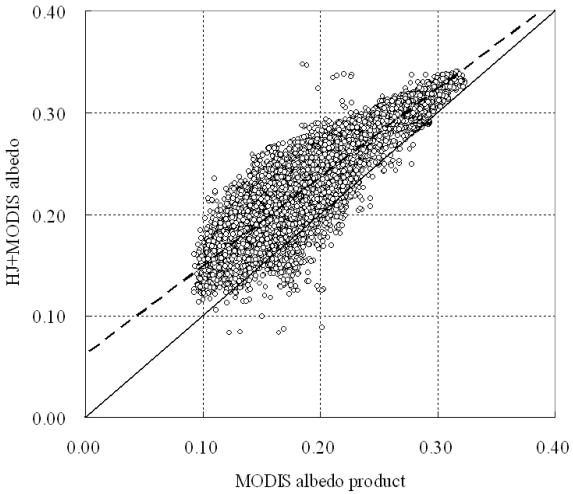

June 20, 2009

⑤ HJ and MODIS combined to retrieve LAI

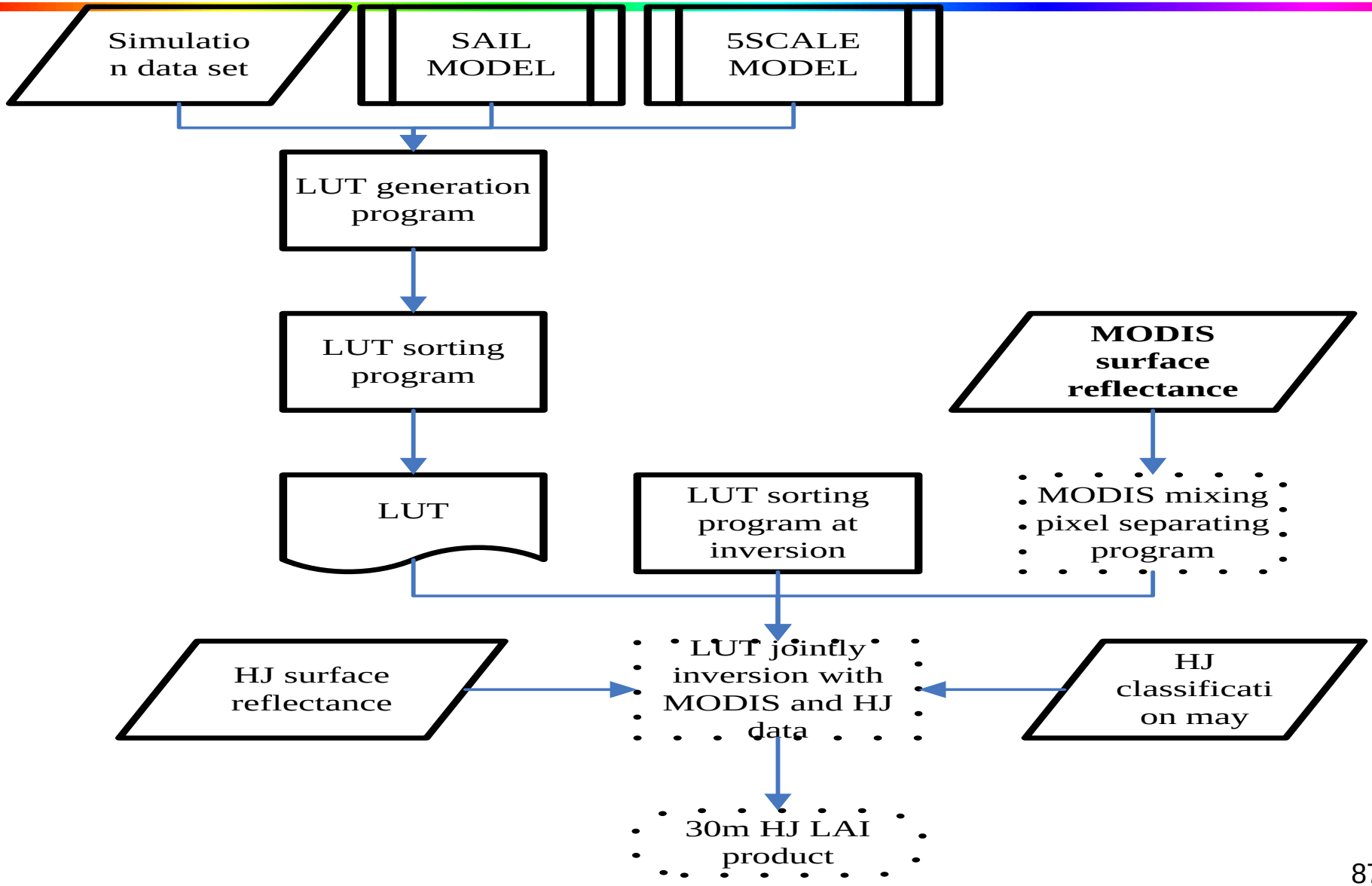

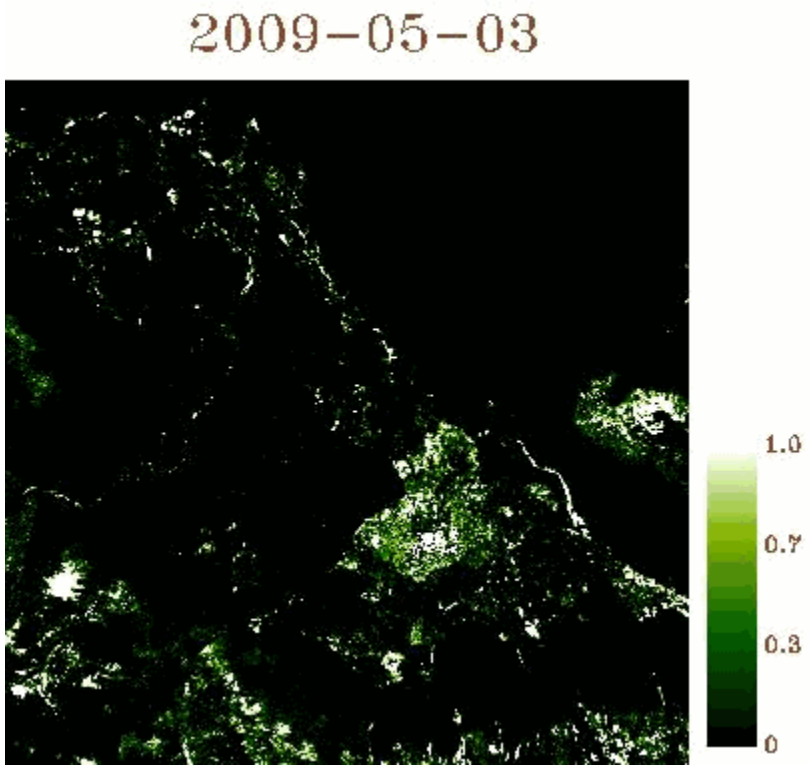

LAI

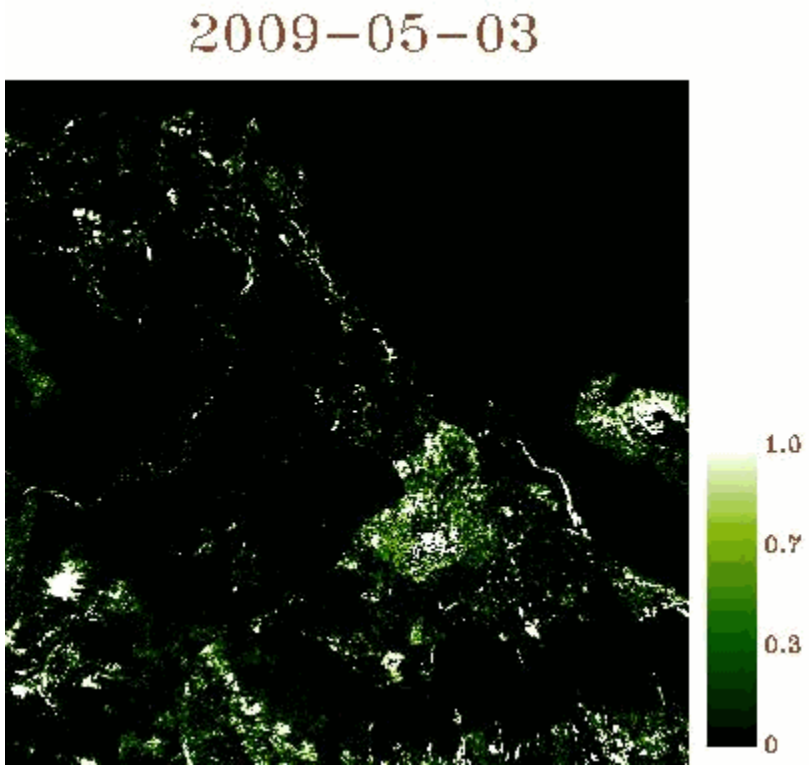

FVC

⑥Land temperature retrieval algorithm

- **single-channel algorithms for Polar-Orbit Satellite:**
  - **Qin et al.(2001) mono-window algorithm**
  - **Jiménez-Muñoz and Sobrino(2003) generalized single-channel algorithm**

- **Problem: Angular effect was not considered**
- **Simulation results indicate the LST errors are increased with view angle and water vapor content.**
- **30° would lead more than 1K error on LST.**

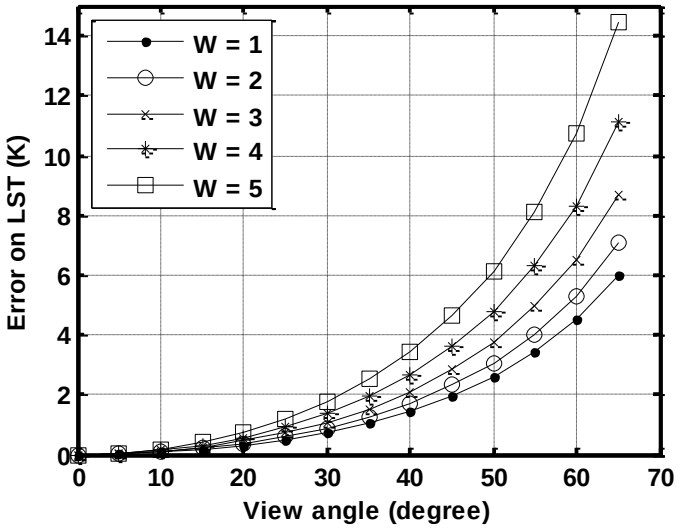

- **angular-dependent single-channel algorithms for HJ-1B wanted:**
  - **Parametric model based algorithm**

- Ellicott et al.(2009) proposed a parametric model for atmospheric correction of MODIS TIR data base on NCEP reanalysis data, which can calculate the atmospheric transmittance, upwelling and downwelling radiance with almost the same accuracy as MODTRAN but less computational time.
- Is it adaptable to HJ-1B/IRS data? Three parameters with angular effect are needed:
  - Layer Transmittance
  - Layer Upwelling and Downwelling Radiances
  - Total Transmittance and Radiances

Layer Transmittance

In the TIR, the optical thickness for layer l in channel i can be described as the sum of three components for **water vapor, water-vapor continuum, and other gases**:

$$\tau_{l,i} = \tau_{l,i}^{\mathrm{H_2O}} + \tau_{l,i}^{\mathrm{H_2Oc}} + \tau_{l,i}^{\mathrm{other}}$$

The layer optical thickness of water vapor:

$$\tau_{l,i}^{\mathrm{H_2O}} = \exp(a_{0,\mathrm{H_2O},i} + a_{1,\mathrm{H_2O},i}\rho_{\mathrm{H_2O}} + a_{2,\mathrm{H_2O},i}\rho_{\mathrm{H_2O}}^2)$$

$$\rho_{\mathrm{H_2O}} = \log(\frac{\rho_{0,\mathrm{H_2O}}}{\cos(\theta_{\mathrm{v}})})$$

Where $\rho_{0,\mathrm{H2O}}$ is the water vapor content of the layer (g/m^2)

θ_{v} is the view angle, a_0, a_1, a_2 are band coefficients that depend on T_l (equivalent temperature) and P_l (equivalent pressure).

Layer Transmittance

The layer optical thickness of **other gases**

$$\tau_{l,i}^{\text{other}} = \exp(a_{0,\text{other},i}\rho_{\text{other}}^{a_1,\text{other}}) \qquad \rho_{\text{other}} = \frac{D}{\cos(\theta_{\text{v}})}$$

where D is the layer depth in km, a_0, a_1 are band coefficients that depend on T_l and P_l

The layer optical thickness of **water vapor continuum** use the CKD model integrated in MODTRAN directly.

The **layer transmittance** is

$$t_{l,i} = \exp(-\tau_{l,i}^{\mathrm{H_2O}} - \tau_{l,i}^{\mathrm{H_2Oc}} - \tau_{l,i}^{\text{other}})$$

Layer Upwelling and Downwelling Radiances

The **layer atmospheric upwelling radiance** is computed using

$$L_{l,\text{atm}\uparrow i} = (1 - t_{l,i}) L_i(T_{l,\text{atm\_}eq})$$

$$T_{l,\text{atm\_eq}} = wT_{l,\text{bot}} + (1-w)T_{l,\text{top}}$$

where w is weighted factor = 0.5, $T_{l,\text{bot}}$ and $T_{l,\text{top}}$ is bottom and top layer temperature

The **layer atmospheric downwelling radiance** is computed using

$$L_{l,\text{atm}\downarrow i} = (1 - t_{l,i}(\theta_{\text{emis}\downarrow})) L_i(T_{l,\text{atm\_}eq})$$

where $\theta_{\text{emis}\downarrow} = 53°$

Total Transmittance and Radiances

The atmosphere is sliced in *L* layer with 1 at low altitude and layer *L* at top of atmosphere. The **band atmospheric transmittance t_i** along the optical path is derived from the layer transmittance $t_{l,i}$

$$t_i = \prod_{l=1}^{L} t_{l,i}$$

For the **upwelling radiance**, layer contributions are summed

$$L_{\text{atm}\uparrow i} = \sum_{l=1}^{L} t_{l+1\to L,i} L_{l,\text{atm}\uparrow i} \qquad t_{l+1\to L,i} = \prod_{k=l+1}^{L} t_{k,i}$$

Where $t_{l+1->L,i}$ is transmittance along the path from top of layer l to top of the atmosphere

In parallel, the **downwelling radiance** is

$$L_{\text{atm}\downarrow i} = \sum_{l=1}^{L} t_{1\to l-1,i}(\theta_{\text{emis}\downarrow}) L_{l,\text{atm}\downarrow i}$$

Retrieving the land surface temperature

Planck function $B_\lambda(T) = \dfrac{c_1 \lambda^{-5}}{\exp(\dfrac{c_2}{\lambda T}) - 1}$ + **Spectral response function**

Channel Radiance $B_i(T_i) = \dfrac{\int_{\lambda_1}^{\lambda_2} B_\lambda(T_i) f(\lambda) d\lambda}{\int_{\lambda_1}^{\lambda_2} f(\lambda) d\lambda}$

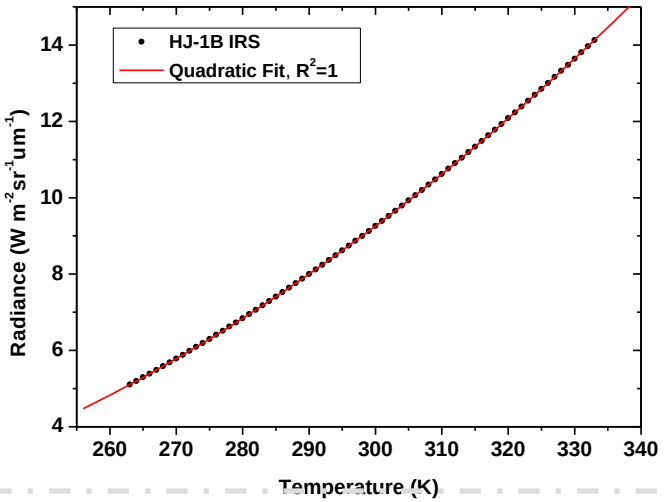

Regression function $B_i(T_i) = aT_i^2 + bT_i + c$

$$T_s = \frac{-b + \sqrt{b^2 - 4a[c - B_i(T_s)]}}{2a}$$

Validation

- Algorithm validation using simulated data
  - **TIGR3 database (2311 profiles) + MODTRAN 4**
- Algorithm validation using remote sensing data
  - **In-situ ground LST measurements with pixel scale are unavailable by now**
  - **MODIS LST product has high accuracy (1K), so we compare HJ1B with MODIS LST product**

Algorithm validation using RS data

- Validation site: Heihe river basin
- Area: 285×285 pixels (HJ-1B band4)
- Land cover type :farmland, Gobi and desert
- 6 days HJ-1B and MODIS images
- Overpass time difference of IRS and MODIS are less than 10 minutes
- Water vapor content (w) was provided by MOD05 product
- Land surface emissivity calculated using NDVI Threshold method (Sorbino et al, 2008)

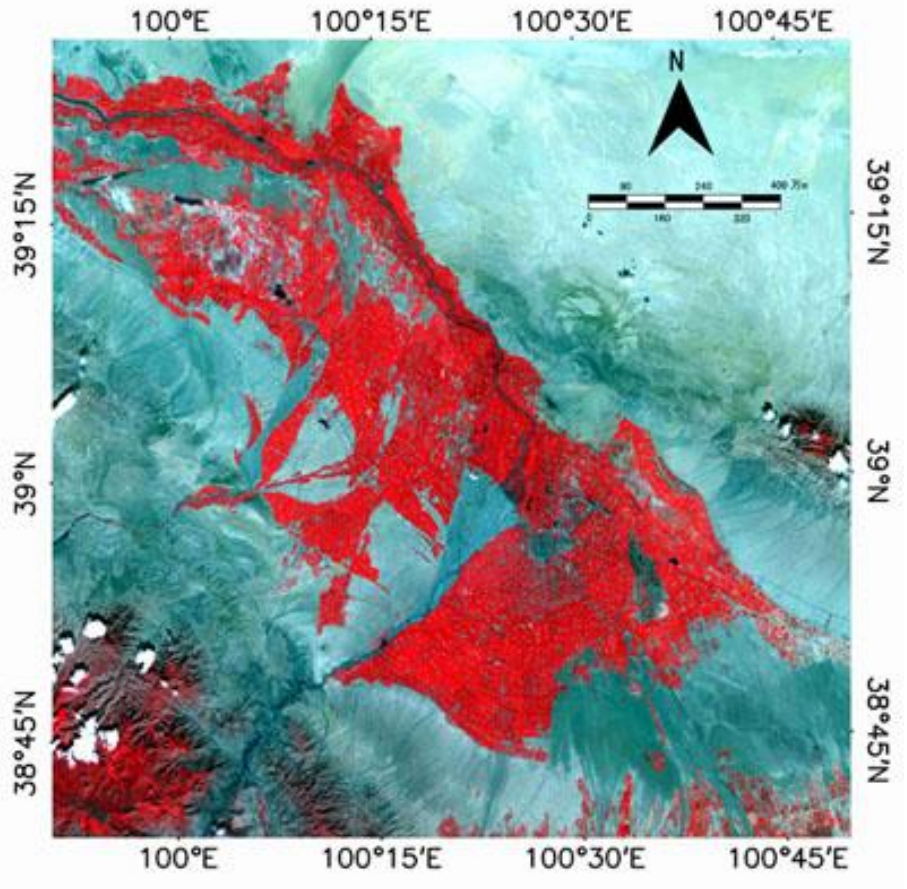

- Air temperature was obtained from Yingke automatic weather station
- NCEP (N39°, E100° and N39°, E101°)

Algorithm validation using RS data

Date and the overpass time of the IRS, MODIS

Data (day/month/year)	w*(g/cm²)	Overpass Time (UTC)	
		HJ-1B IRS	MODIS
22/05/2009	0.62	04:13	04:20
07/06//2009	0.96	04:24	04:15
30/06/2009	1.63	04:17	04:25
27/07/2009	1.42	04:12	04:05
19/08/2009	1.36	04:04	04:10
27/09/2009	1.27	04:07	04:12

*w is the mean value of water vapor content of the study region

- The HJ-1B/IRS and MODIS images have been geo-referenced to the Universal Transverse Mercator(UTM) coordinate system.
- HJ-1B/IRS LST results are re-sampled to 1km pixel size to match with MODIS LST product.
- MODIS LST product have been subtracted to HJ-1B/IRS LST images obtained by our algorithm to compare the results.

Algorithm validation using RS data

Values of difference between HJ1B and MODIS LST product

Date (day/month/year)	Regression based algorithm			Parametric model based algorithm		
	Bias (K)	RMSE (K)	Percentage (%) (<±6K)	Bias (K)	RMSE (K)	Percentage (%) (<±6K)
22/05/2009	1.327	2.169	96.763	0.078	1.864	97.86
07/06/2009	1.542	2.115	97.78	-0.161	1.483	98.533
30/06/2009	1.657	2.726	88.175	-0.815	2.281	88.81
27/07/2009	1.871	2.722	93.156	1.331	2.243	93.777
19/08/2009	0.831	1.834	96.486	-0.377	1.754	96.922
27/09/2009	1.111	1.732	95.812	0.091	1.507	96.182
Average	1.390	2.216	94.695	0.025	1.855	95.347

Algorithm validation using RS data

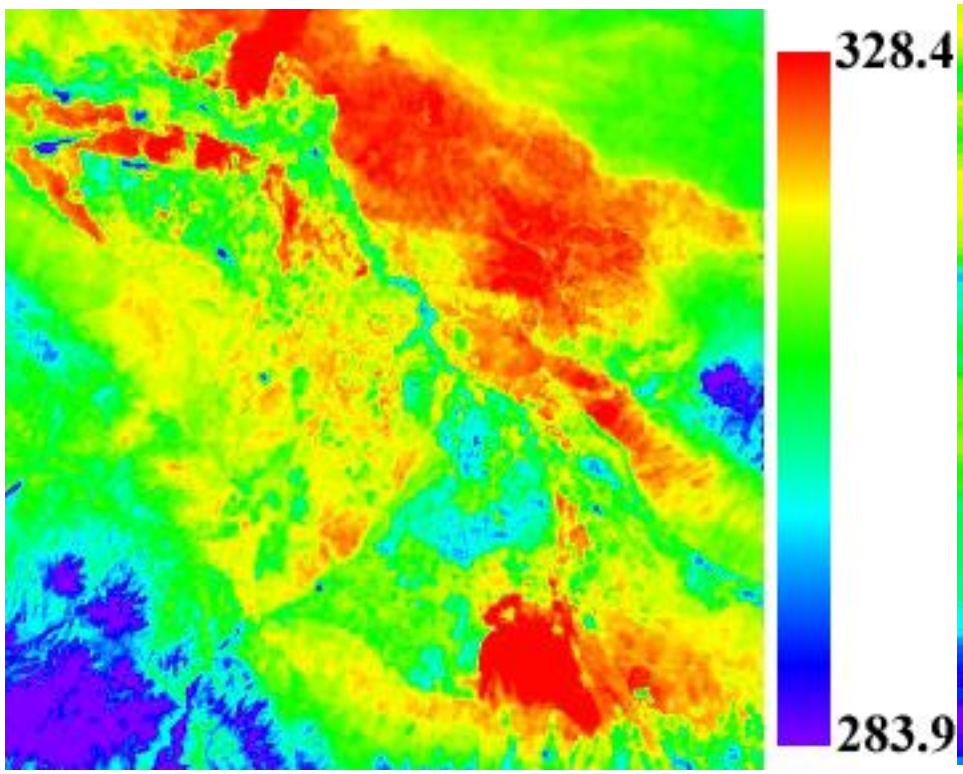

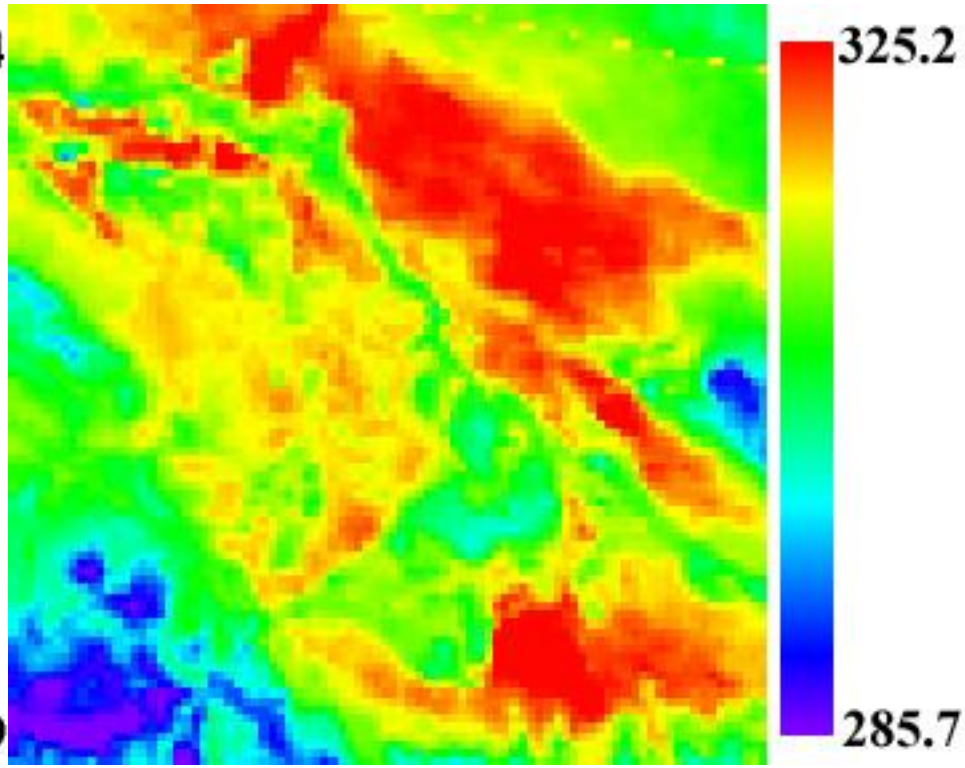

LST images of the study area on May 22, 2009
(a)HJ-1B/IRS LST image (b)MOIDS LST product
(MOIDS product is re-sampled to a resolution of 300m)

(3) Model Assimilation for Environmental monitoring

a. Assimilation for evapotranspiration

b. Assimilation for ecological model

a. evapotranspiration

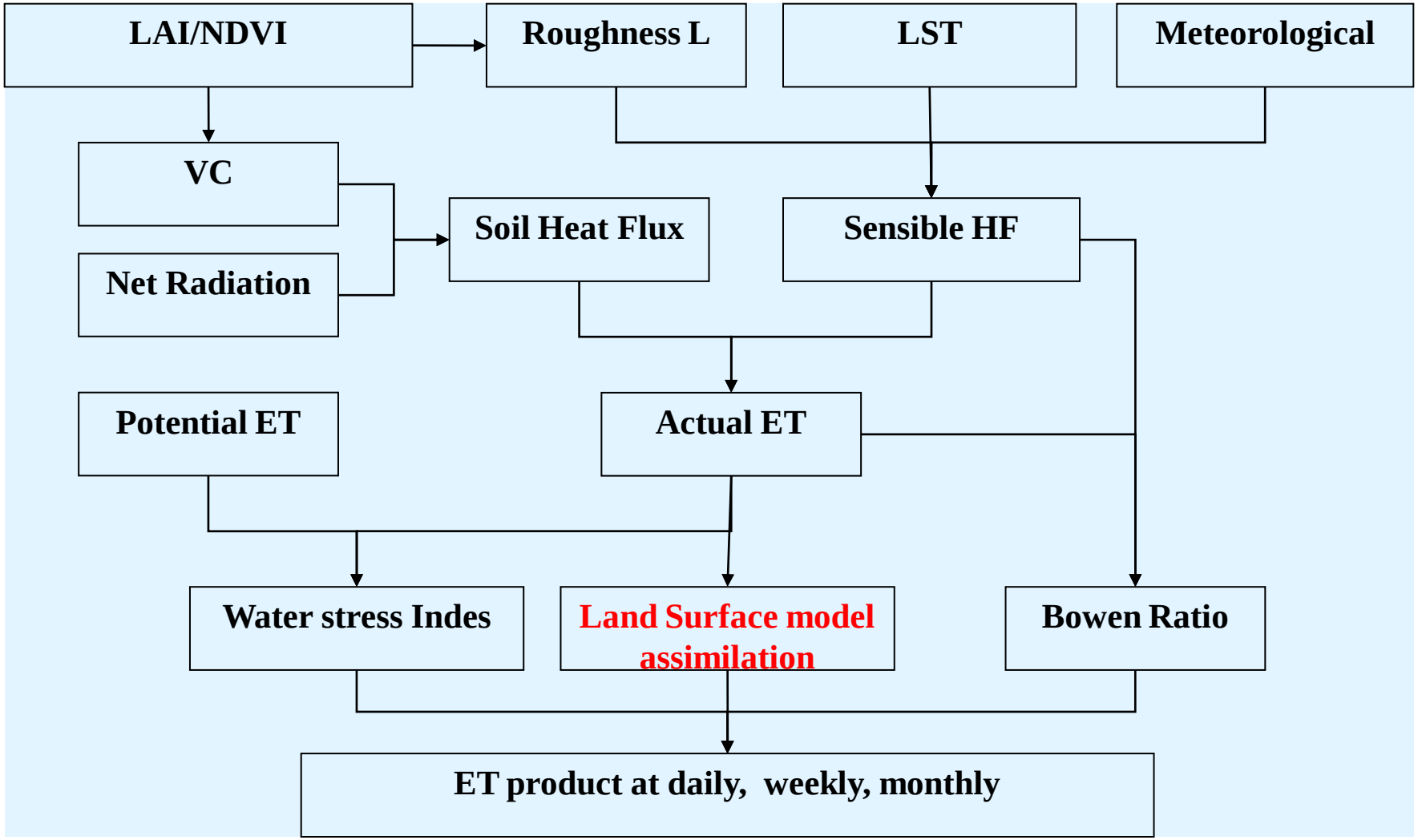

Land surface Evapotranspiration estimation flow chat

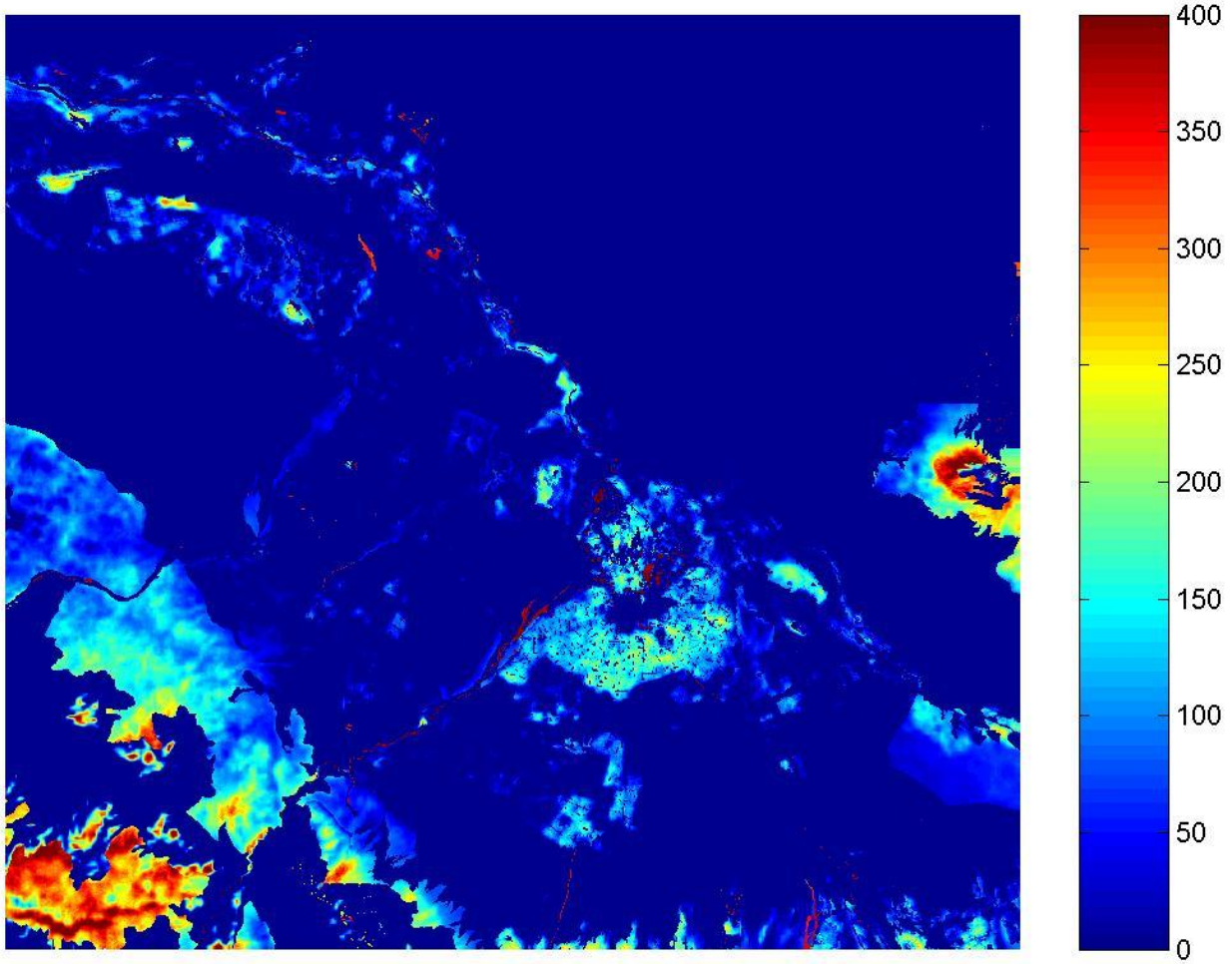

ET distribution in Heihe Basin, Gansu Province, China, on May 22, 2009（Wm-2)

b. Assimilation for ecological model

To generate LAI product

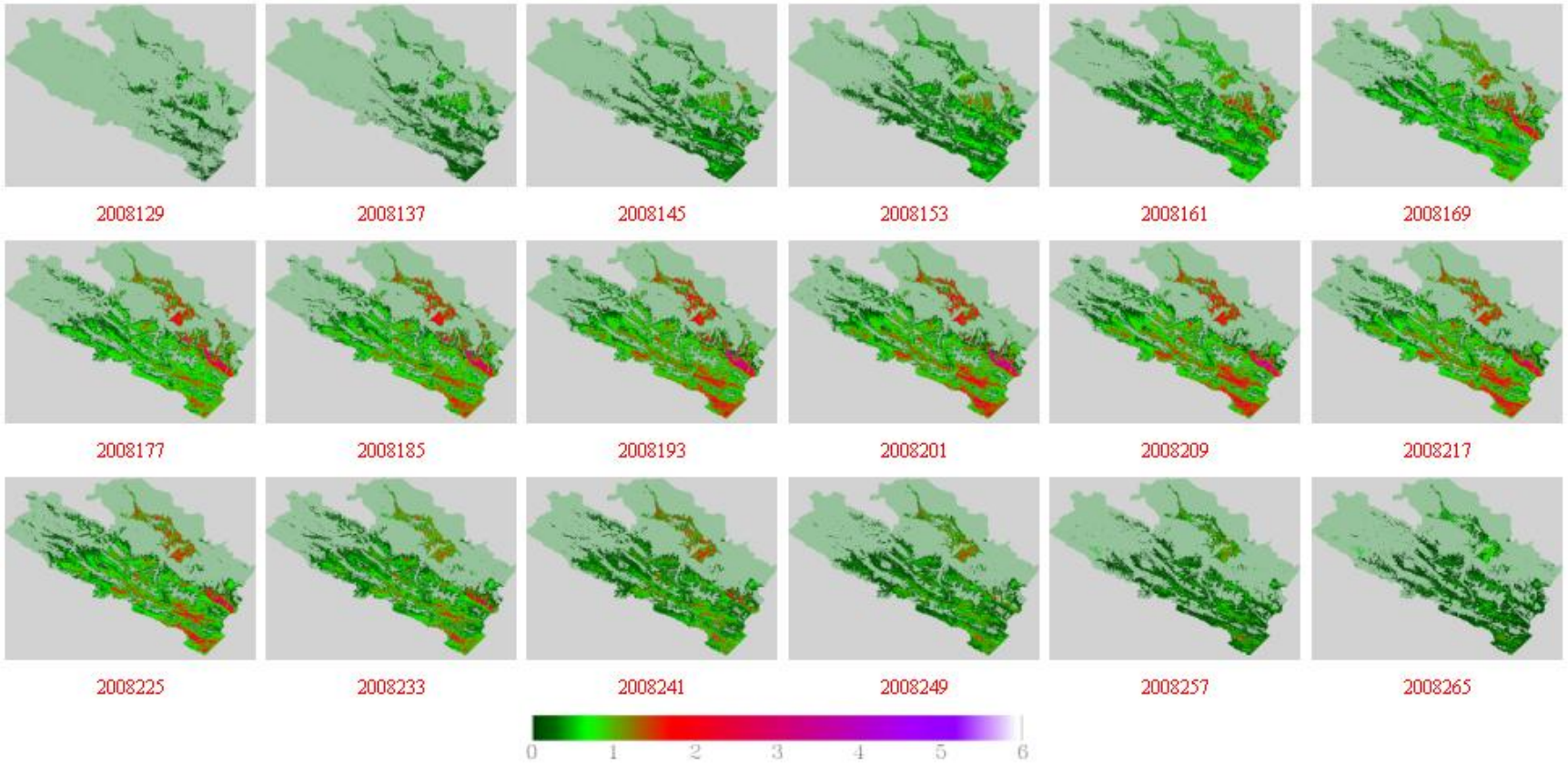

Provided by Prof. Shunlin Liang et. al.

Bondville,IL validation

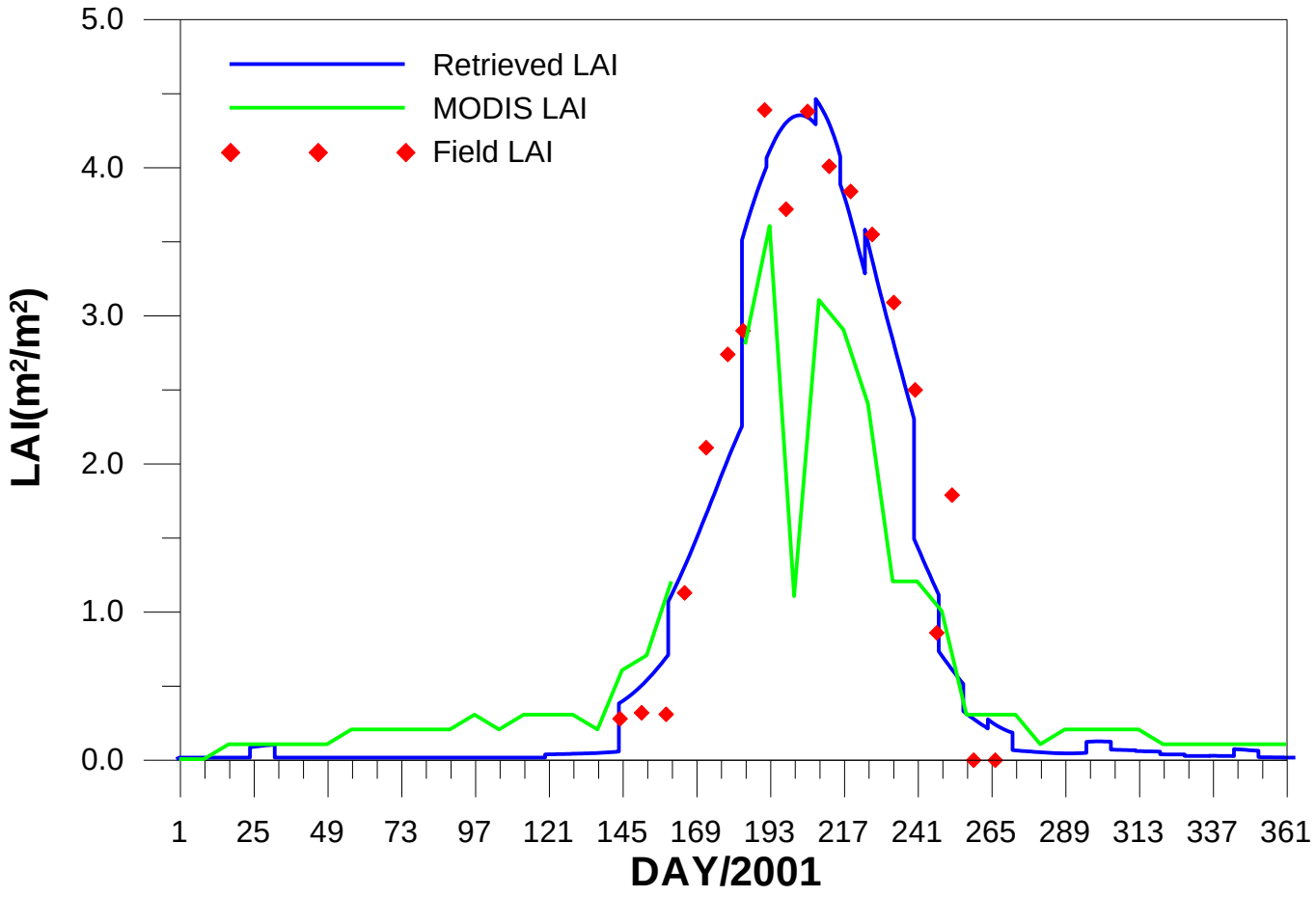

4. Multi-scale field experiment system design

(1) Field observation stations

The comprehensive experiment station in Huailai, Hebei Province

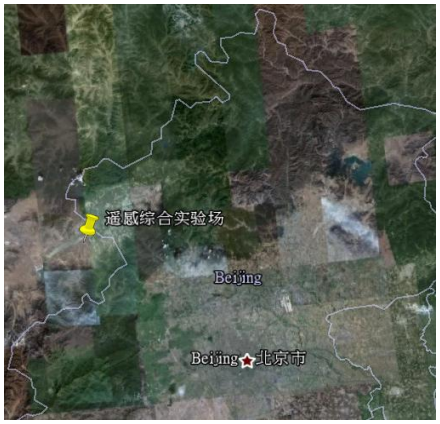

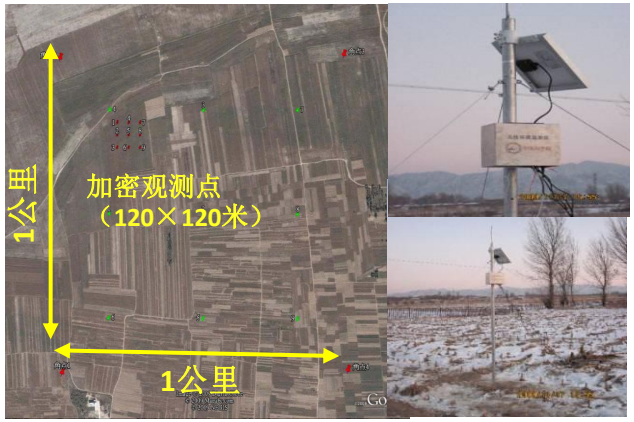

The super monitoring station for air quality in Beijing

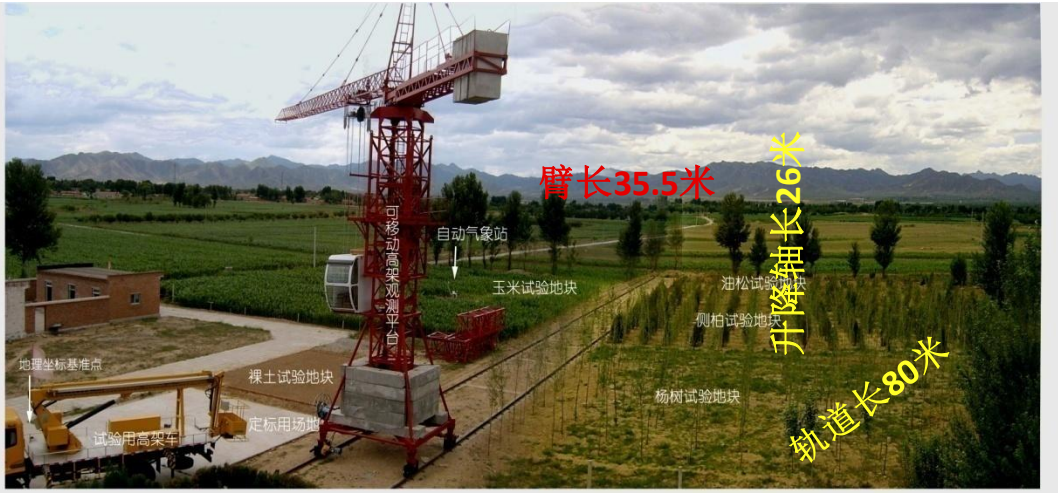

.....

- Field observation stations

The comprehensive experiment station in Huailai, Hebei Province

The super monitoring station for air quality in Beijing

……

- Field observation station

The comprehensive experiment station in Huailai, Hebei Province

The long-term flux observation station of typical underlying surface around Beijing

The super monitoring station for air quality in Beijing

The ecological observation station for environment and health at Poyang Lake

.....

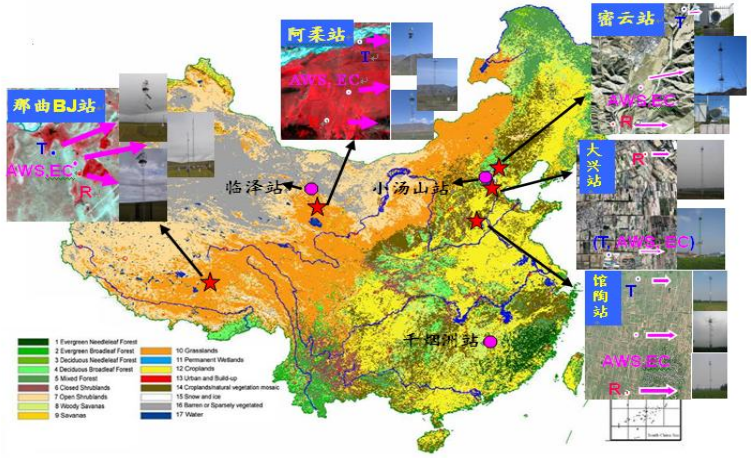

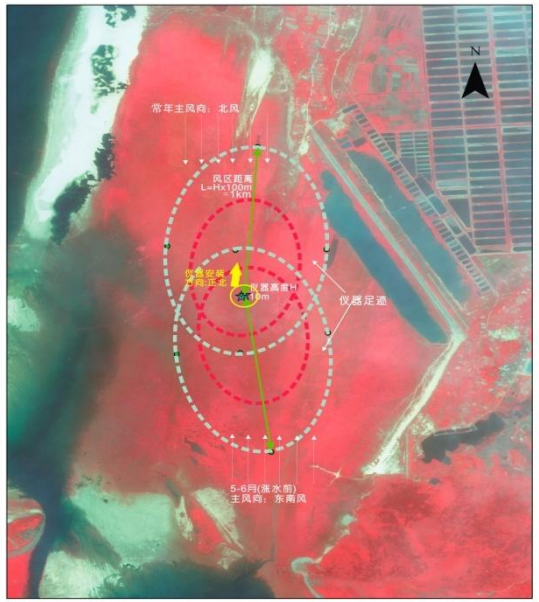

（2）Wireless system design for pixel “true value”

- 1KM*1KM area:
- soil moisture, temperature for 18 point
- LST、LAI、ALBEDO and Radiation at several points
- Wireless network automatically record and transfer

(3) Heat flux/ Latent Flux observation at pixel scale with LAS

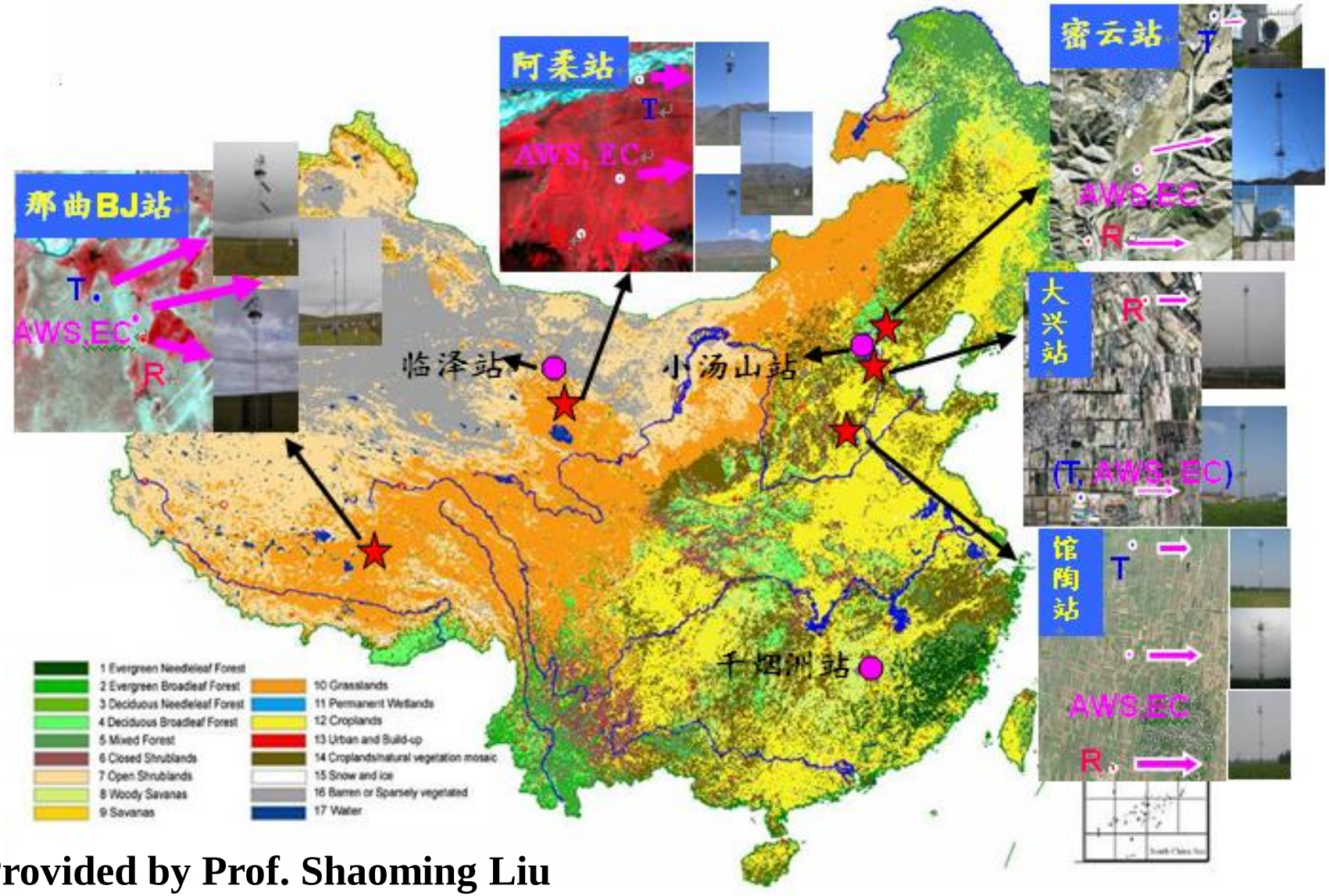

Provided by Prof. Shaoming Liu

5. Software system development and product generation

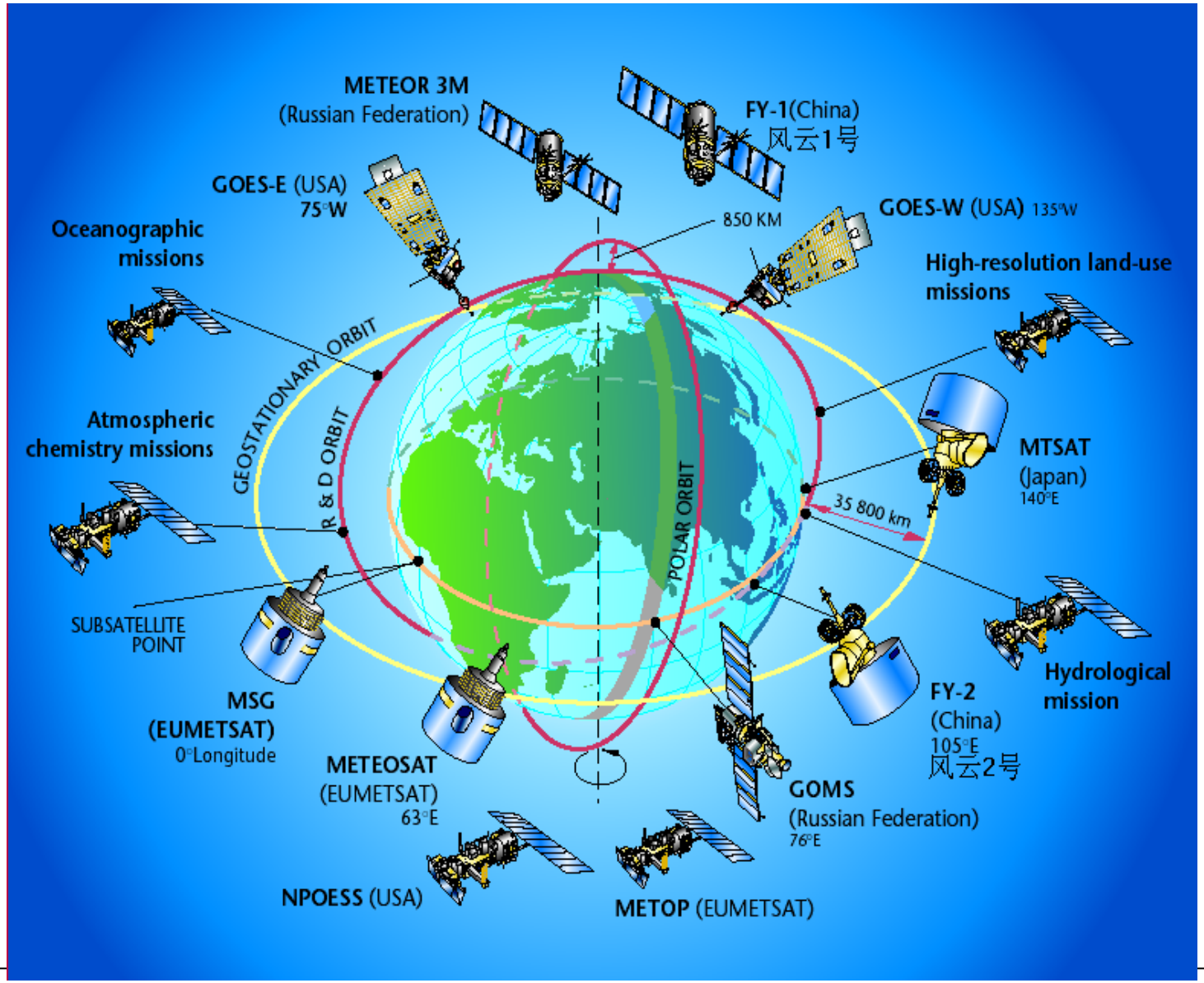

5. Product generation Software system development

Quantitative Remote Sensing Producing System Based On Multi-source Remote Sensing Data

This system takes advantages of multi-source remote sensing data, including moderate and low resolution data, such as **EOS/MODIS, NOAA/AVHRR, FY3/MERSI, FY3/VIRR etc. and high resolution data, such as Landsat/TM/ETM+ and HJ-1, as well as stationary satellite data and high spectral resolution data, to produce quantitative remote sensing parameters like LAI, albedo and so on. The main functions of this system are as follows:**

(1) Data management subsystem(DBMS): multi-source remote sensing data (MSRSD), auxiliary data(AD), and quantitative remote sensing products(QRSP);

(2) Data preprocessing subsystem(DPS): cross-calibaration, geometric correction, reprojectiong and gridding;

(3) Quantitative remote sensing parameter producing subsystem(QRSPPS): based on multi-source remote sensing data.

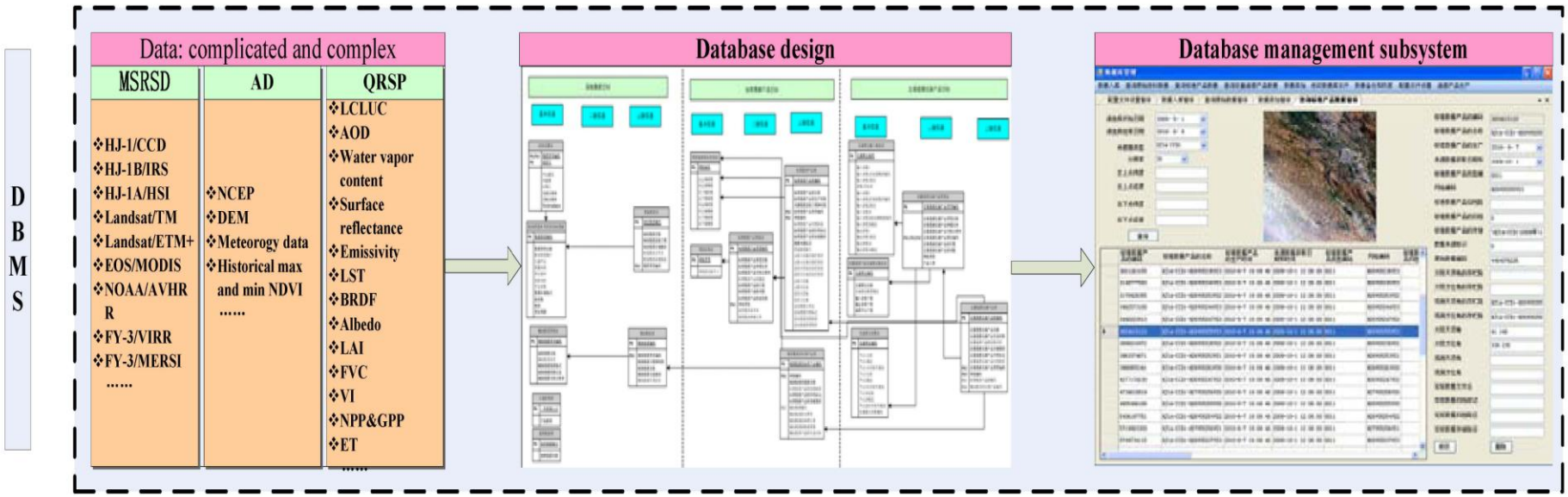

DPS

Preprocessing subsystem design

functions	design
❖Data parsing ❖Radiometric calibaration ❖Radiometric cross calibration ❖Repojection ❖Geometric correction ❖Gridding ❖Data uploading and downloading ……	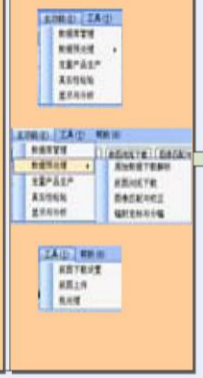

Software function module examples

Radiometric calibration example

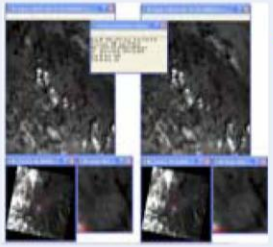

Original and base imagery

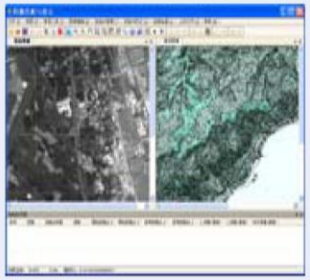

Geometric correction process

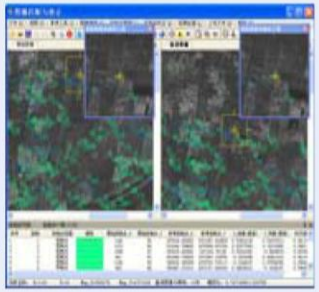

Results validation

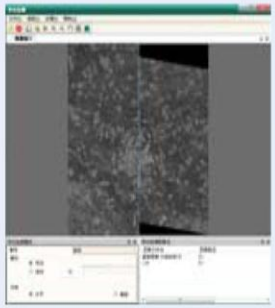

QRSPPS

Products system design

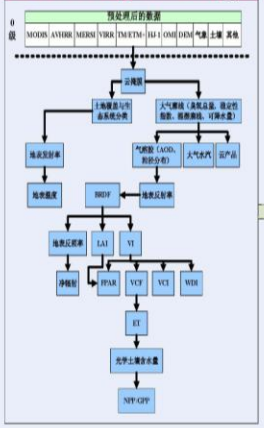

Products workflow design

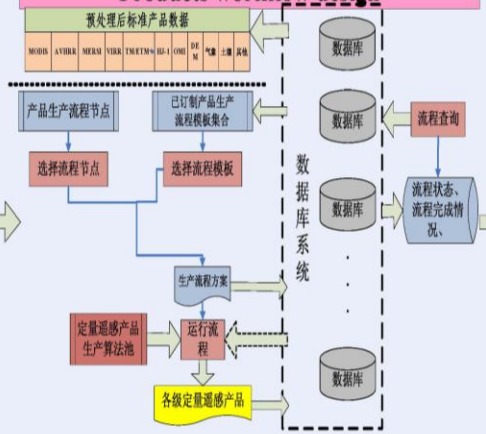

Realization of QRSPPS

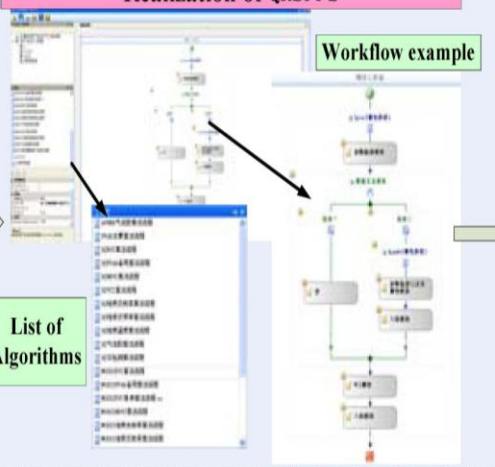

Products examples

Albedo

LST

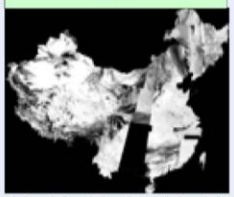

6. Discussion

(1) How to quantitatively describe the directional differences of land surface parameter observed at different scales by different satellites?

Radiation transfer modeling at large scale for complex surface

(2) How to combine accumulated earth observation data to generate the long-term, consistent and accurate land surface products?

Synergic inversion based on information content and error propagation using Multi-scale, multi-spectral (VIS-NIR-TIR-MIR), multi-satellites (Geostationary and polar orbiting, USA, China, European and others)?

(3) How to validate the remote sensing inversed land surface parameters at different scale?

Multi-scale and long term field observation and Scaling transformation?

(4) How to combine remote sensing observation with the land surface process model?

Assimilation?

Huang Huaguo, Liu Qinhuo, Qin Wenhan, Thermal Emission Hot-Spot Effect of Crop Canopies—Part I: Simulation, IEEE JOURNAL OF SELECTED TOPICS IN APPLIED EARTH OBSERVATIONS AND REMOTE SENSING, VOL. 3, NO. 3, SEPTEMBER 2010

Sihan Liu, Qiang Liu, Qinhuo Liu, Jianguang Wen, and Xiaowen Li, The Angular and Spectral Kernel Model for BRDF and Albedo Retrieval, IEEE JOURNAL OF SELECTED TOPICS IN APPLIED EARTH OBSERVATIONS AND REMOTE SENSING, VOL. 3, NO. 3, SEPTEMBER 2010

Xin Xiaozhou, Liu Qinhuo, 2010, The Two-layer Surface Energy Balance Parameterization Scheme (TSEBPS) for estimation of land surface heat fluxes, HYDROLOGY AND EARTH SYSTEM SCIENCES, No.14, No. 3, P. 491-504

Yang Guijun, Liu Qinhuo, Liu Qiang, Xiao Qing, Huang WenJiang, 2010, DIRECTIONAL SIMULATION OF THERMAL INFRARED RADIATION AND 3D RADIATIVE TRANSFER MODEL OF CANOPY, JOURNAL OF INFRARED AND MILLIMETER WAVES, Vol. 29, No. 1, P. 38-44

Guijun Yang, Qinhuo Liu, Qiang Liu, Wenjiang Huang, Jihua Wang. Simulation of high-resolution mid-infrared (3-5 μm) images using an atmosphere radiative transfer analytic model. International Journal of Remote Sensing. 2009Vol.30.No. 22 P.6003-6022

HUAGUO HUANG, MIN CHEN, QINHUO LIU, QIANG LIU， YANG ZHANG, LIQIONG ZHAO and WENHAN QIN，2009, A realistic structure model for large-scale surface leaving radiance simulation of forest canopy and accuracy assessment，International Journal of Remote Sensing，Vol. 30, No. 20, 20 October 2009, 5421–5439

Yang, GJ; Liu, QH; Liu, Q, et al., 2009, Mid-Infrared Atmosphere Radiation Transfer Analytic Model and Remote Sensing Images Simulation, SPECTROSCOPY AND SPECTRAL ANALYSIS, Vol. 29, No. 3, P. 629-634

Wen, JG; Liu, QH; Liu, Q, et al., 2009, Parametrized BRDF for atmospheric and topographic correction and albedo estimation in Jiangxi rugged terrain, China, INTERNATIONAL JOURNAL OF REMOTE SENSING, Vol. 30, No. 11, P2875-2896

JIANGUANG WEN, QIANG LIU, QINHUO LIU, QING XIAO，and XIAOWEN LI，2009, Scale effect and scale correction of land-surface albedo in rugged terrain，International Journal of Remote Sensing， Vol. 30, No. 20, 20 October 2009, 5397–5420

Xin Li, Xiaowen Li, Zengyuan Li, Mingguo Ma, Jian Wang, Qing Xiao, Qiang Liu, Tao Che, Erxue Chen, Guangjian Yan, Zeyong Hu, Lixin Zhang, Rongzhong Chu,1 Peixi Su, Qinhuo Liu, Shaomin Liu, Jindi Wang, Zheng Niu, Yan Chen, Rui Jin,Weizhen Wang, Youhua Ran, Xiaozhou Xin, and Huazhong Ren， 2009, Watershed Allied Telemetry Experimental Research，JOURNAL OF GEOPHYSICAL RESEARCH, VOL. 114, D22103, doi:10.1029/2008JD011590, 2009

Jing Li, Qiang Liu, Qinhuo Liu, Yong Tang, Qing Xiao, A Patch Spectral Purification Method to Extract Field Patch Average Parameter from Moderate Resolution Data. International Journal of Remote Sensing Vol.29, Nos.17-18, September 2008, 4993-5011.

WEN JianGuang, Liu QinHuo, XIAO Qing, LIU Qiang, LI XiaoWen, Modeling the land surface reflectance for optical remote sensing data in rugged terrain. Science in China Series D: Earth Sciences Aug.2008 Vol.51, No.8 1169-1178

CHENG Jie, LIU **QinHuo, LI XiaoWen, XIAO Qing, LIU Qiang, DU YongMing. The Correlation Based Temperature Emissivity Separation Algorithm. Science in** China Ser. D 2008,Vol.38(3):357-369

Yang, GJ; **Liu, QH; Liu, Q, Xiao Q, Gu XF, 2008, Adjacency effect analysis in imaging simulation of high-resolution mid-infrared (3 similar to 5 mu m) remote sensing, JOURNAL OF INFRARED AND MILLIMETER WAVES, Volume: 27, Issue: 3** Pages: 233-240

Chen, LF; Gao, YH; Yang, L, **Liu QH, et. al., 2008, MODIS-derived daily PAR simulation from cloud-free images and its validation, SOLAR ENERGY** Volume: 82 Issue: 6, Pages: 528-534

Cheng, J; **Liu, QH; Li, XW, et al. 2008, Algorithm study on soil mid-infrared emissivity extraction, JOURNAL OF INFRARED AND MILLIMETER WAVES, Volume: 27, Issue: 1** Pages: 21-26

Cheng, J; Xiao, Q; Li, XW, **Liu QH, Du YM, 2008, Multi-layer perceptron neural network based algorithm for simultaneous retrieving temperature and emissivity from hyperspectral FTIR data, SPECTROSCOPY AND SPECTRAL ANALYSIS, Volume: 28, Issue: 4, Pages: 780-783**

Chen, LF; Gao, YH; Li, L, **Liu QH, et al., 2008, Forest NPP estimation based on MODIS data under cloudless condition, SCIENCE IN CHINA SERIES D-EARTH SCIENCES, Volume: 51, Issue: 3** Pages: 331-338

Yao, YJ (Yao, Yanjuan); Liu, QH (Liu, **Qinhuo); Liu, Q (Liu, Qiang); Li, XW (Li, Xiaowen) .LAI retrieval and uncertainty evaluations for typical row-planted crops at different growth stages .REMOTE SENSING OF ENVIRONMENT, 112 (1): 94-106 JAN 15 2008**

Du, YM (Du, Yongming); Liu, QH (Liu, **Qinhuo); Chen, LF (Chen, Liangfu); Liu, QA (Liu, Qiang); Yu, T (Yu, Tao) .Modeling directional brightness temperature of the winter wheat canopy at the ear stage .IEEE TRANSACTIONS ON GEOSCIENCE AND REMOTE SENSING, 45 (11): 3721-3739 Part 2 NOV 2007**

Liu, QH (Liu, Qinhuo); Huang, HG (Huang, Huaguo); Qin, WH (Qin, Wenhan); Fu, KH (Fu, Kaihua); Li, XW (Li, Xiaowen) .An extended 3-D radiosity-graphics combined model for studying thermal-emission directionality of crop canopy .IEEE TRANSACTIONS ON GEOSCIENCE AND REMOTE SENSING, 45 (9): 2900-2918 SEP 2007

Sun, GY (Sun, Genyun); **Liu, QH (Liu, Qinhuo); Liu, Q (Liu, Qiang); Ji, CYY (Ji, Changyuan); Li, XM (Li,** Xiamen) . A novel approach for edge detection based on the theory of universal gravity .PATTERN RECOGNITION, 40 (10): 2766-2775 OCT 2007

Yang, GJ (Yang Gui-Jun); **Liu, QH (Liu Qin-Huo); Huang, HG (Huang Hua-Guo); Liu, Q (Liu Qiang); Gu, XF (Gu Xing-Fa) .Methods for simulating infrared remote sensing images based on scene models .JOURNAL OF INFRARED AND MILLIMETER WAVES, 26 (1): 15-21 FEB 2007**


Thank you very much for your attention!
You are welcome to visit IRSA. More cooperation and communication are expected!